The genetic architecture of human brainstem structures and their involvement in common brain disorders

Torbjørn Elvsåshagen[1,2,3,*], Shahram Bahrami[1,*], Dennis van der Meer[1,4], Ingrid Agartz[1,3,5,6], Dag Alnæs[1], Deanna M. Barch[7], Ramona Baur-Streubel[8], Alessandro Bertolino[9,10], Mona K. Beyer[3,11], Giuseppe Blasi[9], Stefan Borgwardt[12,13,14], Birgitte Boye[15,16], Jan Buitelaar[17,18], Erlend Bøen[15], Elisabeth Gulowsen Celius[2,3], Simon Cervenka[6], Annette Conzelmann[19], David Coynel[20,21], Pasquale Di Carlo[10], Srdjan Djurovic[22,23], Sarah Eisenacher[24], Thomas Espeseth[25], Helena Fatouros-Bergman[6], Lena Flyckt[6], Barbara Franke[26], Oleksandr Frei[1], Barbara Gelao[9], Hanne Flinstad Harbo[2,3], Catharina A. Hartman[27], Asta Håberg[28,29], Dirk Heslenfeld[30,31], Pieter Hoekstra[32], Einar A. Høgestøl[2,3], Rune Jonassen[25,33], Erik G. Jönsson[1,3,6], Karolinska Schizophrenia Project (KaSP) consortium[34], Peter Kirsch[35,36], Iwona Kłoszewska[37], Trine Vik Lagerberg[1], Nils Inge Landrø[5,25], Stephanie Le Hellard[23], Klaus-Peter Lesch[38,39,40], Luigi A. Maglanoc[1,25], Ulrik F. Malt[3], Patrizia Mecocci[41], Ingrid Melle[1,3], Andreas Meyer-Lindenberg[24], Torgeir Moberget[1,25], Jan Egil Nordvik[42], Lars Nyberg[43], Kevin S. O`Connell[1], Jaap Oosterlaan[30,44], Marco Papalino[10], Andreas Papassotiropoulos[20,21,45,46], Paul Pauli[8], Giulio Pergola[10], Karin Persson[47,48], Dominique de Quervain[20,21,45], Andreas Reif[49], Jarek Rokicki[1], Daan van Rooij[17], Alexey A. Shadrin[1], André Schmidt[12], Emanuel Schwarz[24], Geir Selbæk[3,47,48], Hilkka Soininen[50,51], Piotr Sowa[11], Vidar M. Steen[23,52], Magda Tsolaki[53], Bruno Vellas[54], Lei Wang[55], Eric Westman[13,56], Georg Ziegler[38], Mathias Zink[24,57], Ole A. Andreassen[1,3], Lars T. Westlye[1,25], Tobias Kaufmann[1,3]

[1]NORMENT, Division of Mental Health and Addiction, Oslo University Hospital, Oslo, Norway

[2]Department of Neurology, Division of Clinical Neuroscience, Oslo University Hospital, Oslo, Norway

[3]Institute of Clinical Medicine, University of Oslo, Oslo, Norway

[4]School of Mental Health and Neuroscience, Faculty of Health, Medicine and Life Sciences, Maastricht University, Maastricht, The Netherlands

[5]Department of Psychiatry, Diakonhjemmet Hospital, Oslo, Norway

[6]Centre for Psychiatry Research, Department of Clinical Neuroscience, Karolinska Institutet & Stockholm Health Care Services, Stockholm County Council, Stockholm, Sweden

[7]Departments of Psychological & Brain Sciences, Psychiatry, and Radiology, Washington University in St. Louis, St. Louis, USA

[8]Department of Psychology I, University of Würzburg, Würzburg, Germany

[9]Institute of Psychiatry, University of Bari, Bari, Italy

[10]Department of Basic Medical Science, Neuroscience, and Sense Organs, University of Bari Aldo Moro, Bari, Italy

[11]Division of Radiology and Nuclear Medicine, Oslo University Hospital, Oslo, Norway

[12]Department of Psychiatry (UPK), University of Basel, Basel, Switzerland

[13]Institute of Psychiatry, King's College, London, UK

[14]Department of Psychiatry and Psychotherapy, University of Lübeck, Lübeck, Germany

[15]Psychosomatic and CL Psychiatry, Division of Mental Health and Addiction, Oslo University Hospital, Oslo, Norway

[16]Department of Behavioural Sciences in Medicine, University of Oslo, Oslo, Norway

[17]Department of Cognitive Neuroscience, Donders Institute for Brain, Cognition and Behaviour, Radboud University Medical Center, Nijmegen, The Netherlands

[18]Karakter Child and Adolescent Psychiatry University Centre, Nijmegen, The Netherlands

[19]Children and Adolescence Psychiatry, University of Tübingen, Tübingen, Germany

[20]Transfaculty Research Platform Molecular and Cognitive Neurosciences, University of Basel, CH-4055 Basel, Switzerland

[21]Division of Cognitive Neuroscience, Department of Psychology, University of Basel, Basel, Switzerland

[22]Department of Medical Genetics, Oslo University Hospital, Oslo, Norway

[23]NORMENT, Department of Clinical Science, University of Bergen, Bergen, Norway

[24]Department of Psychiatry and Psychotherapy, Central Institute of Mental Health, Medical Faculty Mannheim, Heidelberg University, Mannheim, Germany

[25]Department of Psychology, University of Oslo, Oslo, Norway

[26]Departments of Human Genetics and Psychiatry, Donders Institute for Brain, Cognition and Behaviour, Radboud University Medical Center, Nijmegen, The Netherlands

[27]Department of Psychiatry, University of Groningen, University Medical Center Groningen, Groningen, The Netherlands

[28]Department of Neuromedicine and Movement Science, Norwegian University of Science and Technology, Trondheim, Norway

[29]Department of Radiology and Nuclear Medicine, St. Olavs Hospital, Trondheim, Norway

[30]Clinical Neuropsychology section, Vrije Universiteit Amsterdam, Amsterdam, The Netherlands

[31]Department of Cognitive Psychology, Vrije Universiteit Amsterdam, Amsterdam, The Netherlands

[32]Department of Child and Adolescent Psychiatry, University Medical Center Groningen, University of Groningen, Groningen, The Netherlands

[33]Faculty of Health Sciences, Oslo Metropolitan University, Oslo, Norway

[34]Members of Karolinska Schizophrenia Project (KaSP) consortium are listed at the end of the manuscript as collaborators

[35]Department of Clinical Psychology, Central Institute of Mental Health, Medical Faculty Mannheim, Heidelberg University, Mannheim, Germany

[36]Bernstein Center for Computational Neuroscience Heidelberg/Mannheim, Mannheim, Germany

[37]Department of Old Age Psychiatry and Psychotic Disorders, Medical University of Lodz, Lodz, Poland

[38]Division of Molecular Psychiatry, Center of Mental Health, University of Würzburg, Würzburg, Germany

[39]Laboratory of Psychiatric Neurobiology, Institute of Molecular Medicine, Sechenov First Moscow State Medical University, Moscow, Russia

[40]Dept. of Psychiatry and Neuropsychology, School for Mental Health and Neuroscience (MHeNS), Maastricht University, Maastricht, The Netherlands

[41]Institute of Gerontology and Geriatrics, University of Perugia, Perugia, Italy

[42]The CatoSenteret Rehabilitation Center, Son, Norway

[43]Departments of Radiation Sciences and Integrative Medical Biology, Umeå Center for Functional Brain Imaging, Umeå University, Umeå, Sweden

[44]Emma Children's Hospital Amsterdam UMC, University of Amsterdam, Emma Neuroscience Group, Department of Pediatrics, Amsterdam Reproduction & Development, Amsterdam, The Netherlands

[45]Psychiatric University Clinics, University of Basel, Basel, Switzerland

[46]Department Biozentrum, Life Sciences Training Facility, University of Basel, Basel, Switzerland

[47]Department of Geriatric Medicine, Oslo University Hospital, Oslo, Norway

[48]Norwegian National Advisory Unit on Ageing and Health, Vestfold Hospital Trust, Tønsberg, Norway

[49]Department of Psychiatry, Psychosomatic Medicine and Psychotherapy, University Hospital Frankfurt, Frankfurt am Main, Germany

[50]Department of Neurology, Institute of Clinical Medicine, University of Eastern Finland, Kuopio, Finland

[51]Neurocenter, Neurology, Kuopio University Hospital, Kuopio, Finland

[52]Dr. E. Martens Research Group for Biological Psychiatry, Department of Medical Genetics, Haukeland University Hospital, Bergen, Norway

[53]Department of Neurology, Aristotle University of Thessaloniki, Thessaloniki, Greece

[54]INSERM U 1027, University of Toulouse, Toulouse, France

[55]Feinberg School of Medicine, Northwestern University, Chicago, Illinois, USA

[56]Department of Neurobiology, Care Sciences and Society, Karolinska Institute, Stockholm, Sweden

[57]District hospital Mittelfranken, Ansbach, Germany

[58]Department of Physiology and Pharmacology, Karolinska Institutet, Stockholm, Sweden

[59]Neuroimmunology Unit, Department of Clinical Neuroscience, Karolinska Institutet, Stockholm, Sweden

***These authors contributed equally to this work**

@ Corresponding authors:

Torbjørn Elvsåshagen, M.D., Ph.D, Shahram Bahrami, Ph.D, & Tobias Kaufmann, Ph.D

E-mails: torbjorn.elvsashagen@medisin.uio.no, shahram.bahrami@medisin.uio.no, tobias.kaufmann@medisin.uio.no

Postal address: Norwegian Centre for Mental Disorders Research, Oslo University Hospital, PoBox 4956 Nydalen, Norway

Telephone: +47 23 02 73 50, Fax: +47 23 02 73 33

Counts:

Abstract: 144 words

Main text body: 4011 words

References: 74 in the main text

Figures: 5 in the main text

Keywords:

Brainstem, genetic architecture, magnetic resonance imaging, neurological disorders, psychiatric disorders, multisite

ABSTRACT

Brainstem regions support critical bodily functions, yet their genetic architectures and involvement in brain disorders remain understudied. Here, we examined volumes of brainstem structures using magnetic resonance imaging in 43,353 individuals. In 27,034 genotyped healthy participants, we identified 16 genetic loci associated with whole brainstem volume and 10, 23, 3, and 9 loci associated with volumes of the midbrain, pons, superior cerebellar peduncle, and medulla oblongata, respectively. These loci were mapped to 305 genes, including genes linked to brainstem development and common brain disorders. We detected genetic overlap between the brainstem volumes and eight psychiatric and neurological disorders. Using imaging data from 16,319 additional individuals, we observed differential volume alterations in schizophrenia, bipolar disorder, multiple sclerosis, mild cognitive impairment, dementia, and Parkinson's disease. Together, our results provide new insights into the genetic underpinnings of brainstem structures and support their involvement in common brain disorders.

Main

The brainstem is a critical regulator of vital bodily functions and includes the midbrain, pons, and the medulla oblongata[1,2]. Regions of the brainstem subserve emotions and behavior and are implicated in the pathophysiology of psychiatric and neurological diseases[3-6]. The monoaminergic brainstem nuclei may play central roles in mood, psychotic, and autism spectrum disorders[7-10]. Atrophy and lesions of brainstem structures are hallmarks of neurodegenerative and other neurological diseases[5,11]. Despite their importance in human health and disease, the brainstem structures remain markedly understudied.

Magnetic resonance imaging (MRI) studies have revealed cortical and subcortical structural alterations in psychiatric and neurological disorders[12-15], and the discovery of genetic contributions to brain structure variation has begun[16-18]. However, no large-scale neuroimaging study has focused on the genetic architecture of brainstem regions and their involvement in common brain disorders. The unprecedented availability of large imaging genetics resources[19] and recent development of a Bayesian brainstem segmentation algorithm[20] allowed us to estimate the volumes of midbrain, pons, medulla oblongata, superior cerebellar peduncle (SCP, which interconnects the pons and the cerebellum), and the whole brainstem in a large sample. We employed three complementary approaches to increase our knowledge of the genetic underpinnings of brainstem structures and their roles in common brain disorders. First, we conducted genome-wide association studies (GWAS) in healthy individuals to identify genetic loci associated with volumes of the brainstem structures. Second, we used summary statistics from recent large-scale GWAS of common brain disorders to assess genetic overlap between the disorders and volumes of the brainstem regions. Finally, we examined volumes of the brainstem structures in individuals with psychiatric or neurological illnesses in comparison to healthy controls.

Results

We obtained raw T1 3D brain MRI data from a total of *n* = 49,815 individuals, collected through collaborations, data sharing platforms, and from in-house samples (Supplementary Tables 1-2). The MRI data was segmented into the whole brainstem, midbrain, pons, SCP, and medulla oblongata using Freesurfer 6.0[21] and Bayesian brainstem segmentation, robust to differences in MRI scanners and pulse sequence details[20]. We assessed the delineations in all 49,815 data sets by visually inspecting twelve sagittal view figures of the segmentations for each participant (Supplementary Fig. 1). This procedure was conducted blind to case-control status and excluded 13% (*n* = 6,462) of the data sets, mainly due to insufficient field of view, image quality, and segmentation errors in the clinical samples. The final study sample of *n* = 43,353 participants (Supplementary Table 3) comprised healthy participants (*n* = 38,299, age range 3-95 years) and individuals with psychiatric or neurological disorders (*n* = 5,054, age range 5-96 years).

GWAS reveals 61 genetic loci associated with brainstem volumes. The study sample included 27,034 genotyped healthy individuals aged 40-70 years from the UK Biobank[22]. Using MRI and single-nucleotide polymorphism (SNP) data from these participants, we conducted GWAS with PLINK v2.0[23] on volumes of the midbrain, pons, SCP, medulla oblongata, and whole brainstem. All GWAS accounted for age, age², sex, scanning site, intracranial volume (ICV), genotyping batch, and the first ten genetic principal components to control for population stratification. In addition, the GWAS for the midbrain, pons, SCP, and medulla oblongata accounted for whole brainstem volume, thus revealing genetic signals beyond commonality in volume, analogous to a recent study of hippocampal subfields[24]. The GWAS for the brainstem structures were also run without covarying for whole brainstem volume.

SNP-based heritability estimated using LD score regression[25] on the GWAS summary statistics was 32% for the whole brainstem, 29% for the midbrain, 31% for pons, 15% for SCP, and 23% for the medulla oblongata (all s.e. < 5%), illustrating the substantial genetic influence on brainstem volumes (Fig. 1a). We found genome-wide significant hits (P < 5e-8) for all brainstem volumes and identified a total of 125 independent significant SNPs across structures located in 61 genomic loci, using the Functional Mapping and Annotation of GWAS (FUMA) platform v1.3.3c[26] (Fig. 1b-c and Supplementary Table 4). Sixteen genetic loci were associated with whole brainstem volume and 10, 23, 3, and 9 loci were associated with volumes of the midbrain, pons, SCP, and medulla oblongata, respectively. Sixteen loci were associated with more than one brainstem volume, thus resulting in 45 unique brainstem-associated genetic regions. Individual Manhattan and quantile-quantile (Q-Q) plots for each brainstem volume are provided in Supplementary Figs. 2-3. Supplementary Fig. 4 shows regional plots for the most significant genetic locus for each brainstem volume. Heritability estimates and GWAS hits for the brainstem regions without covarying for whole brainstem volume are provided in Supplementary Figs. 5-6 and Supplementary Table 5.

We functionally annotated SNPs across the brainstem volumes that were in linkage disequilibrium ($r^2 \geq 0.6$) with one of the independent significant SNPs using FUMA. A majority of these SNPs were intronic (60.3%) or intergenic (23.7%) and 1.5% were exonic (Supplementary Tables 6-10). About 94% of the SNPs had a minimum chromatin state of 1 to 7, thus suggesting they were in open chromatin regions[27]. Supplementary Fig. 7 provides information for functional SNP categories for each brainstem volume. Two of the lead SNPs were exonic and associated with medulla oblongata (rs13107325) and whole brainstem (rs13388394) volumes. The combined annotation-dependent depletion (CADD) scores of those SNPs were 23.1 (rs13107325) and 17.7 (rs13388394), thus indicating deleterious protein

effects[28]. rs13107325 is located in *SLC39A8* and has previously been associated with multiple traits, including schizophrenia (SCZ) and Parkinson's disease (PD)[29].

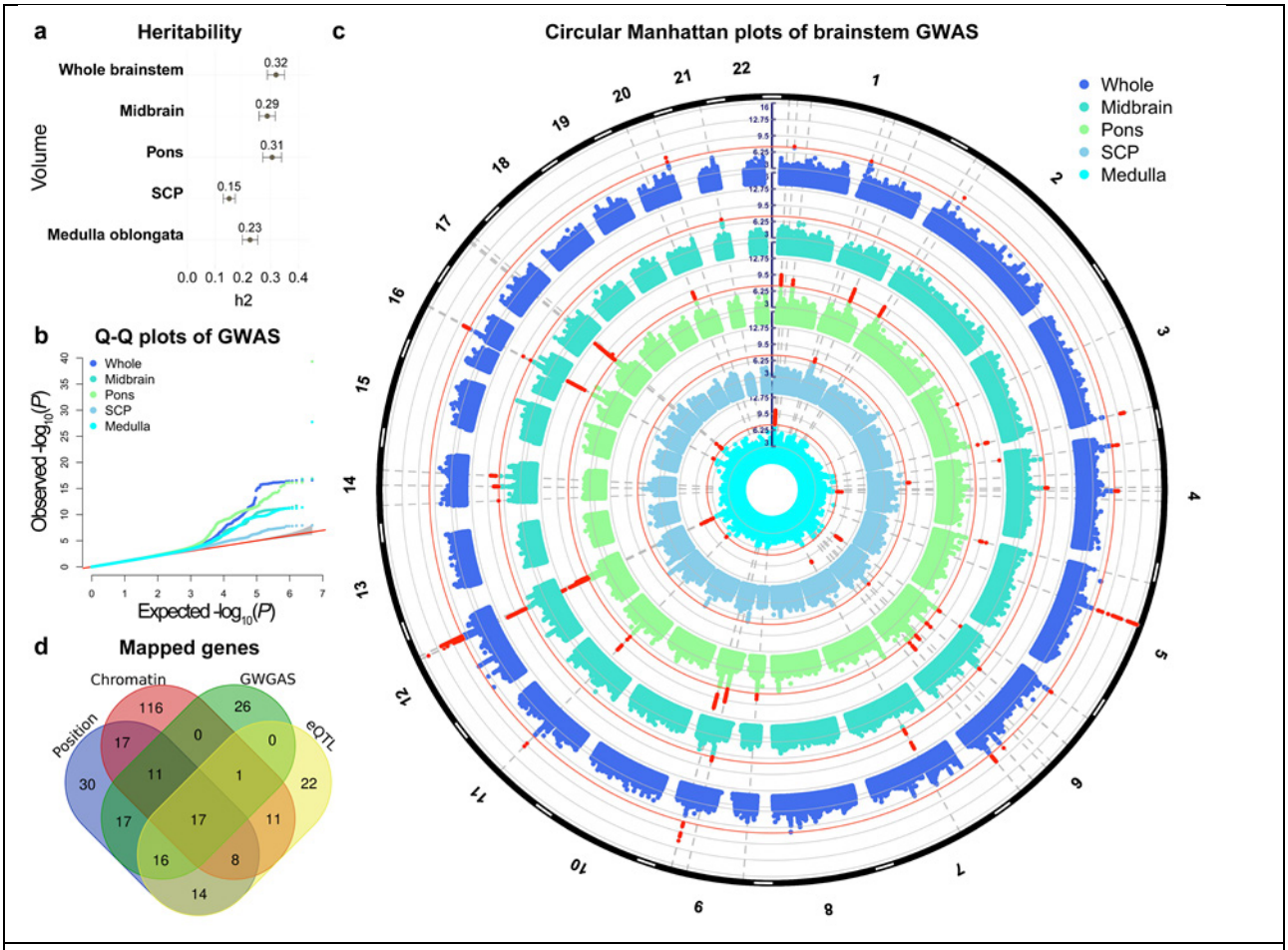

Fig. 1 | GWAS identifies 61 loci associated with brainstem volumes. a, Heritability estimates for the brainstem volumes of n = 27,034 healthy individuals. All brainstem volumes showed substantial heritability, with highest estimates for the whole brainstem (h_2 = 0.32) and pons (h_2 = 0.31) and lowest for the medulla oblongata (h_2 = 0.23) and SCP (h_2 = 0.15). **b**, Q-Q plots for the brainstem volumes. **c**, Circular Manhattan plots of GWAS for brainstem volumes. The outermost plot in blue reflects the GWAS of whole brainstem volume, whereas, from the periphery to center, the turquoise, green, grey/blue, and cyan plots indicate the GWAS of the midbrain, pons, SCP, and medulla oblongata volumes, respectively. Red circular lines indicate genome-wide significance and the red radial lines are significant loci. **d**, Venn diagram showing number of genes mapped by the four different strategies, i.e., positional gene, expression quantitative trait loci (eQTL), and chromatin interaction mapping, and identification by the GWGAS. Seventeen genes were identified by all four approaches. Whole; whole brainstem. SCP; superior cerebellar peduncle. Medulla; medulla oblongata. GW(G)AS; genome-wide (gene-based) association analyses.

Implicated genes and genome-wide gene-based associations. We used positional, expression quantitative trait loci (eQTL), and chromatin interaction mapping in FUMA[26] to map the 125 independent significant SNPs to genes. These three strategies identified 280 unique genes, where 130, 89, and 181 genes were mapped by positional, eQTL, and chromatin interaction mapping, respectively. 168 of these were implicated by one mapping strategy, 68 genes by two strategies, and 25 of the genes were implicated by three strategies (Fig. 1d, and Supplementary Table 11). Supplementary Fig. 8 provides visualisation of mapped genes for each brainstem volume in Circos plots.

We then conducted genome-wide gene-based association analyses (GWGAS) using MAGMA[30] and detected 87 unique genes across the brainstem volumes (Fig. 2 and Supplementary Table 12). Thirty-six were associated with whole brainstem volume and 22, 37, 10, and 17 genes were associated with volumes of the midbrain, pons, SCP, and the medulla oblongata, respectively. Twenty-two of the genes were only associated with whole brainstem volume, whereas 13, 14, 6, 5 genes were only significant for midbrain, pons, SCP, and the medulla oblongata volumes. The most strongly associated gene for each volume identified by the GWGAS was *RFX4* (P = 2.8e-15), *PARPBP* (P = 1.7e-11), *DRAM1* (P = 6.2e-15), *LMX1A* (P = 1.7e-10), and *HOXB3* (P = 2.0e-12) for the whole brainstem, midbrain, pons, SCP, and medulla oblongata, respectively. Supplementary Fig. 9 provides Q-Q plots for these GWGAS. We also found that 25 of the genes identified by GWGAS were not mapped by the GWAS analyses, resulting in a total number of 305 brainstem-linked genes identified by either GWAS or GWGAS. Moreover, supporting robustness, seventeen of the 87 genes identified by the GWGAS were also implicated by all three FUMA mapping strategies (Fig. 1d, Supplementary Table 13).

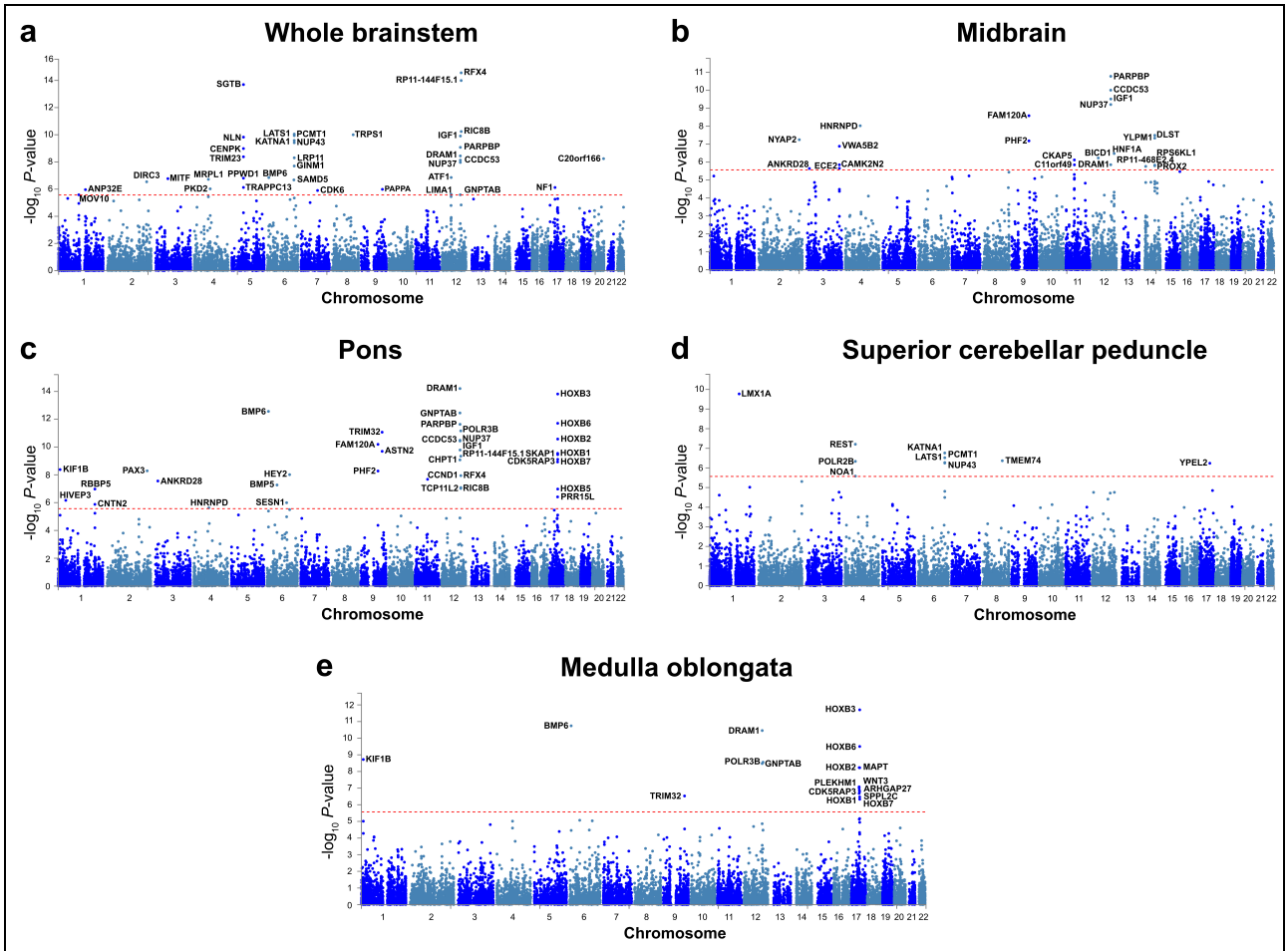

Fig. 2 | Manhattan plots from the genome-wide gene-based association analyses for volumes of the whole brainstem (**a**), midbrain (**b**), pons (**c**), superior cerebellar peduncle (**d**), and medulla oblongata (**e**). Thirty-six genes were associated with whole brainstem volume and 22, 37, 10, and 17 genes were associated with volumes of the midbrain, pons, superior cerebellar peduncle, and the medulla oblongata, respectively. Twenty-two of the genes were only associated with whole brainstem volume, whereas 13, 14, 6, 5 genes were only significant for volumes of the midbrain, pons, superior cerebellar peduncle, and the medulla oblongata. The red horizontal lines indicate genome-wide significance.

Gene sets implicated by the significant genes. We conducted gene sets analyses and identified 78 Gene Ontology sets significantly associated with whole brainstem volume, and 34, 58, 6, and 56 gene sets associated with volumes of the midbrain, pons, SCP, and medulla oblongata, respectively (Supplementary Table 14). The most significant gene set for whole brainstem volume was *natural killer cell mediated immunity* (P = 2.47e-10), *positive regulation of epithelial*

cell proliferation for midbrain (P = 8.97e-06), *anterior posterior pattern specification* for pons (P = 1.68e-11), *imp biosynthetic process* for SCP (P = 4.96e-06), and *embryonic skeletal system development* for medulla oblongata (P = 2.66e-14). Notably, *HOX* genes, which encode transcription factors with central roles in nervous system development[31,32] were included in the nine most significant gene sets for pons and in the 24 gene sets most strongly associated with medulla oblongata. We also employed the ConsensusPathDB[33] to identify over-represented pathways for the mapped genes and found 13, 1, 25, and 58 significant pathways for volumes of the whole brainstem, pons, SCP, and medulla oblongata, respectively (Supplementary Table 15).

Genetic overlap between brainstem volumes and common brain disorders. To further examine the polygenic architecture of brainstem volumes and the potential genetic overlap between brainstem regions and common brain disorders, we used GWAS summary statistics for attention-deficit/hyperactivity disorder (ADHD), autism spectrum disorder (ASD), bipolar disorder (BD), major depression (MD), SCZ, Alzheimer's disease (AD), multiple sclerosis (MS), and PD, as outlined in Methods. We then generated conditional Q-Q plots[34-36] for the brainstem regions and the eight clinical conditions. The conditional Q-Q plots compare the association with one trait (e.g., whole brainstem volume) across all SNPs and within SNPs strata determined by the significance of their association with another trait (e.g., SCZ). Polygenic overlap exists if the proportion of SNPs associated with the first trait increases as a function of the strength of association for the second trait and is visualized as a successive leftward deflection from the null distribution[34]. The conditional Q-Q plots for brainstem volumes and the clinical conditions showed successive increments of SNP enrichment for whole brainstem, midbrain, pons, SCP, and medulla oblongata (Supplementary Fig. 10), consistent with polygenic overlap across volumes

and disorders. Conditional Q-Q plots illustrating the genetic overlap between whole brainstem volume and SCZ, BD, and PD are provided in Fig. 3a-c.

We leveraged the genetic overlap to discover more of the genetic underpinnings of brainstem volumes by employing conditional false discovery rate (FDR) statistics[37,38]. The conditional FDR builds on an empirical Bayesian statistical framework, combines summary statistics from a trait of interest with those of a conditional trait, and thus increases power to detect genetic variants associated with the primary trait. We ran the conditional FDR analyses for each of the brainstem volumes conditioned on the eight disorders and discovered a total of 208 genetic loci for the whole brainstem, and 111, 270, 55, and 125 loci for the midbrain, pons, SCP, and medulla oblongata, respectively. These regions were located in 52 unique genetic loci for whole brainstem volume, and 29, 63, 21, and 25 unique loci for volumes of the midbrain, pons, SCP, and medulla oblongata, respectively (Fig. 3d, Supplementary Tables 16-20). The loci identified by the conditional FDR included all brainstem-associated genetic regions discovered by the GWAS. Supplementary Fig. 11 provides Manhattan plots for the genetic loci detected by the conditional FDR analyses for each brainstem region.

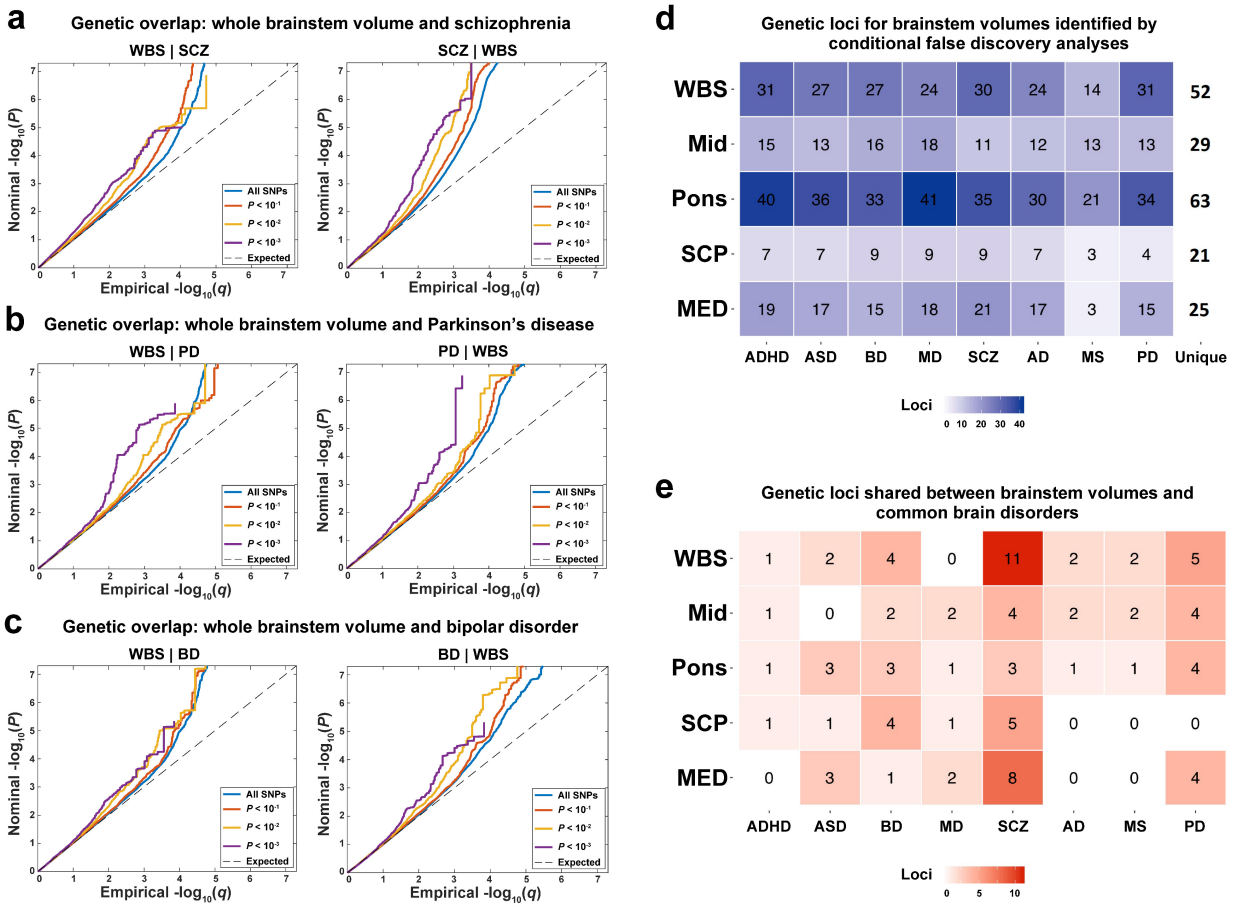

Fig. 3 | **a**, Conditional Q-Q plots for whole brainstem volume conditioned on SCZ (left) and vice versa (right), demonstrating genetic overlap. **b**, Conditional Q-Q plots for whole brainstem volume conditioned on PD (left) and vice versa (right), showing genetic overlap between these phenotypes. **c**, Conditional Q-Q plots for whole brainstem volume conditioned on BD (left) and vice versa (right), demonstrating genetic overlap. **d**, Enhanced discovery of genetic loci for each of the brainstem volumes when conditional false discovery rate analyses were run for each of the brainstem volumes conditioned on the eight brain disorders. These analyses revealed a total of 208 genetic loci for whole brainstem volume, and 111, 270, 55, and 125 loci for volumes of the midbrain, pons, SCP, and medulla oblongata, respectively. These genetic regions were located in 52 unique genetic loci for whole brainstem volume, and 29, 63, 21, and 25 unique loci for volumes of the midbrain, pons, SCP, and medulla oblongata. **e**, conjunctional false discovery rate analysis detected shared genetic loci across brainstem volumes and the eight clinical conditions. The largest numbers of shared loci were found for SCZ (31), BD (14), and PD (17), whereas 8, 4, 6, 9, and 5 genetic loci were jointly shared for ASD, ADHD, MD, AD, and MS, respectively, and the brainstem volumes. WBS; whole brainstem. MID; midbrain. SCP; superior cerebellar peduncle. MED; medulla oblongata. ADHD; attention-deficit/hyperactivity disorder. ASD; autism spectrum disorders. BD; bipolar disorder. MD; major depression. SCZ; schizophrenia. AD; Alzheimer's disease. MS; multiple sclerosis. PD; Parkinson's disease.

To further characterize the genetic overlap between brainstem volumes and the eight clinical conditions, we performed conjunctional FDR analyses, which enable detection of genetic loci shared between two phenotypes[34-36]. These analyses revealed shared loci across the brainstem structures and the clinical conditions (Fig. 3e). We found the largest number of loci shared between brainstem volumes and SCZ (31), BD (14), and PD (17). For ASD, ADHD, MD, AD, and MS, there were 9, 4, 6, 5, and 5 genetic loci jointly associated with the brainstem volumes and the disorders, respectively (Fig. 3e). Notably, the shared genetic loci exhibited a mixed pattern of allelic effect directions, i.e., disorder-linked genetic variants were associated with both larger and smaller brainstem volumes. Manhattan plots and details for the genetic loci shared between the eight clinical conditions and the brainstem volumes are provided in Fig. 4a-h and in Supplementary Table 21.

We ran Gene Ontology gene sets analyses for genes nearest to the shared loci across the brainstem regions for each disorder and found 33 significant gene sets for SCZ, mainly involving central nervous system, neuronal, and cellular developmental processes (Supplementary Table 22). There were no significant gene sets for the other disorders.

We also examined genetic correlations between brainstem volumes and the common brain disorders using LD score regression[25] (Supplementary Fig. 12). There were correlations with uncorrected $P < 0.05$, including positive associations between brainstem volumes and PD, yet these were not significant after multiple testing corrections.

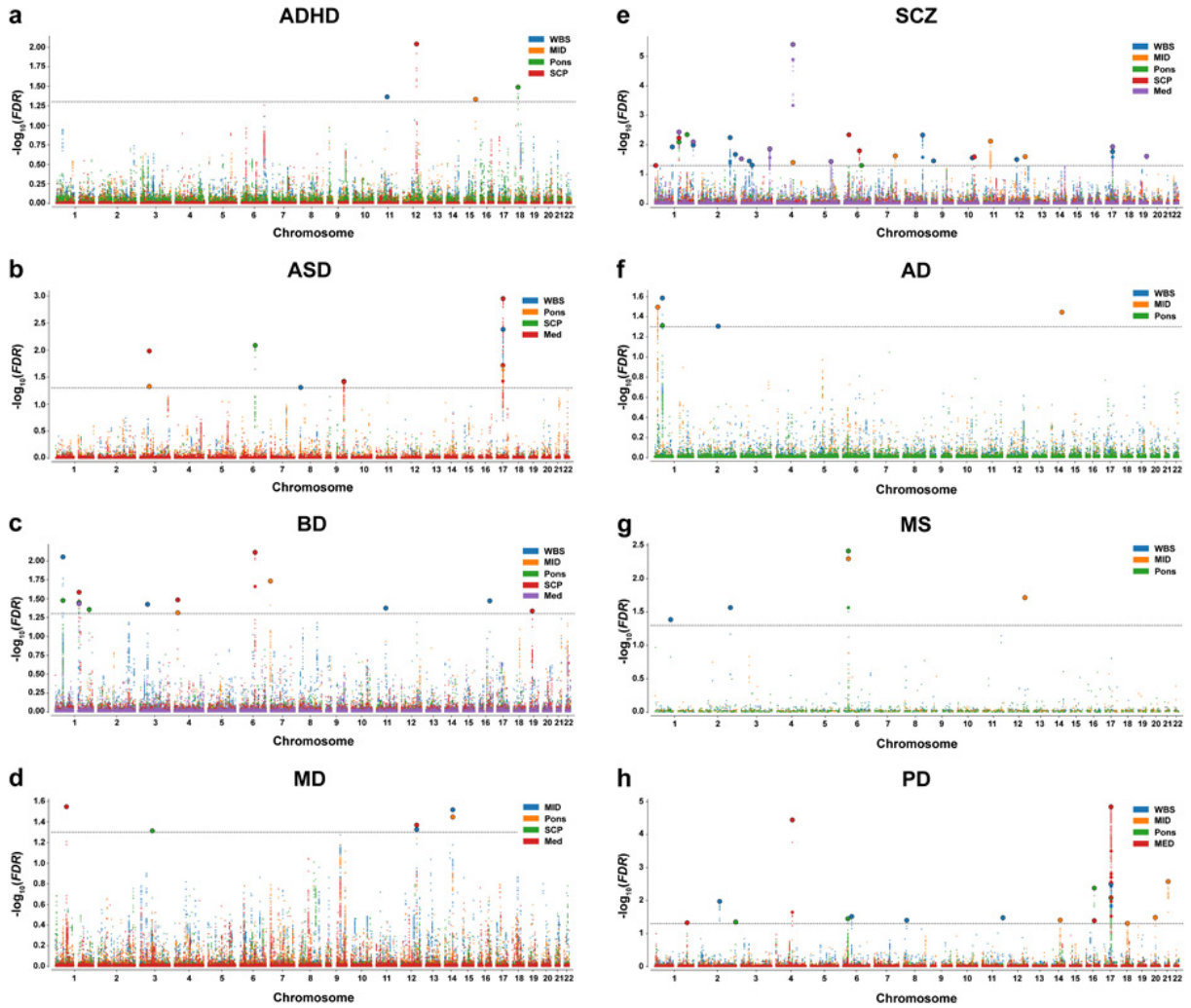

Fig. 4 | Manhattan plots for genetic loci shared between brainstem volumes and eight common brain disorders: **a**, 4 shared loci in ADHD, **b**, 9 shared loci in ASD, **c**, 14 shared loci in BD, **d**, 6 shared loci in MD, **e**, 31 shared loci in SCZ, **f**, 5 shared loci in AD, **g**, 5 shared loci in MS, and **h**, 17 shared loci in PD. WBS; whole brainstem. MID; midbrain. SCP; superior cerebellar peduncle. MED; medulla oblongata. ADHD; attention-deficit/hyperactivity disorder. ASD; autism spectrum disorders. BD; bipolar disorder. MD; major depression. SCZ; schizophrenia. AD; Alzheimer's disease. MS; multiple sclerosis. PD; Parkinson's disease.

Brainstem volumes in common brain disorders. We compared brainstem volumes between individuals with common brain disorders and healthy controls (HC) (age range 5-96 years): ADHD (n = 681 patients/n = 992 HC), ASD (n = 125/n = 140), BD (n = 464/n = 1,513), major depressive disorder (MDD; n = 211/n = 93), SCZ (n = 1,044/n = 2,079), prodromal SCZ or at risk

mental state (SCZRISK; n = 91/n = 402), non-SCZ psychosis spectrum diagnoses (PSYMIX; n = 308/n = 1,430), dementia (n = 756/n = 1,921), mild cognitive impairment (MCI; n = 987/n = 1,655), MS (n = 257/n = 1,053), and PD (n = 138/n = 67). Supplementary Tables 1-3 provide information on the individual cohorts. Linear models were run covarying for sex, age, age², ICV, and scanner site using R[39]. The analyses for volumes of midbrain, pons, SCP, and medulla oblongata were run both with and without covarying for whole brainstem volume, and were adjusted for multiple testing using FDR (Benjamini-Hochberg, accounting for all 99 tests). Fig. 5 depicts the resulting case-control differences.

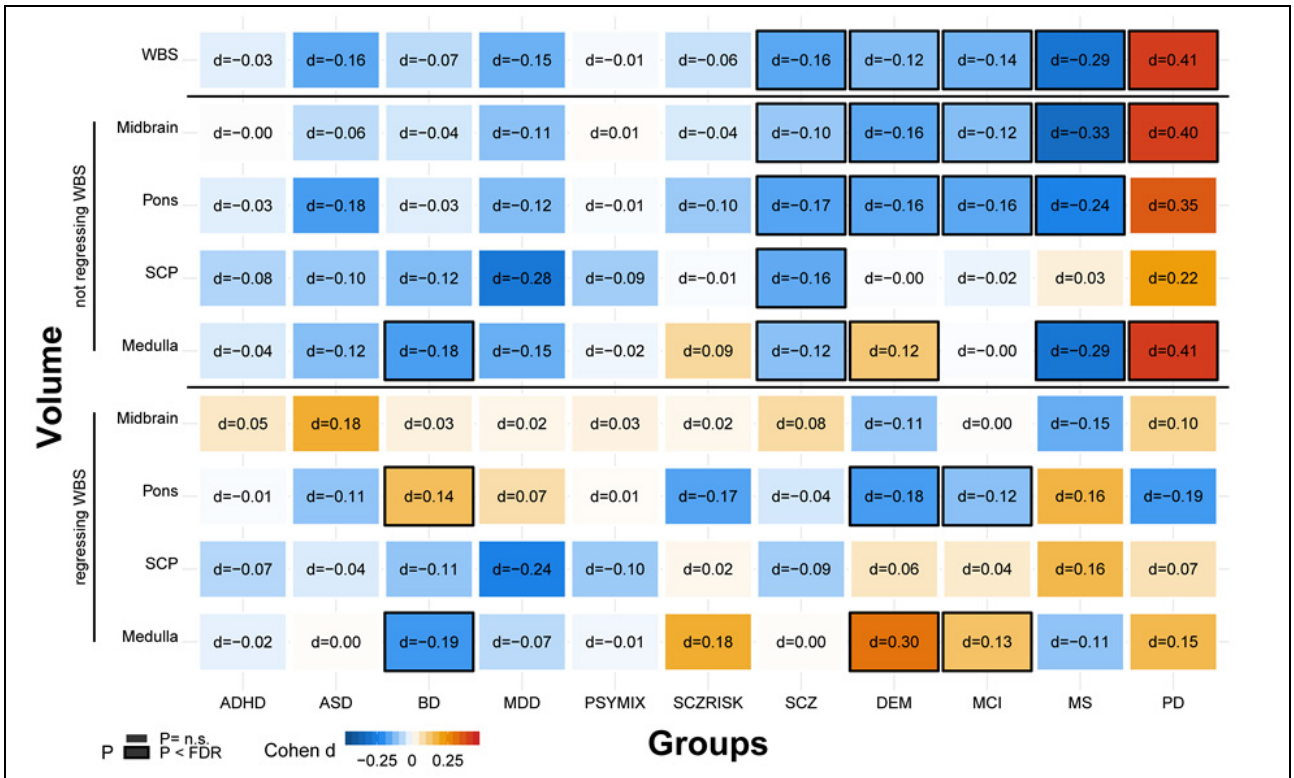

Fig. 5 | Volumes of brainstem structures in individuals with common brain disorders compared to healthy controls. There were differential volumetric alterations in individuals with BD, SCZ, DEM, MCI, MS, and PD after adjusting for multiple testing. ADHD; attention-deficit/hyperactivity disorder. ASD; autism spectrum disorders. BD; bipolar disorder. MDD; major depressive disorder. PSYMIX; non-SCZ psychosis spectrum diagnoses. SCZRISK; prodromal SCZ or at risk mental state. SCZ; schizophrenia. DEM; dementia. MCI; mild cognitive impairment. MS; multiple sclerosis. PD; Parkinson's disease. WBS; whole brainstem. SCP; superior cerebellar peduncle. Medulla; medulla oblongata.

BD was associated with smaller medulla oblongata volume and larger pons volume, when accounting for the whole brainstem. Individuals with SCZ showed smaller volumes of all brainstem structures compared to HC, but not significantly for the midbrain, pons, and medulla oblongata when regressing out whole brainstem volume, consistent with a general effect across the brainstem regions. Volumes of whole brainstem, midbrain, and pons were smaller in the individuals with dementia compared to HC, whereas medulla oblongata volume was larger. A highly similar pattern was found for individuals with MCI, with smaller volumes of the whole brainstem, midbrain, and pons, and larger medulla oblongata volume when accounting for whole brainstem. Individuals with MS showed smaller volumes of the whole brainstem, midbrain, pons, and medulla oblongata, whereas individuals with PD had larger volume of the whole brainstem, midbrain, and medulla oblongata.

We ran further analyses of associations between brainstem volumes and clinical characteristics in the individuals with MCI, dementia, MS, SCZ, and PD and details of these analyses are provided in Supplementary Figs. 13-14. There were significant associations between Mini-Mental State Examination[40] scores and brainstem volumes in dementia and MCI, indicating smaller pons and larger medulla oblongata volumes in more severely affected individuals (all $P <$ 2e-04). In MS, there were brainstem volume decreases also in the subgroup of patients without infratentorial lesions (n = 91; all $P < 0.05$) and significant negative associations between the Expanded Disability Status Scale[41] scores and brainstem volumes in patients with infratentorial lesions (n = 153; $P < 0.05$). There was no significant association between the Global Assessment of Functioning scale[42] or Positive and Negative Syndrome Scale[43] scores and brainstem volumes in individuals with SCZ. We found no evidence for tremor severity influencing brainstem volumes in individuals with PD.

Discussion

The midbrain, pons, and medulla oblongata have central roles in human health and disease, yet no large-scale neuroimaging study has focused on their structure and genetic underpinnings. Here, we discovered novel genetic loci associated with brainstem volumes and found genetic overlap with eight psychiatric and neurological disorders, revealing that the brainstem may play important roles in common brain disorders. Indeed, leveraging clinical imaging data we found differential alterations of brainstem volumes in individuals with SCZ, BD, MS, dementia, MCI, and PD.

We identified 61 genetic loci associated with brainstem volumes using GWAS. Sixteen of these loci were associated with more than one volume, thus resulting in 45 unique brainstem-associated genetic regions. There is to our knowledge no previous study of the genetic underpinnings of midbrain, pons, SCP, and medulla oblongata volumes, yet a recent landmark study of ~8,400 individuals in UK Biobank identified four SNPs on chromosomes four (rs10027331), nine (rs10983069), 11 (rs10792032), and 12 (rs11111090) associated with Freesurfer-based volume of the whole brainstem[44]. These SNPs are within four of the genetic loci linked to whole brainstem volume in the present study.

The brainstem volume-associated genetic loci detected by the GWAS of this study were linked to 305 genes. Seventeen of these genes were identified by both the GWGAS and by all three FUMA mapping strategies (Supplementary Table 13). Among these genes, *MAPT*, *KIF1B*, *KATNA1*, *NLN,* and *SGTB* are notable. *MAPT* encodes tau protein, which is produced throughout neurons of the brain[45]. Accumulation of tau is a hallmark of the neurodegenerative tauopathies, including AD and frontotemporal dementia[45]. *MAPT* has also been linked to PD[46] and rare mutations and common variants of *MAPT* increase progressive supranuclear palsy risk, where brainstem volume loss is a central disease characteristic[47]. *KIF1B* is involved in axonal transport

of mitochondria and synaptic vesicles and plays important roles in development of myelinated axons[48]. Loss of the gene results in impaired development of brainstem nuclei and impaired formation of synapses in the mouse spinal cord[49]. *KATNA1* is implicated in axon outgrowth regulation[50] and neuronal migration during development[51]. *NLN* regulates neurotensin signaling[52], which has been linked to the pathophysiology of psychiatric and neurological disorders, including SCZ and PD[53,54]. The most significant locus for whole brainstem volume was mapped to *SGTB*, which is expressed at high levels in the brain and promotes neuronal differentiation and neurite outgrowth[55]. Although further studies are needed to clarify the relationship between these genes and brainstem structures, their implication by both the GWGAS and the three FUMA mapping approaches are suggestive of a role in brainstem volume variation.

The Gene Ontology gene sets analyses of the GWAS findings showed that *HOX* genes were included in the nine most significant gene sets for pons and in the 24 gene sets most strongly associated with medulla oblongata volume. In addition, nine *HOX* genes (*HOXB1-9*) were associated with volumes of both pons and medulla oblongata in the GWGAS. *HOX* genes encode Hox proteins, which are transcription factors with central roles in nervous system development[31,32]. The *HOXB1-4* genes are critical for the development of the embryonic hindbrain, which gives rise to the pons, the medulla oblongata, and the cerebellum[32]. For example, *HOXB1* mutations can cause congenital bilateral facial palsy, hearing loss, and strabismus[56]. The *HOX* genes are not, however, expressed in the embryonic midbrain, which develops into the midbrain. Consistent with the embryonic genetic division between the hindbrain and the midbrain, *HOX* genes were not associated with the midbrain in the gene sets or in the GWGAS analyses of the current study.

There was polygenic overlap between the brainstem regions and the eight psychiatric and neurological disorders of the present study. We leveraged the genetic overlap to uncover more of

the genetic architecture of the brainstem volumes and identified 52, 29, 63, 21, and 25 loci associated with volumes of the whole brainstem, midbrain, pons, SCP, and medulla oblongata, respectively, using conditional FDR. These loci included all brainstem-associated genetic regions identified by the GWAS. The polygenic overlap also indicates a role for brainstem regions in common brain disorders and gene sets analyses implicated cellular and neurodevelopmental processes in the genetic loci shared with SCZ.

Further studies of how the overlapping genetic regions influence brainstem structure and the risk for common brain disorders are warranted, yet several of the shared loci are noteworthy. The most significant shared locus for SCZ and the second-most significant shared locus for PD was rs13107325, which was associated with midbrain volume in SCZ and medulla oblongata volume in both disorders. rs13107325 is located in the metal ion transporter gene *SLC39A8*. We also found that rs4845679 was jointly associated with volumes of pons, SCP, and medulla oblongata and both SCZ and BD. The nearest gene for rs4845679 is *KCNN3*, which is expressed at high levels in the adult brain and encodes a protein that contributes to the afterhyperpolarization in neurons[57]. The most significant locus for ASD was rs9891103, which was jointly associated with whole brainstem volume, and its nearest gene was *MAPT*. rs8070942 and rs3865315 were shared between ASD and SCZ, respectively, and medulla oblongata volume. The nearest gene for these SNPs was *KANSL1*, which is expressed in the brain and encodes a nuclear protein involved in histone acetylation[58].

We also found that the genetic loci shared between brainstem structures and the brain disorders exhibited a mixed pattern of allelic effect directions, i.e., disorder-linked genetic variants were associated with both larger (same effect direction) and smaller (opposite effect direction) brainstem volumes. A consistent direction of effect across overlapping genetic loci is a requirement for a significant genetic correlation as assessed using LD score regression[25]. For

example, a recent study showed that SCZ and educational attainment may share >8K causal genetic variants, yet their genetic correlation is close to zero due to shared variants with opposite effect directions[59]. Thus, a mixed pattern of allelic effect directions might be one explanation for the lack of robust genetic correlations between the brainstem volumes and the disorders in the present study.

We detected brainstem volume differences between individuals with SCZ, BD, dementia, MCI, MS, and PD and their respective HC groups. The monoaminergic nuclei of the brainstem are implicated in psychotic and mood disorders[4,60-63], yet there are few volumetric studies of brainstem regions in these illnesses. The results of the present study suggest a general volume decrease across brainstem regions in SCZ, consistent with previous studies of the whole brainstem[64,65]. BD, on the other hand, was associated with reduced volume of the medulla oblongata and a relative sparing or even increase of pons volume in the current study. Whether brainstem differences in SCZ and BD are genetically mediated and involved in the development of these disorders or illness effects that emerge during the course of the diseases mandates future studies.

Compared to healthy peers, individuals with dementia showed smaller volumes of the midbrain and pons and larger relative volume of medulla oblongata. Notably, we found a highly similar pattern in individuals with MCI. To our knowledge, there is no previous study showing reduced brainstem volumes in MCI, although one recent report found greater whole brainstem volume reduction over one year in individuals with MCI that converted to dementia than in those who did not convert[66]. There is a scarcity of structural brainstem studies in dementia, yet the results of the present study are consistent with a few previous findings suggesting volume decreases mainly in midbrain and pons in dementia[20,67,68]. Here, we extend these findings to MCI, thus suggesting that structural midbrain and pons alterations could be present in the early phases

of dementia. The smaller volumes of whole brainstem, midbrain, pons, and the medulla oblongata in individuals with MS are consistent with the limited number of previous volumetric brainstem studies of the disorder[69-71].

We found larger volumes of the whole brainstem, midbrain, and medulla oblongata in the individuals with PD. There was no indication that tremor severity could explain the volume increases. Notably, some previous studies detected enlargement of the brainstem and other brain structures in PD[72-74] and the individuals with PD of the present study were in the early phase of the disorder and none used anti-Parkinson drugs. However, the PD sample was small and replication studies are needed to further explore how clinical characteristics, such as disorder phase and medication use, and potential confounds, including within-scanner motion, may factor into measurements of brainstem volumes in PD.

The resolution of the MRI data of the present study does not allow for analyses of individual brainstem nuclei. We also note that the effect sizes for the brainstem changes in the brain disorders of this study were small to moderate. However, larger effect sizes might be revealed in future studies of brainstem nuclei and the effects observed in the present study should not be interpreted as clinically insignificant. Rather, the findings of this study highlight the potential importance of the brainstem across psychiatric and neurological disorders and should stimulate research efforts to further clarify the roles of brainstem subregions in the etiologies and treatments of common brain disorders.

In summary, the current study provides new insights into the genetic architecture of brainstem regions, identifies the first genetic loci linked to volumes of the midbrain, pons, SCP, and the medulla oblongata, and shows genetic and imaging evidence for an involvement of brainstem regions in common brain disorders. Altogether, these findings encourage further studies of brainstem structures in human health and disease.

Supplementary figures

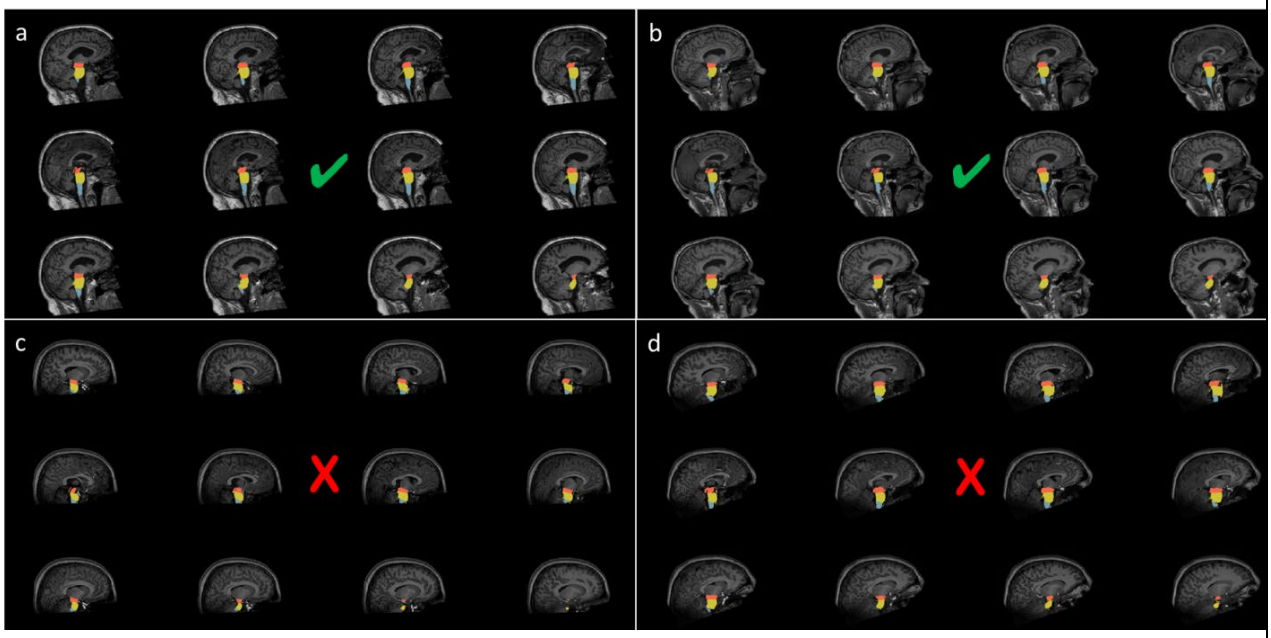

Supplementary Fig. 1 | We manually assessed the delineations in all magnetic resonance imaging data sets (n = 49,815) by visually inspecting twelve sagittal view figures of the segmentations for each participant, as illustrated in **a**-**d**. **a** and **b** are examples of two datasets included in the study, whereas **c** and **d** are data sets excluded due to insufficient field of view (FOV). Data sets were excluded from the study if one of the following requirements was not met: 1. the field of view included the whole brainstem, 2. the superior boundary of the midbrain approximated an axial plane through the mammillary body and the superior edge of the quadrigeminal plate, 3. the boundary between mibrain and pons approximated an axial plane through the superior pontine notch and the inferior edge of the quadrigeminal plate, 4. the boundary between between pons and medulla oblongata approximated an axial plane at the level of the inferior potine notch, 5. the inferior boundary of the medulla oblongata approximated an axial plane at the level of the posterior rim of the foramen magnum, 6. there were no substantial segmentation errors for the anterior and posterior boundaries of midbrain, pons, and medulla oblongata, and 7. the superior boundary of the SCP approximated the inferior boundary of the midbrain tectum, the inferior boundary of the SCP was defined by the merging with the cerebellum, and the anterior boundary of the SCP was defined by the posterior boundary of the pons.This visual quality control procedure excluded 13% (n = 6,462) of the data sets, mainly due to insufficient FOV, image quality, and segmentation errors in the clinical samples. SCP; superior cerebellar peduncle.

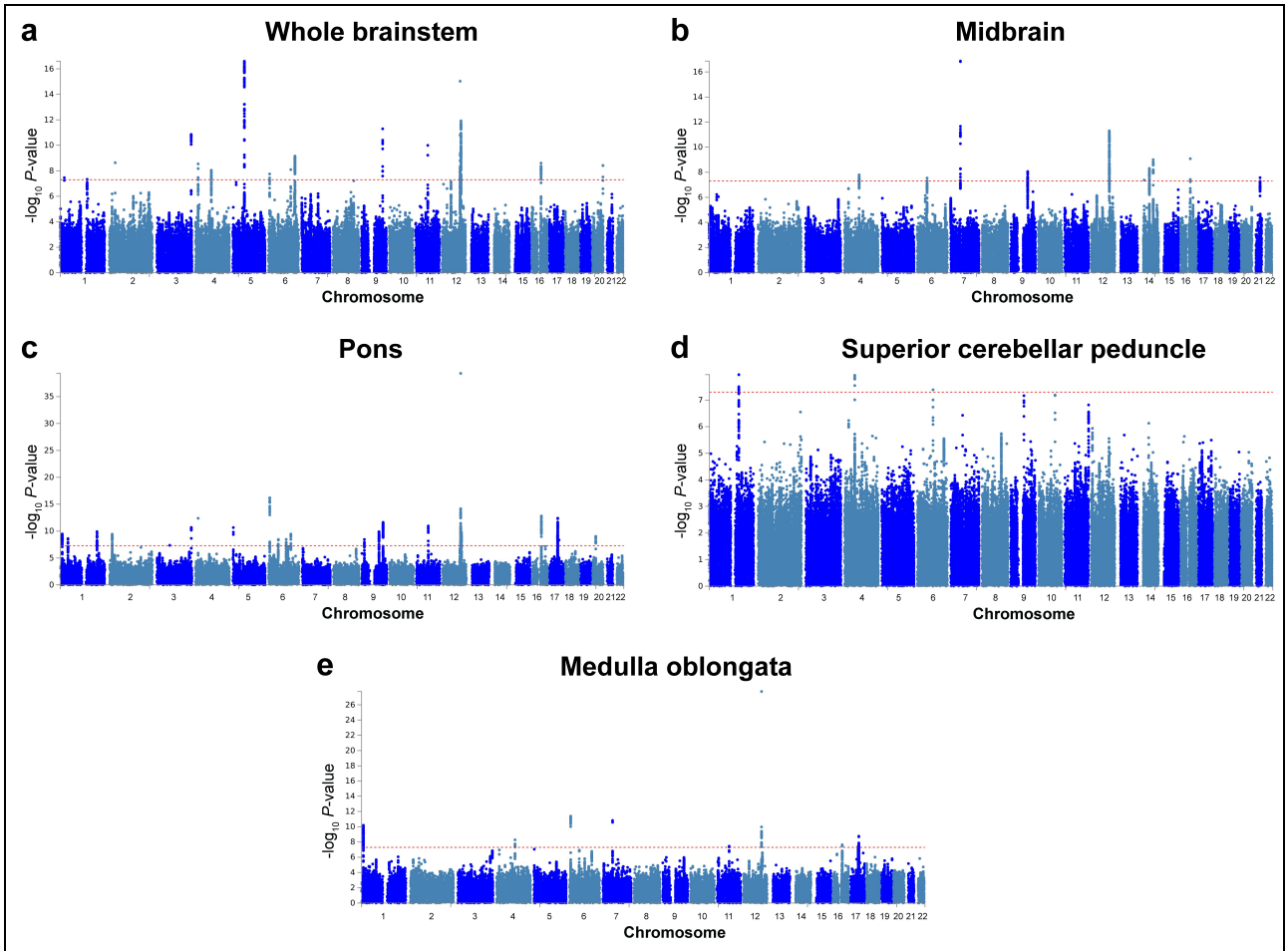

Supplementary Fig. 2 | Manhattan plots for volumes of the whole brainstem (**a**), midbrain (**b**), pons (**c**), superior cerebellar peduncle (d), and medulla oblongata (e) from the genome-wide association studies. 16 genetic loci were associated with whole brainstem volume and 10, 23, 3, and 9 loci were associated with volumes of the midbrain, pons, superior cerebellar peduncle, and medulla oblongata, respectively. The red horizontal lines indicate genome-wide significance.

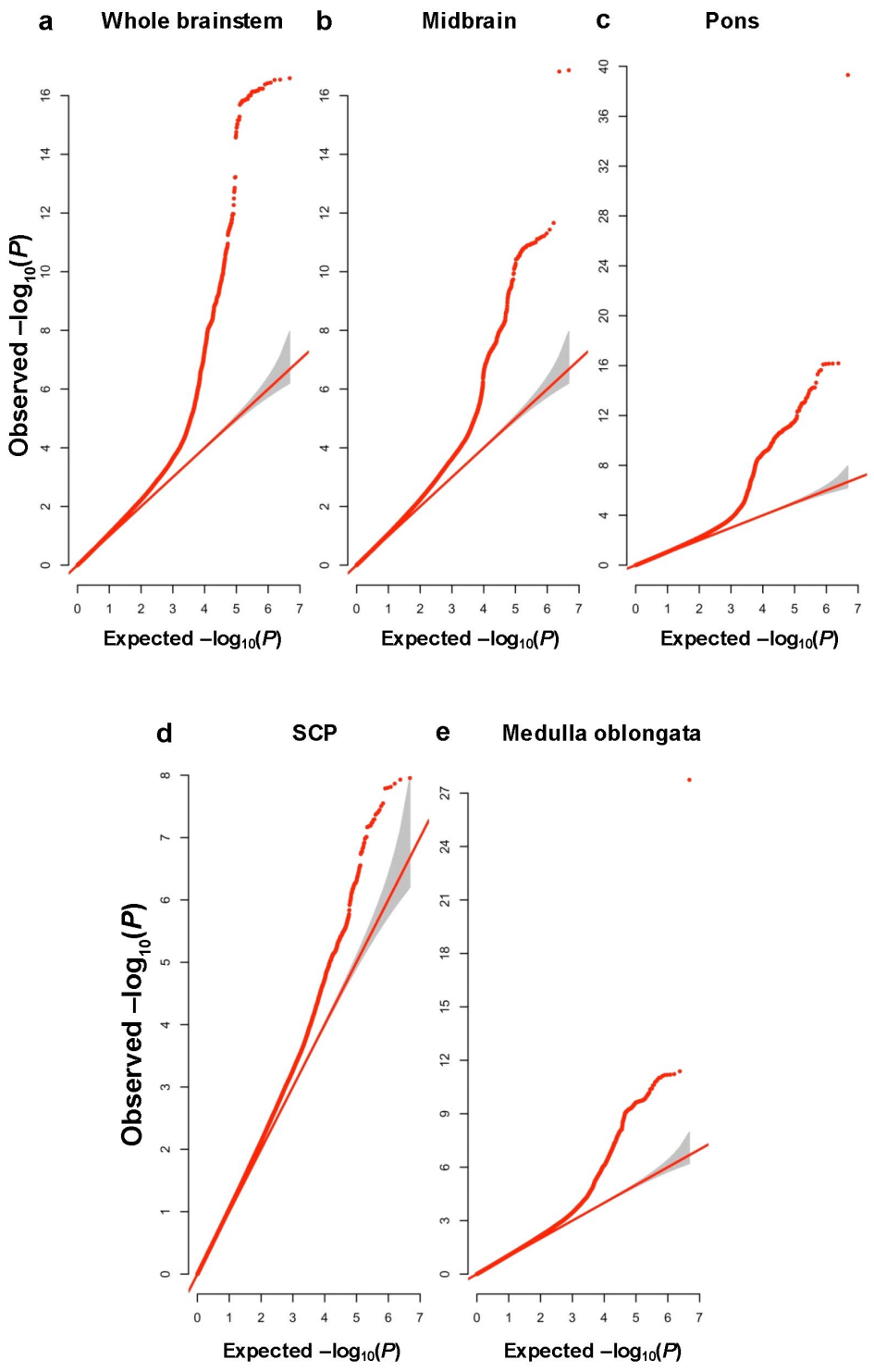

Supplementary Fig. 3 | Q-Q plots for volumes of the whole brainstem (**a**), midbrain (**b**), pons (**c**), superior cerebellar peduncle (**d**), and medulla oblongata (**e**) from the genome-wide association studies. SCP; superior cerebellar peduncle.

a **Whole brainstem-associated locus at chromosome 5**

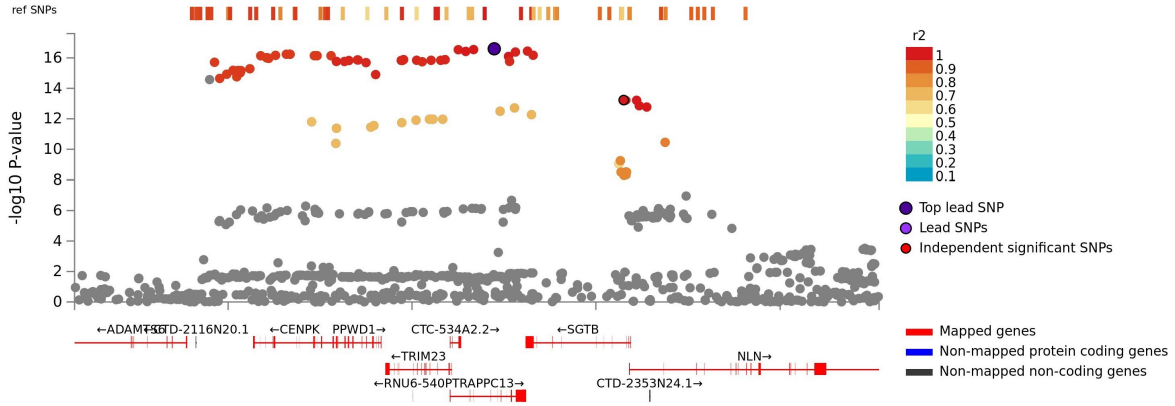

b **Midbrain-associated locus at chromosome 7**

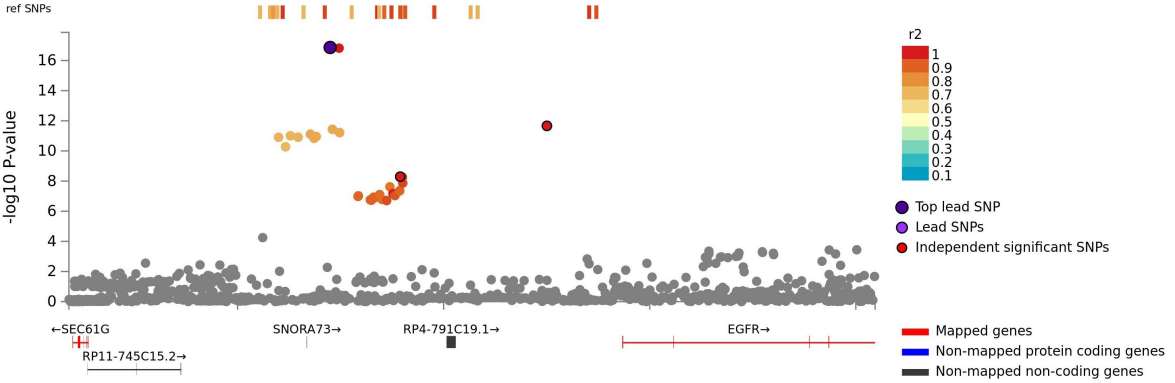

c **Pons-associated locus at chromosome 12**

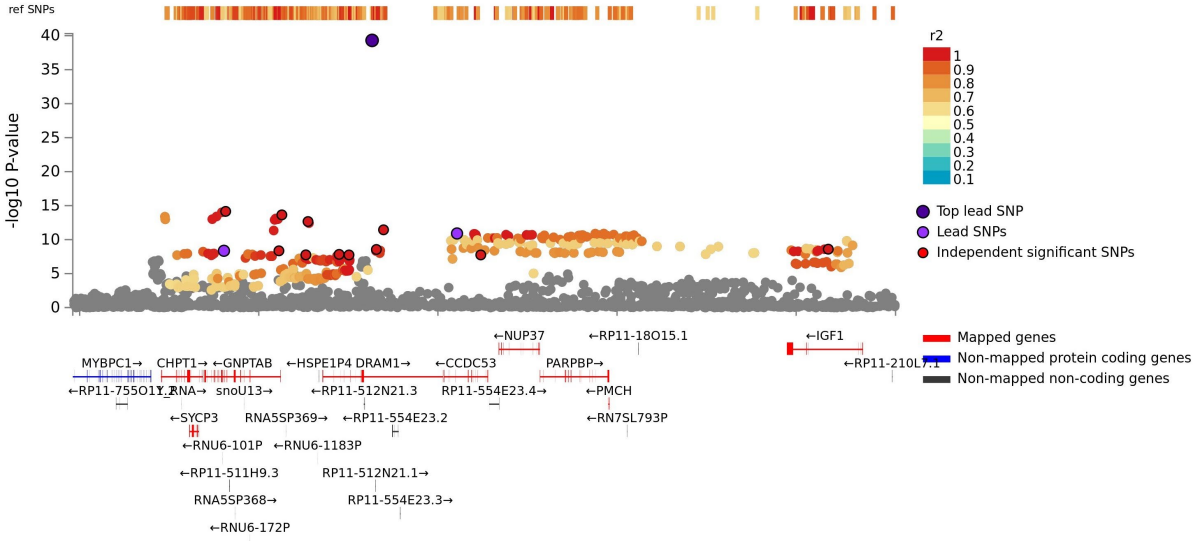

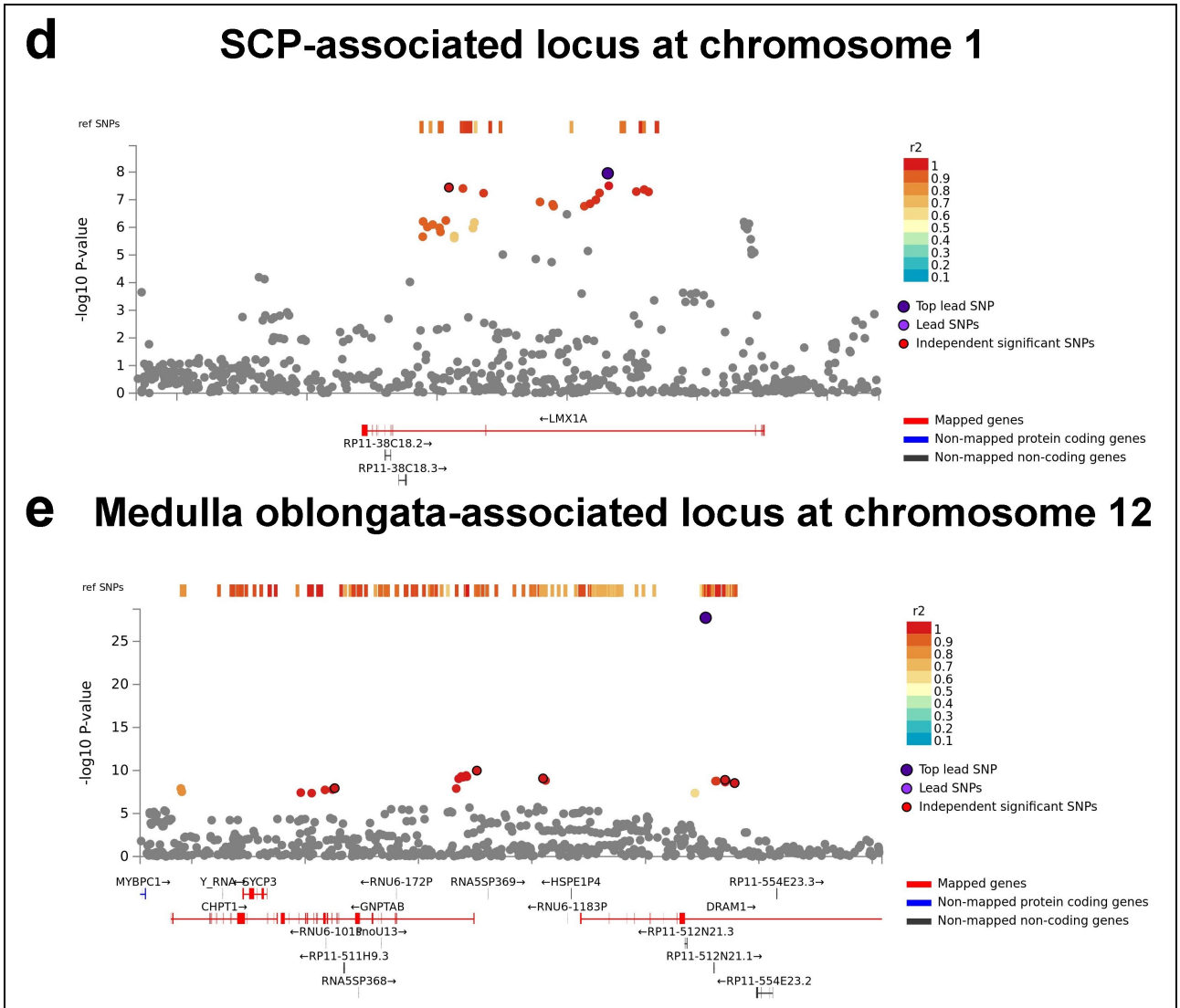

Supplementary Fig. 4 | Regional plots for the most significant genetic locus from the genome-wide association studies for volumes of the whole brainstem at chromosome 5 (**a**), midbrain at chromosome 7 (**b**), pons at chromosome 12 (**c**), superior cerebellar peduncle at chromosome 1 (**d**), and medulla oblongata at chromosome 12 (**e**). SCP; superior cerebellar peduncle.

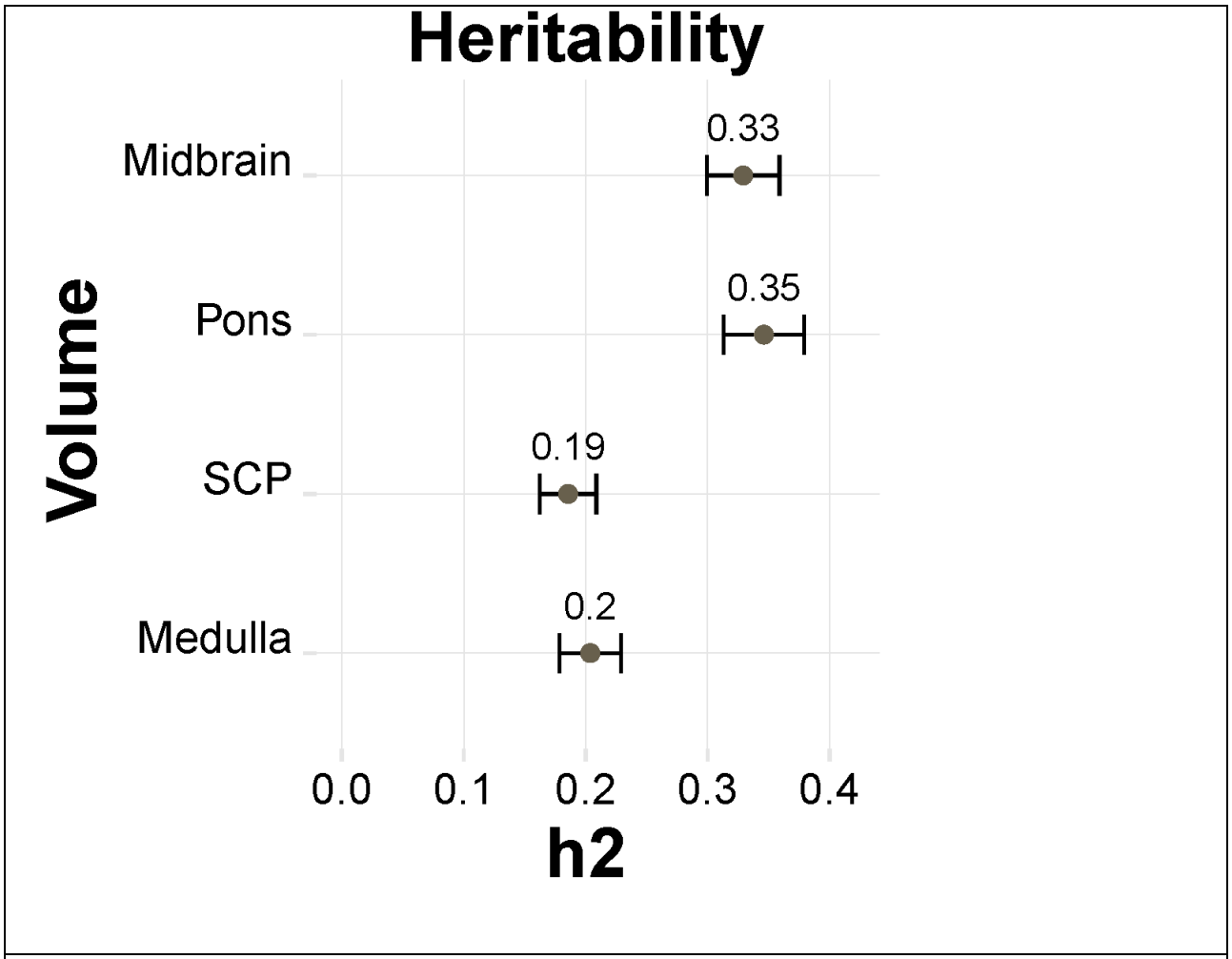

Supplementary Fig. 5 | Heritability estimates for the brainstem volumes of n = 27,034 healthy individuals when not accounting for the whole brainstem. All brainstem volumes showed substantial heritability, which highest estimates for the midbrain (h_2 = 0.33) and pons (h_2 = 0.35) and lowest for the medulla oblongata (h_2 = 0.20) and SCP (h_2 = 0.19). SCP; superior cerebellar peduncle.

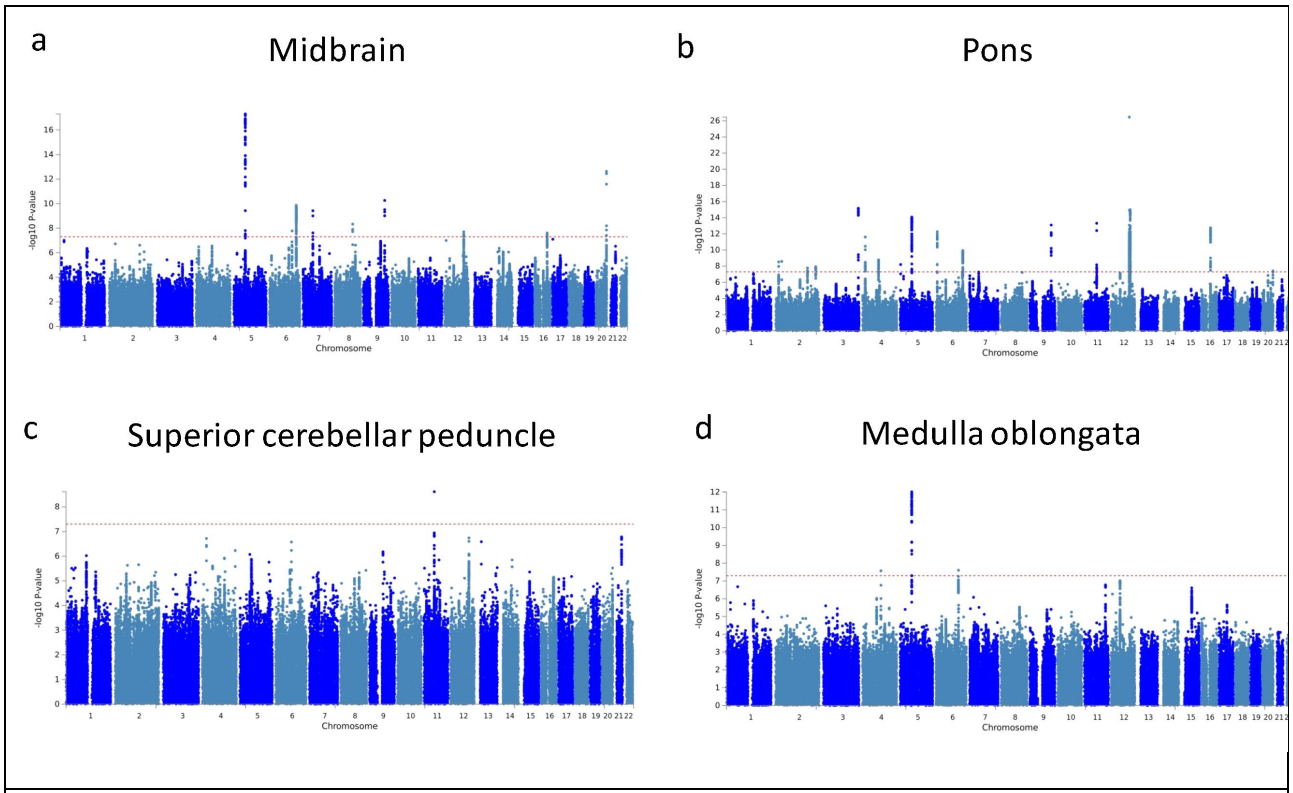

Supplementary Fig. 6 | Manhattan plots for volumes of the midbrain (**a**), pons (**b**), superior cerebellar peduncle (**c**), and medulla oblongata (**d**) from the genome-wide association studies when not accounting for whole brainstem volume. The red horizontal lines indicate genome-wide significance. Additional information for the significant loci is provided in Supplementary Table 5.

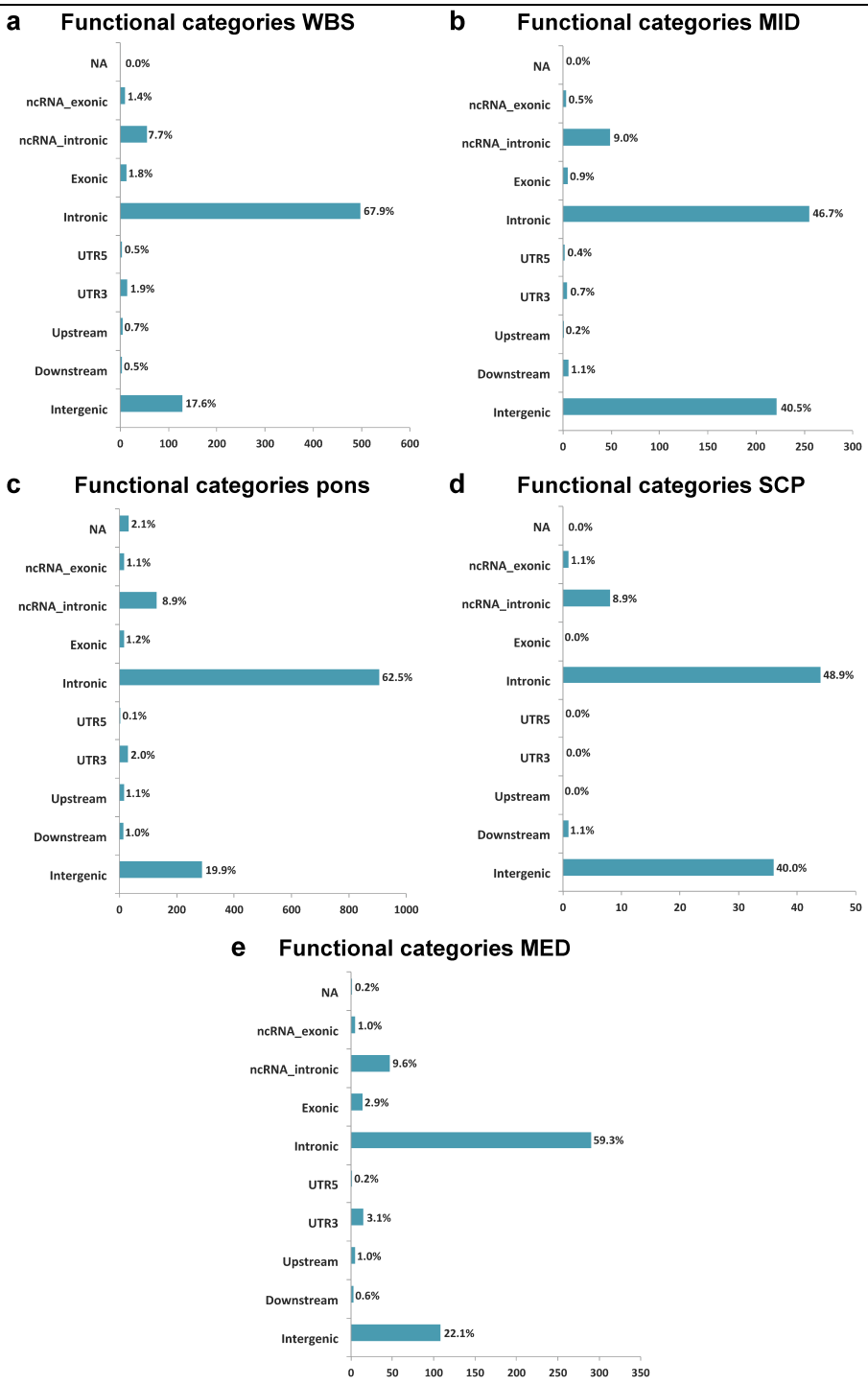

Supplementary Fig. 7 | Functional single-nucleotide polymorphism categories from the genome-wide association studies for volumes of the whole brainstem (**a**), midbrain (**b**), pons (**c**), superior cerebellar peduncle (**d**), and medulla oblongata (**e**). WBS; whole brainstem. MID; midbrain. SCP; superior cerebellar peduncle. MED; medulla oblongata. UTR; untranslated region.

a **Loci for whole brainstem at chromosome 12**

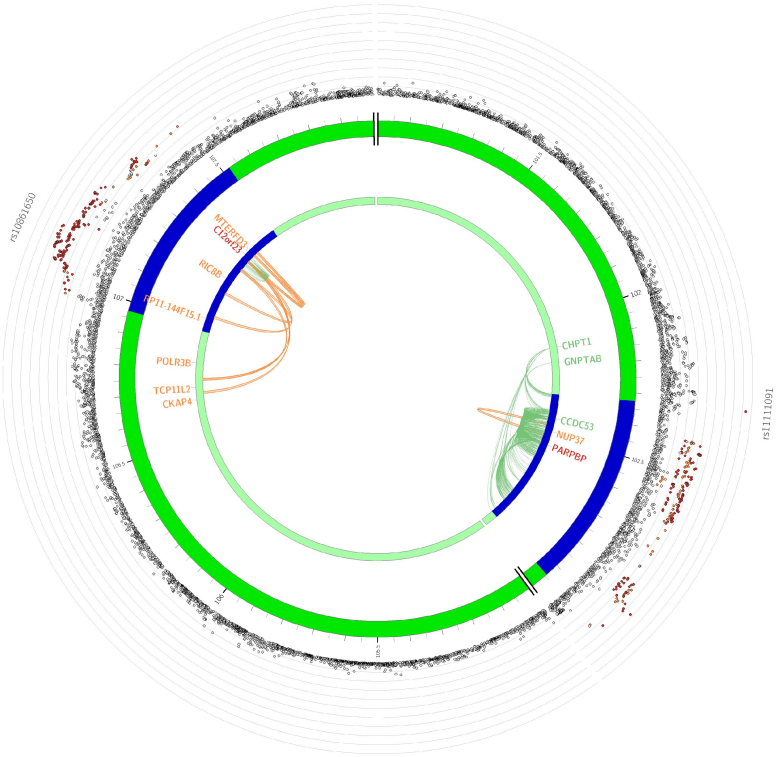

b **Loci for midbrain at chromosome 14**

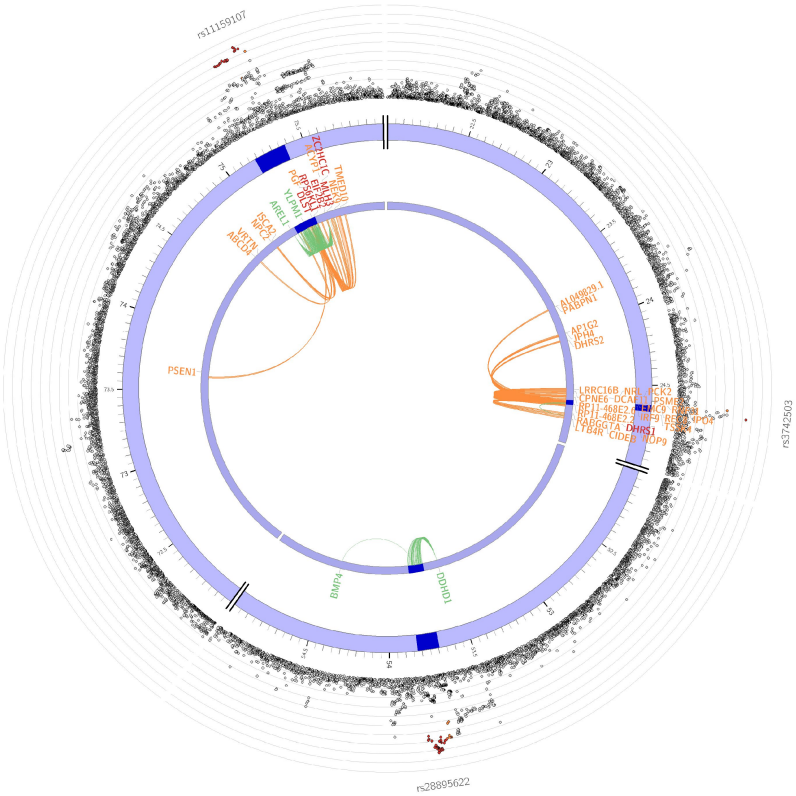

c **Loci for pons at chromosome 1**

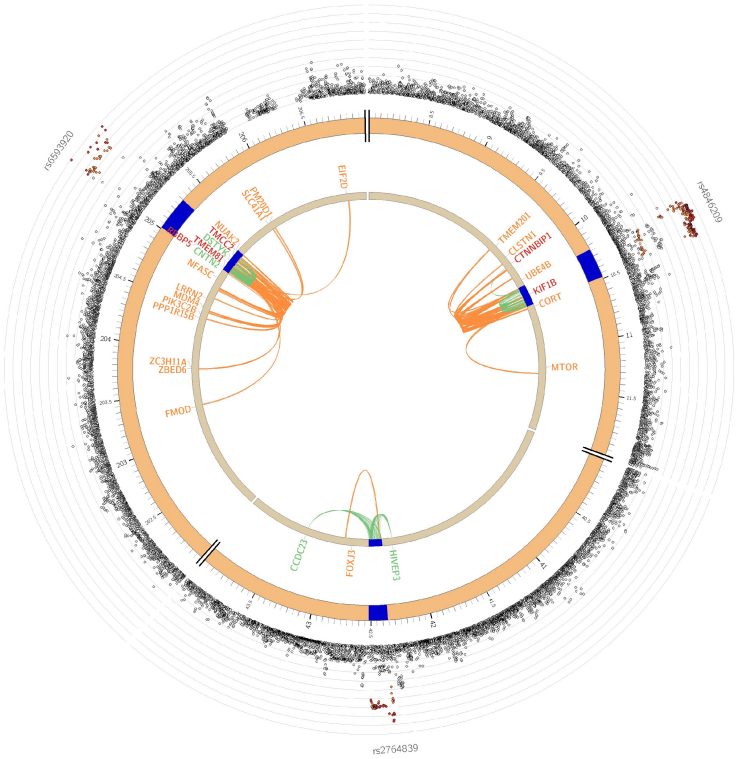

d **Loci for SCP at chromosome 4**

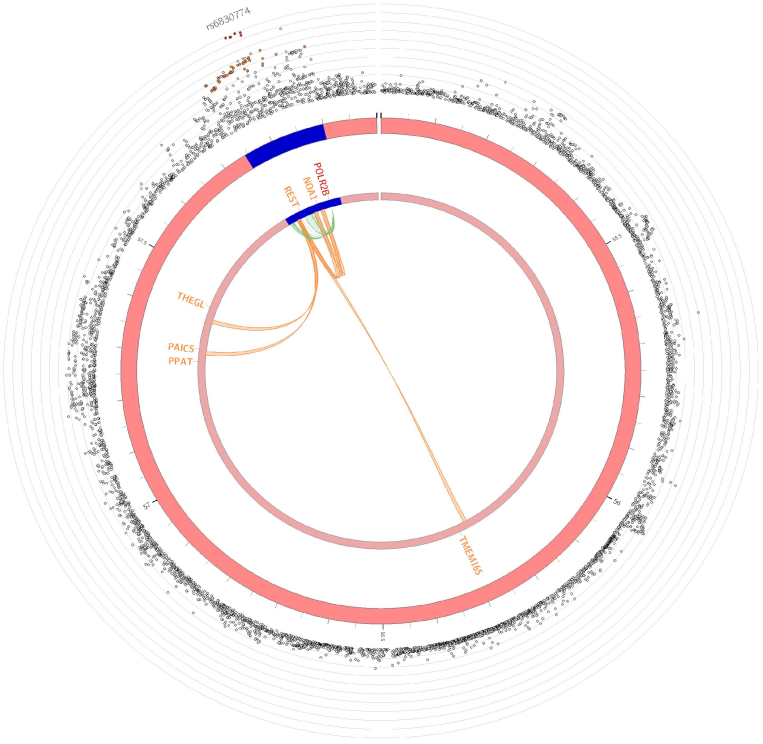

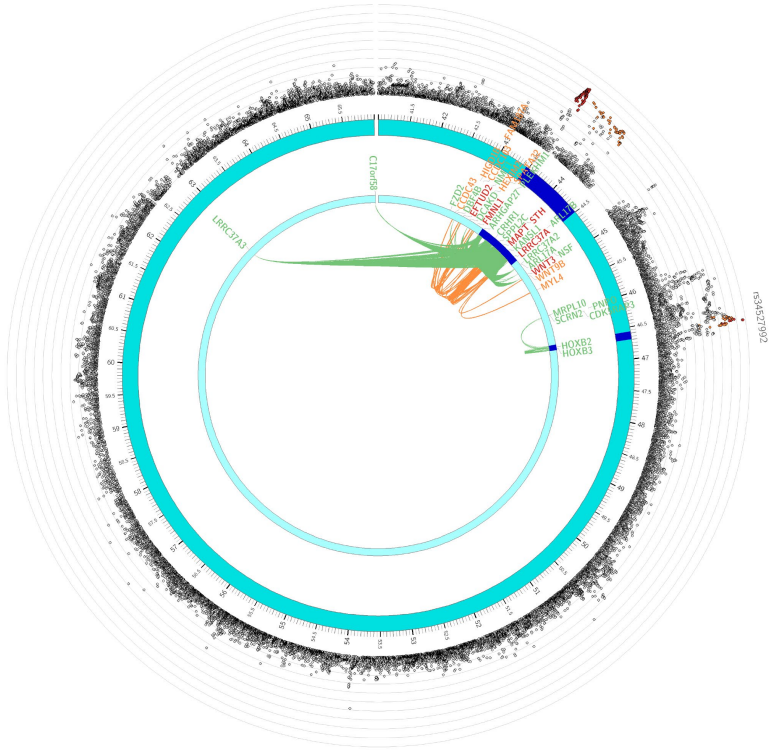

Supplementary Fig. 8 | Examples of Circos plots of mapped genes for the whole brainstem at chromosome 12 (**a**), midbrain at chromosome 14 (**b**), pons at chromosome 1 (**c**), superior cerebellar peduncle at chromosome 4 (**d**), and medulla oblongata at chromosome 4 (**e**). The plots show mapped genes of significant genetic loci from the genome-wide association studies of brainstem volumes (blue regions). The genes were linked to the loci by eQTL mapping (green lines) and chromatin interactions (orange lines). Green color indicates genes implicated by eQTLs, orange color indicates genes mapped by chromatin interactions, and genes implicated by both strategies are in red color. The outer layers show the Manhattan plots of single nucleotide polymorphisms from the genome-wide association studies.

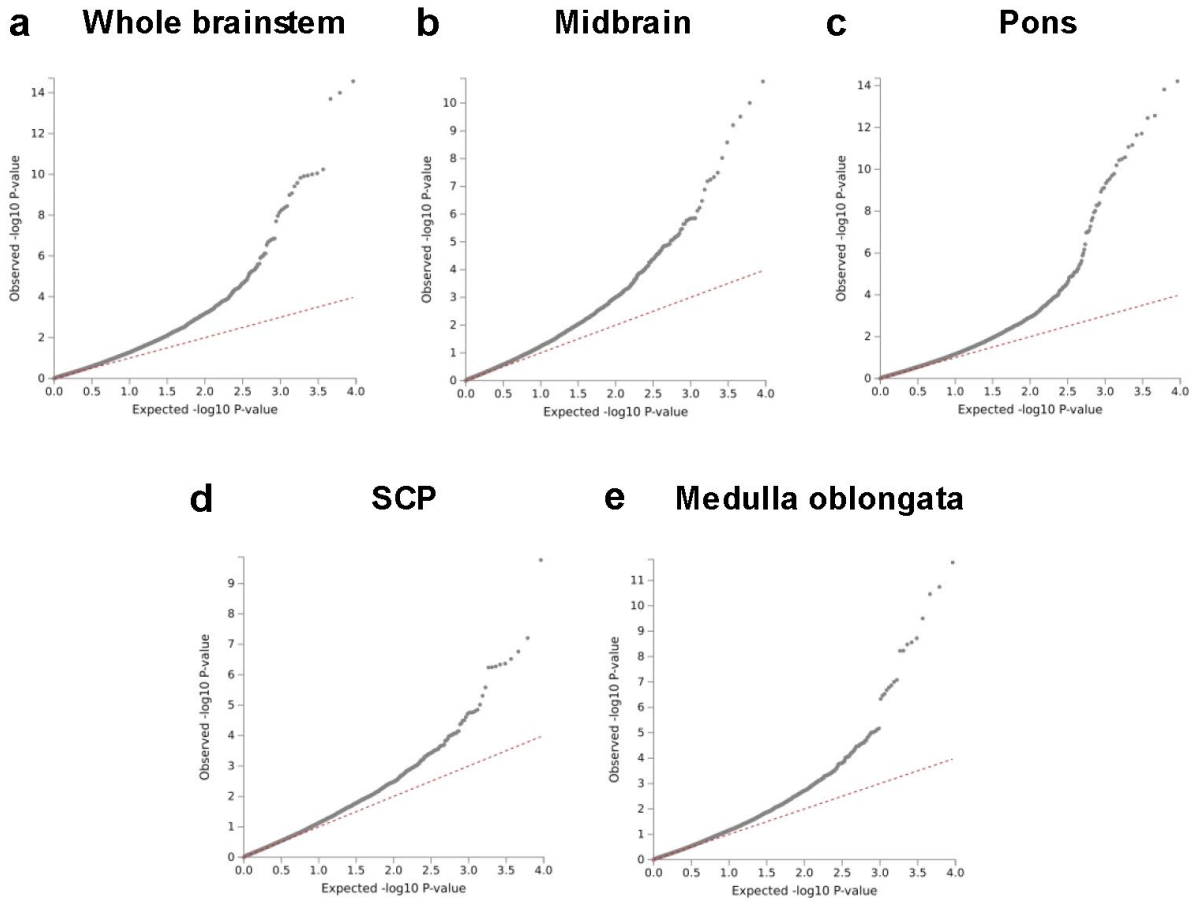

Supplementary Fig. 9 | Q-Q plots for volumes of the whole brainstem (**a**), midbrain (**b**), pons (**c**), superior cerebellar peduncle (**d**), and medulla oblongata (**e**) from the genome-wide gene-based association analyses. SCP; superior cerebellar peduncle.

a **Genetic overlap between brainstem volumes and ADHD**

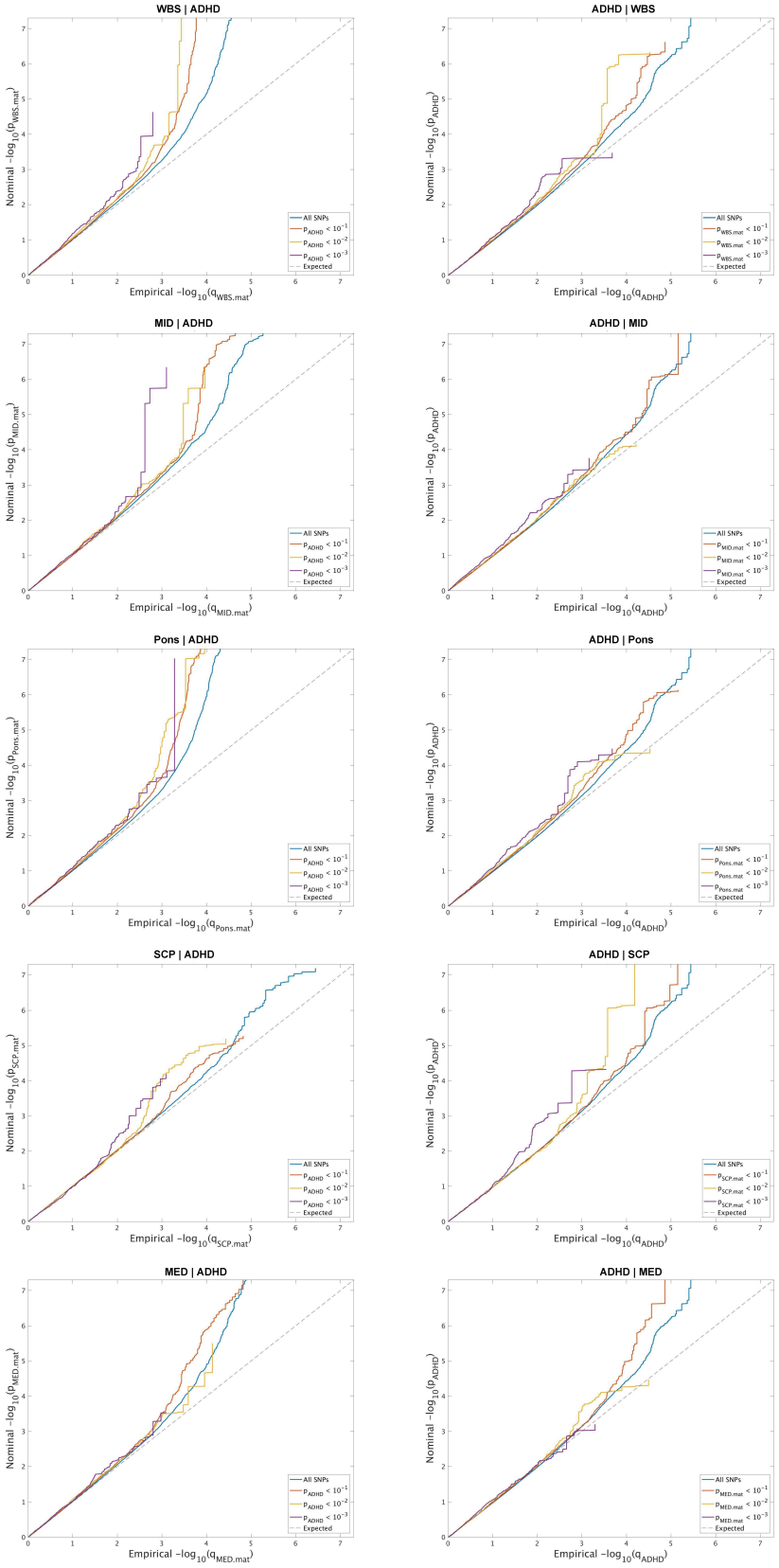

b **Genetic overlap between brainstem volumes and ASD**

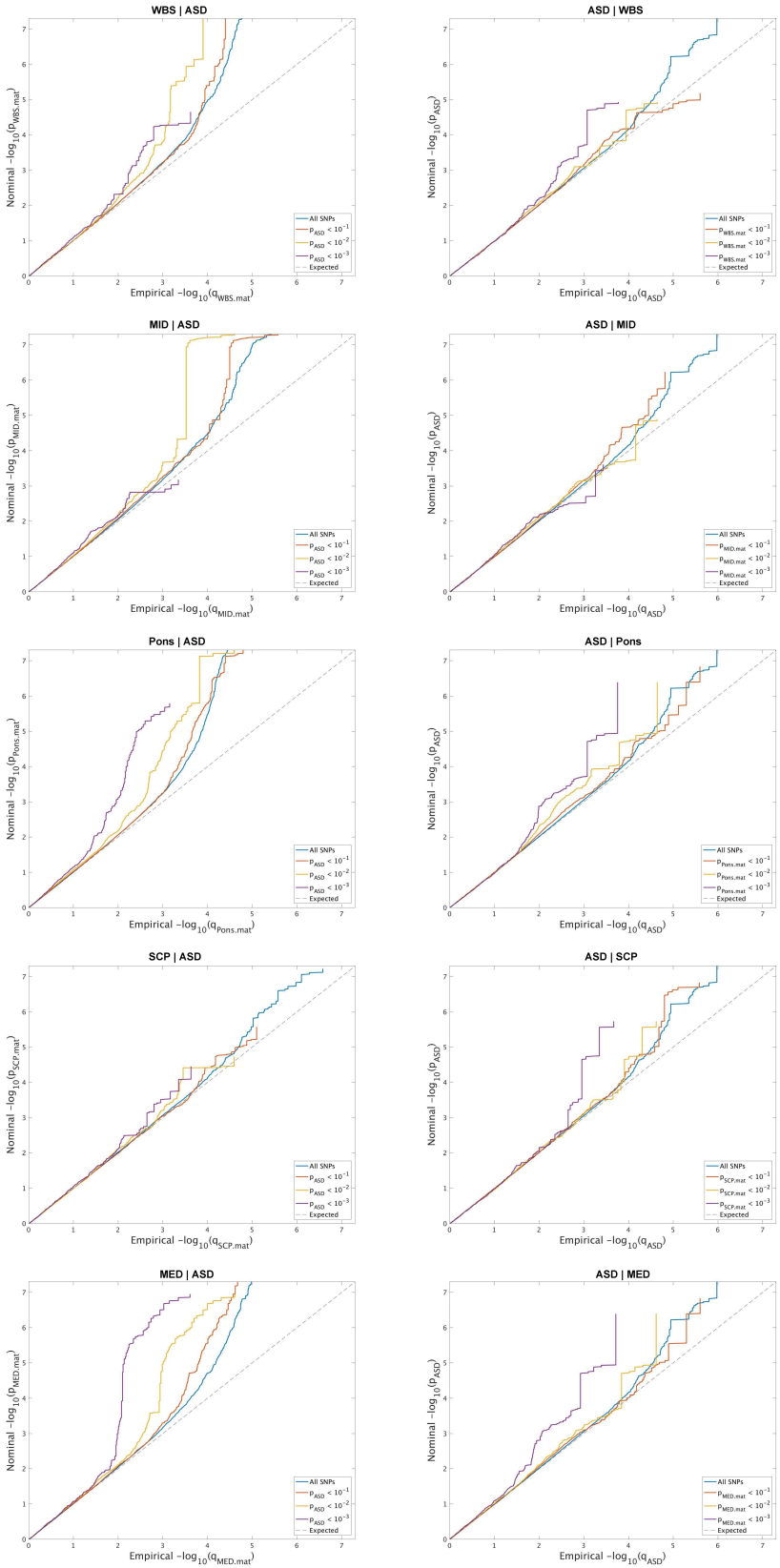

c **Genetic overlap between brainstem volumes and BD**

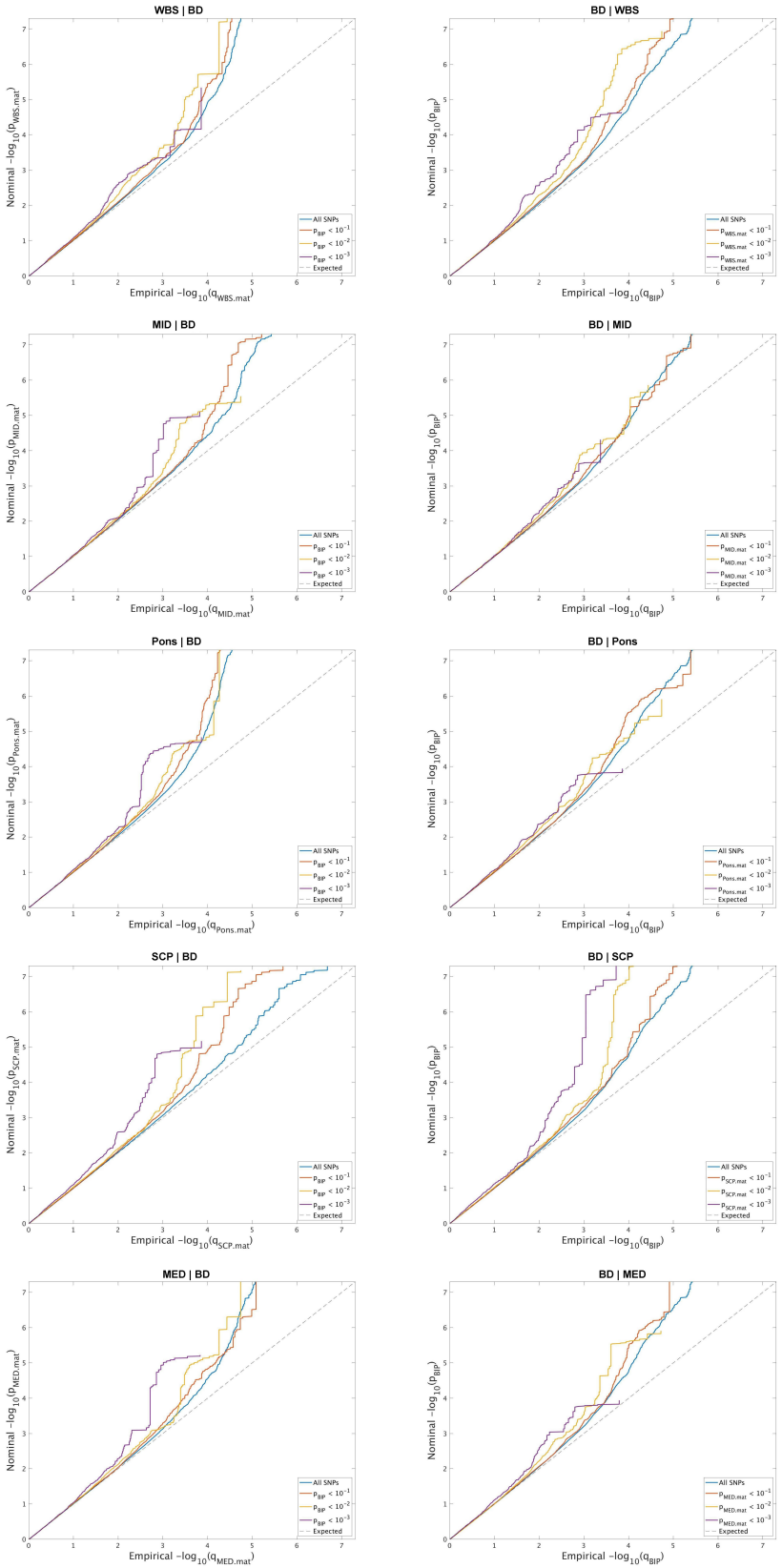

d **Genetic overlap between brainstem volumes and MD**

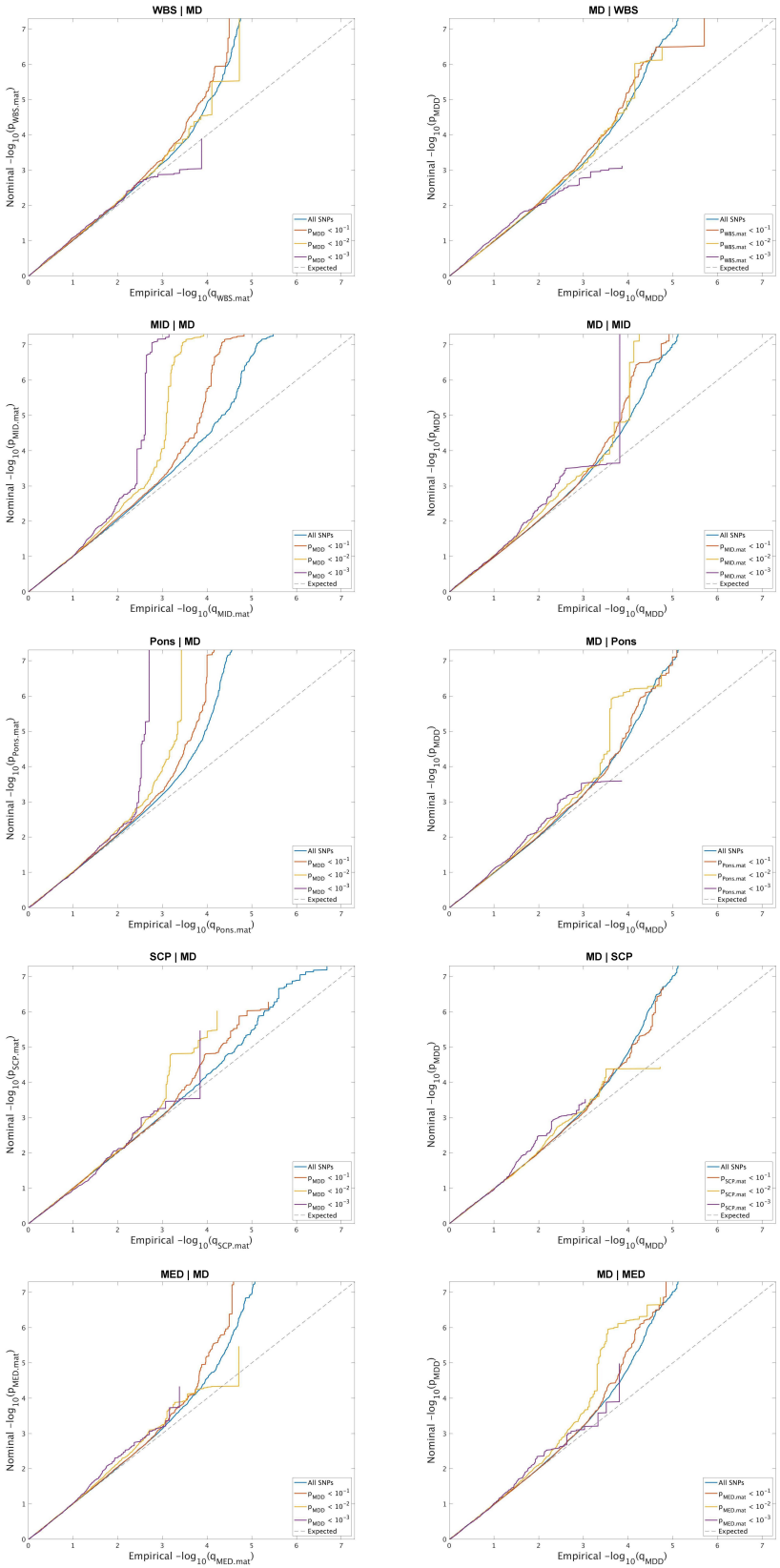

e **Genetic overlap between brainstem volumes and SCZ**

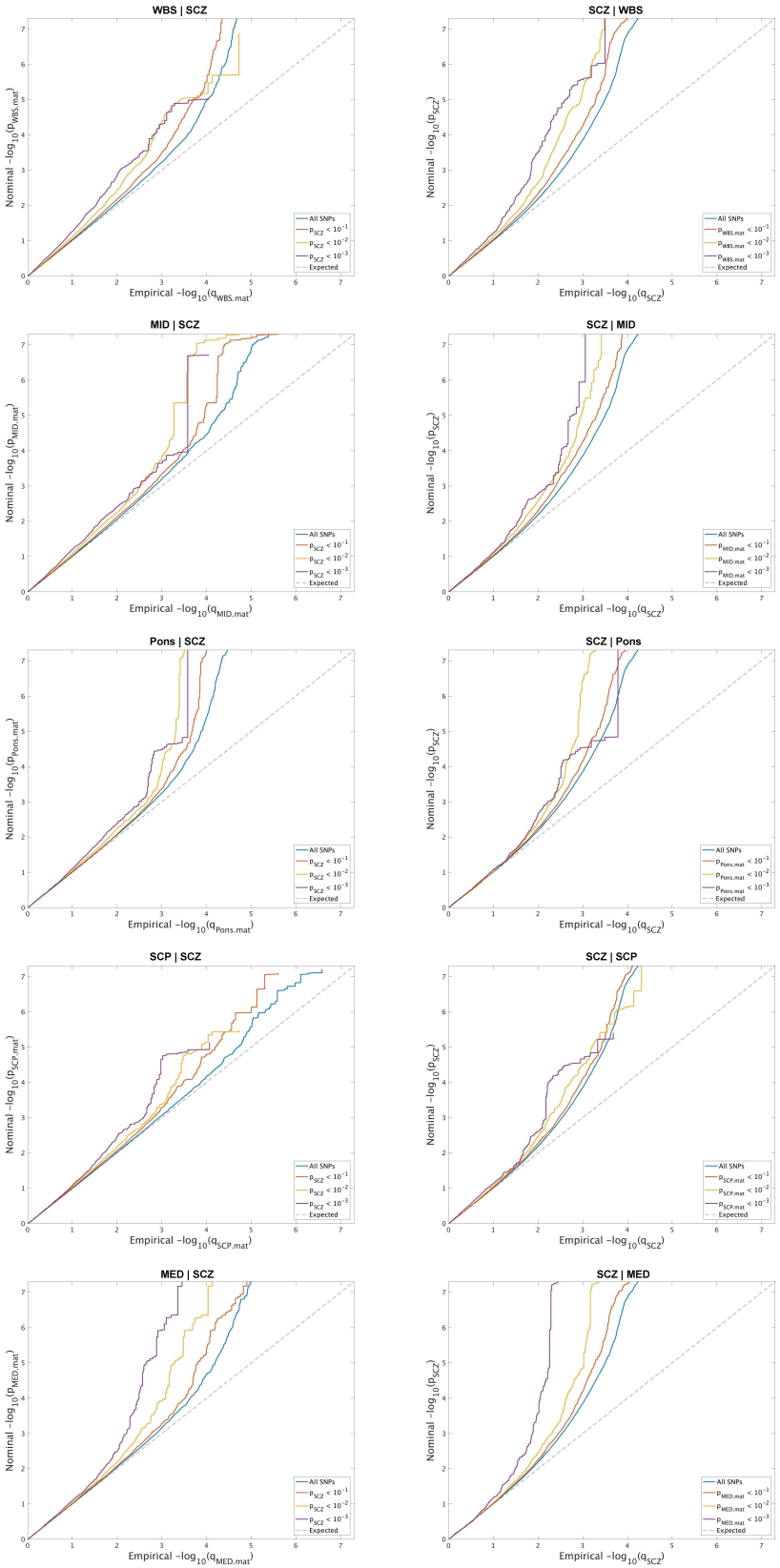

f **Genetic overlap between brainstem volumes and AD**

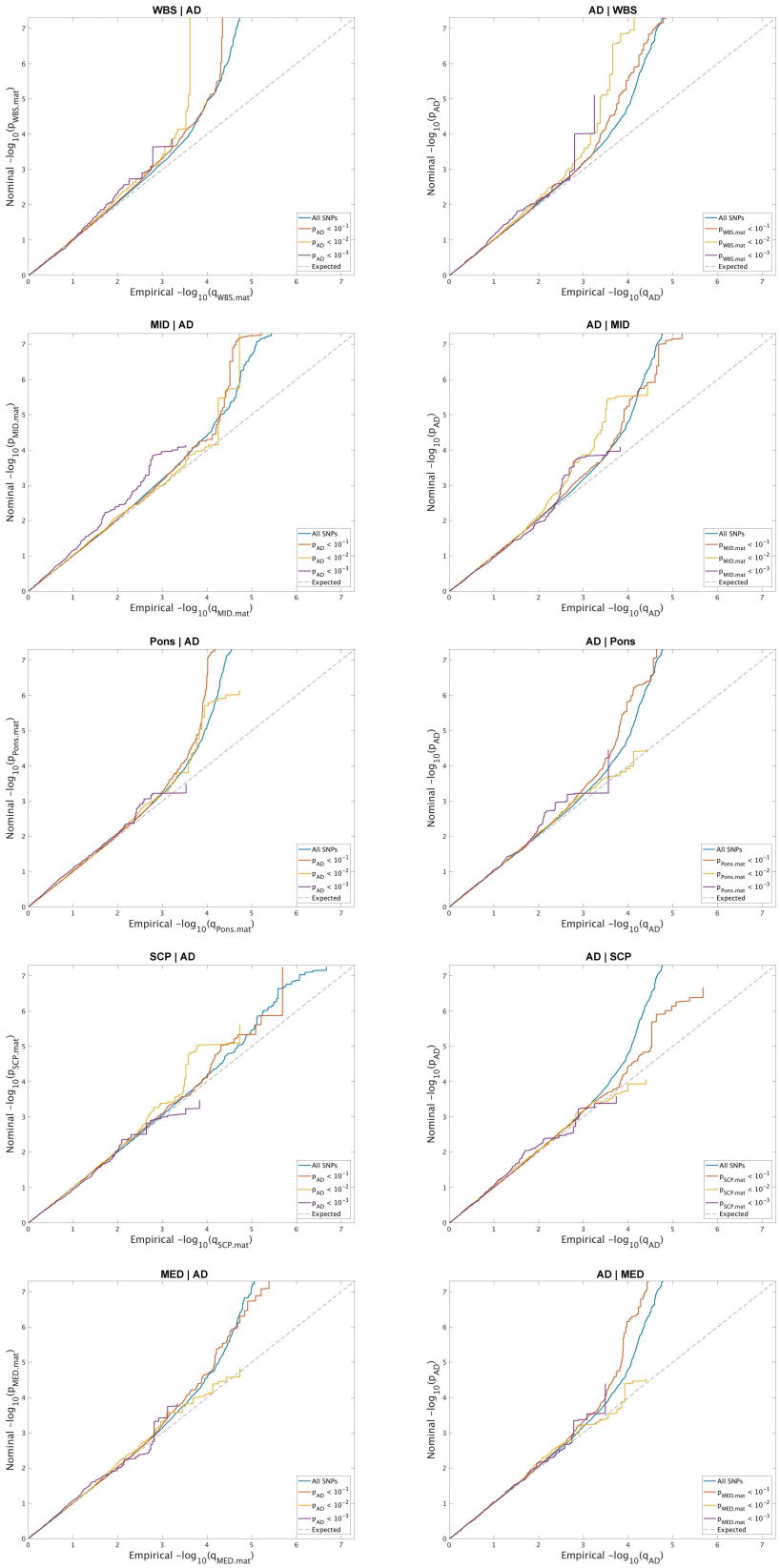

g **Genetic overlap between brainstem volumes and MS**

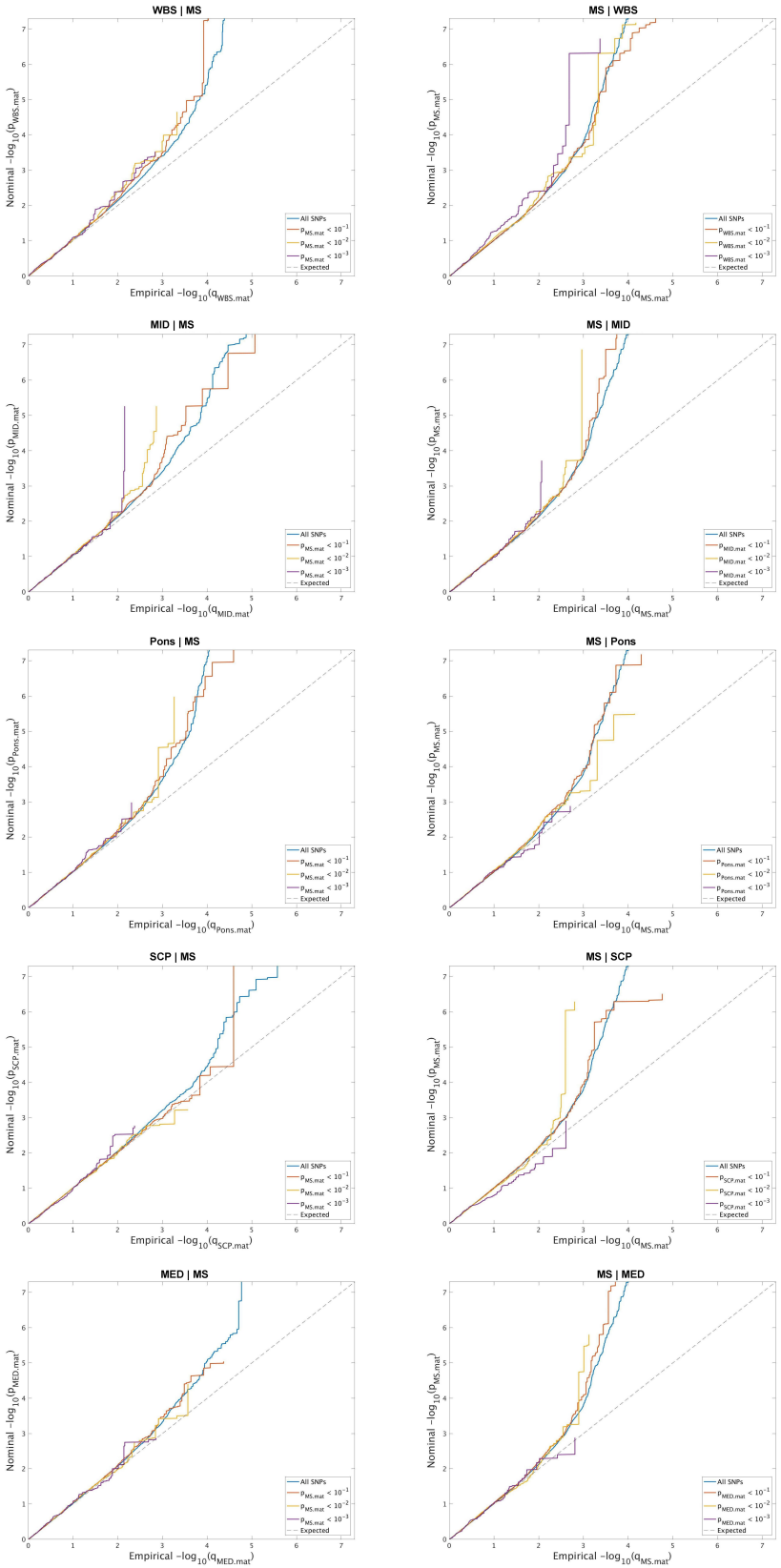

h **Genetic overlap between brainstem volumes and PD**

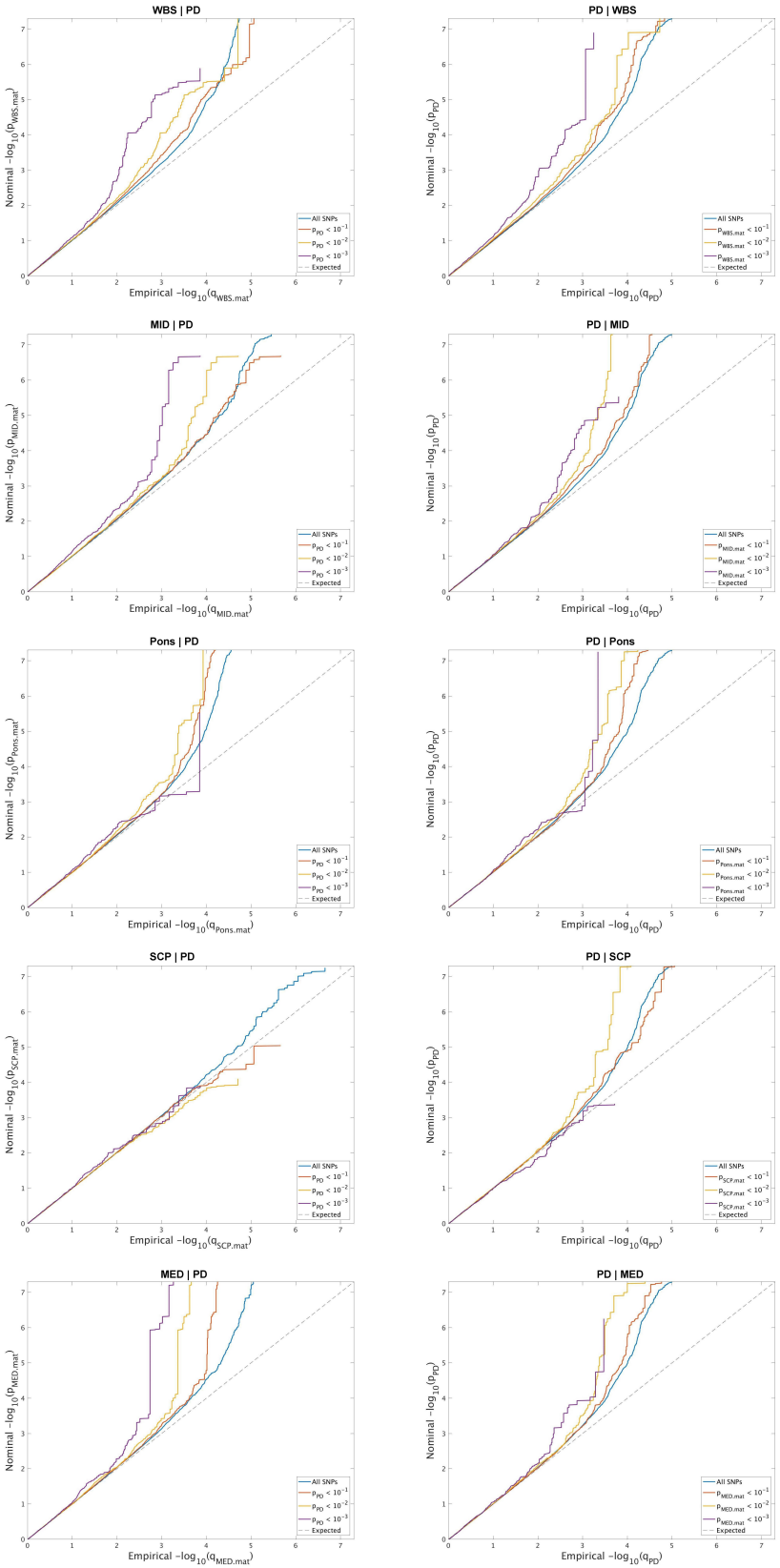

Supplementary Fig. 10 | Conditional Q-Q plots for brainstem volumes given associations with the disorder (left figures) and vice versa (right figures), for attention deficit hyperactivity disorder (**a**), autism spectrum disorder (**b**), bipolar disorder (**c**), major depression (**d**), schizophrenia (**e**), Alzheimer's disease (**f**), multiple sclerosis (**g**), and Parkinson's disease (**h**). ASD; autism spectrum disorders. BD; bipolar disorder. MD; major depression. SCZ; schizophrenia. AD; Alzheimer's disease. MS; multiple sclerosis. PD; Parkinson's disease.

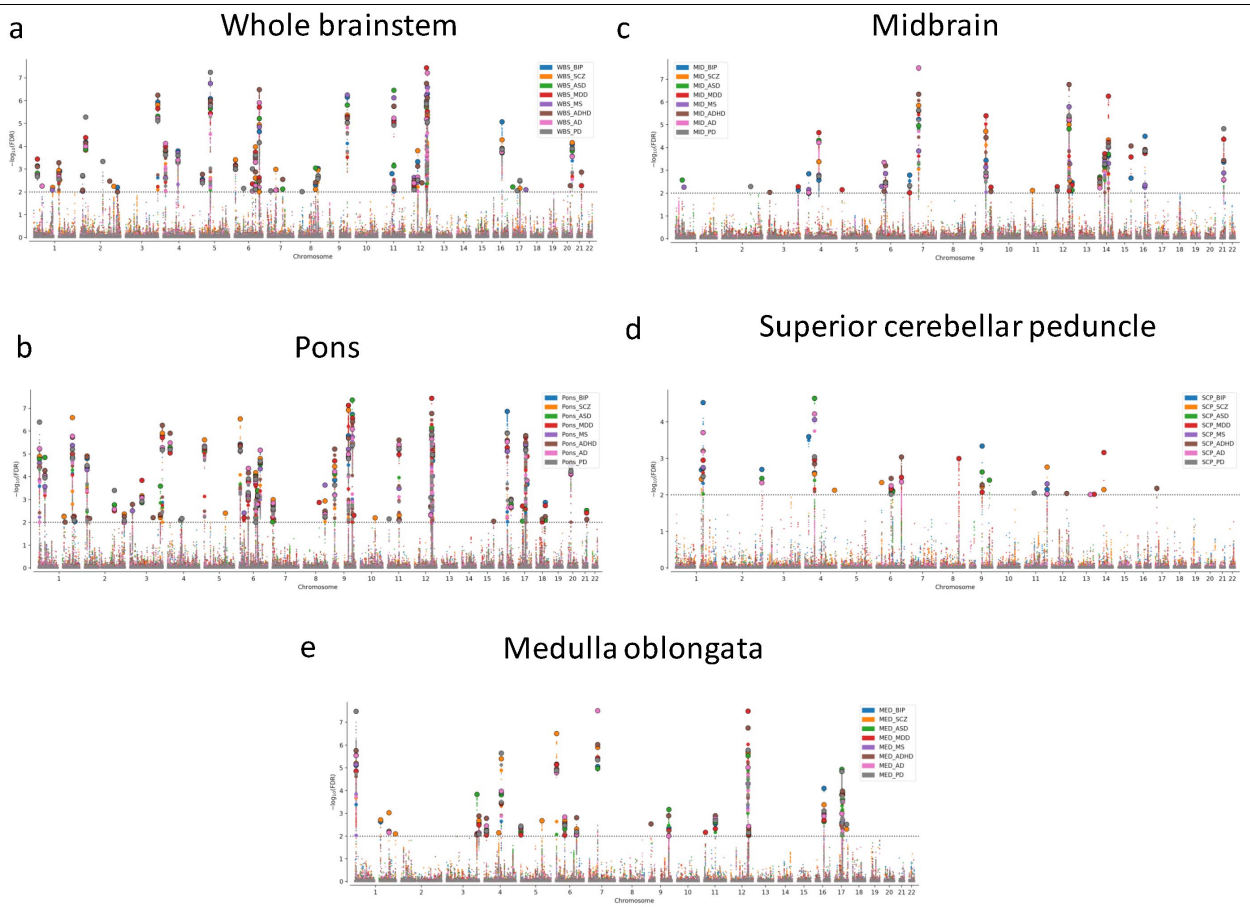

Supplementary Fig. 11 | Manhattan plots of genetic loci for each brainstem region identified by the condition false discovery rate analyses when conditioned on the eight brain disorders. These analyses revealed a total of 208 independent significant single-nucleotide polymorphisms (SNPs) for whole brainstem volume (**a**), 111 SNPs for midbrain volume (**b**), 270 SNPs for pons volume (**c**), 55 SNPs for superior cerebellar peduncle volume (**d**), and 125 SNPs for medulla oblongata volume (**e**). ASD; autism spectrum disorders. BD; bipolar disorder. MD; major depression. SCZ; schizophrenia. AD; Alzheimer's disease. MS; multiple sclerosis. PD; Parkinson's disease.

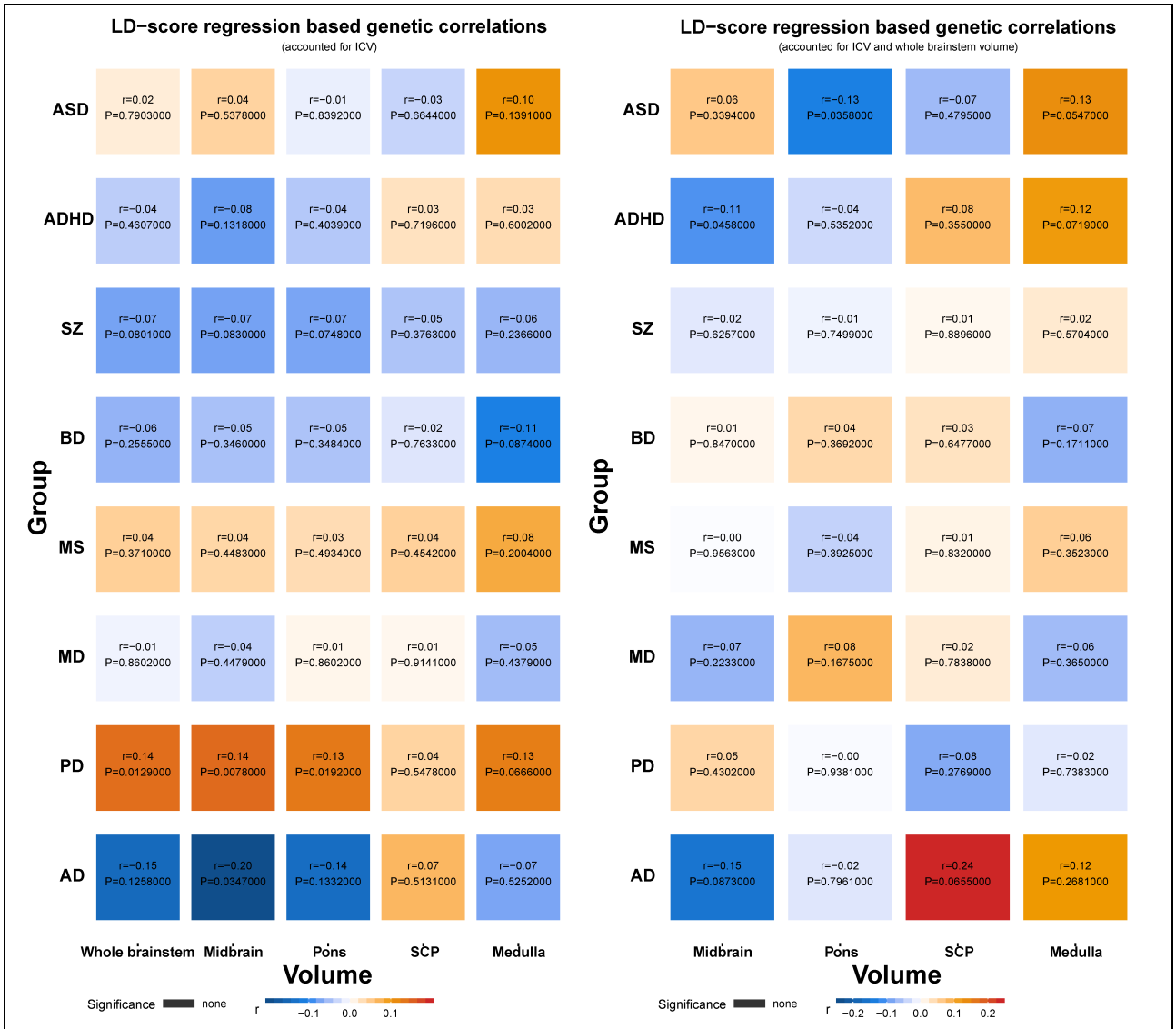

Supplementary Fig. 12 | Genetic correlations between brainstem volumes and eight brain disorders. There were correlations between brainstem volumes and ASD, ADHD, and PD with uncorrected $P < 0.05$, yet these were not significant after multiple testing corrections. ADHD; attention deficit hyperactivity disorder. ASD; autism spectrum disorder. BD; bipolar disorder. MD; major depression. MS; multiple sclerosis. PD; Parkinson's disease. SCZ; schizophrenia.

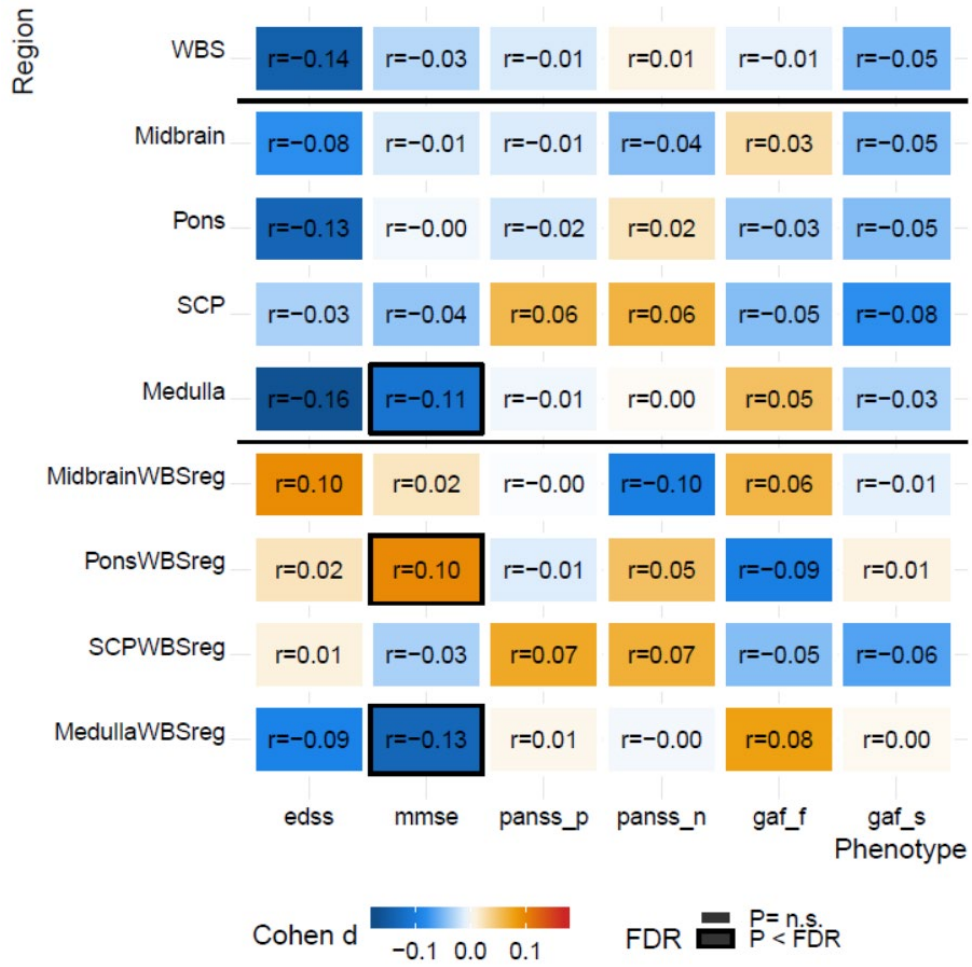

Supplementary Fig. 13 | Associations between brainstem volumes and clinical variables. We ran analyses of associations between brainstem volumes and clinical characteristics in the individuals with MCI, DEM, MS, SCZ, and PD. Across individuals with MCI and DEM (n = 1610), there were negative associations between Mini-Mental State Examination (MMSE) scores[40] and medulla oblongata volume before (r = -0.11 , P = 1.8e-05) and after (r = -0.13, P = 3.5e-07) accounting for whole brainstem volume. In addition, there was a significant positive association between MMSE and pons volume when adjusted for the whole brainstem (r = 0.10, P = 1.7e-04). All MRIs from the individuals with MS were examined by two neuroradiologists and then divided into two groups according to presence of infratentorial lesions. There was no significant difference in brainstem volumes between patients with (n = 153) and without (n = 91) infratentorial lesions (all P > 0.05; results not shown in the figure). Patients without lesions had reduced volumes relative to the controls of the whole brainstem (Cohen's d = -0.23, P = 0.03), midbrain (Cohen's d = - 0.26, P = 0.01), and medulla oblongata (Cohen's d = -0.22, P = 0.03; results not shown in the figure). There were significant reductions in volumes of patients with infratentorial lesions relative to controls for the whole brainstem (Cohen's d = -0.30, P = 3.4e-04), the midbrain (Cohen's d = -0.36, P = 1.9e-05), the pons (Cohen's d = -0.24, P = 3.9e-03), and medulla

oblongata (Cohen's d = - 0.29, P = 4.9e-04; results not shown in the figure). Across individuals with MS, there were no significant associations between brainstem volumes and EDSS (all $P > 0.05$). However, in the individuals with infratentorial lesions, there were negative associations between Expanded Disability Status Scale (EDSS)[41] and volumes of the whole brainstem (r = - 0.21, P = 0.03), pons (r = - 0.20, P = 0.045), and medulla oblongata (r = - 0.24, P = 0.01). There were no significant association between EDSS and volumes of the brainstem in the individuals without infratentorial lesions (all $P > 0.41$). In SCZ, there was no significant association between brainstem volumes and symptom or function scores of the Global Assessment of Functioning scale[42] or positive and negative scores of the Positive and Negative Syndrome Scale[43] (all $P > 0.05$). There were no significant relationships between brainstem volumes and the Movement Disorder Society-sponsored revision of the Unified Parkinson's Disease Rating Scale III sum score[75] or the Hoehn and Yahr Stage score[76] (all $P > 0.05$) in the individuals with PD (results not shown in the figure). MCI; mild cognitive impairment. DEM; dementia. MS; multiple sclerosis. SCZ; schizophrenia. PD; Parkinson's disease. MRI; magnetic resonance imaging.

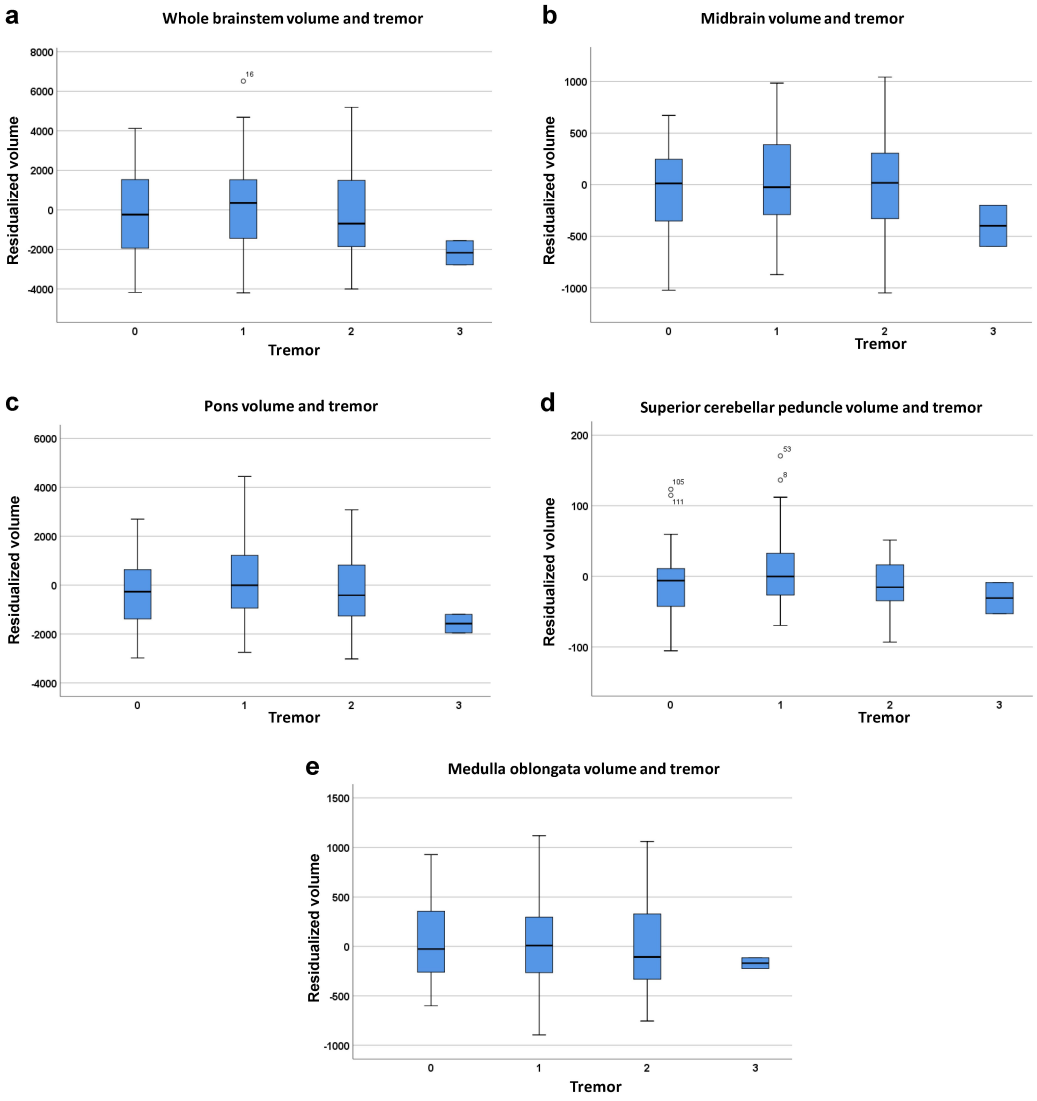

Supplementary Fig. 14 | Tremor and brainstem volumes in individuals with Parkinson's disease (PD).We examined whether the volume increases in the individuals with PD were related to tremor, which could cause increased within-scanner motion and confound the brainstem segmentation. Here, we used item 2.10 of the Unified Parkinson's Disease Rating Scale III[75]:

"Over the past week, have you usually had shaking or tremor? 0: Normal: Not at all. I have no shaking or tremor; 1: Slight: Shaking or tremor occurs but does not cause problems with any activities.; 2: Mild: Shaking or tremor causes problems with only a few activities; 3: Moderate: Shaking or tremor causes problems with many of my daily activities; and 4: Severe: Shaking or tremor causes problems with most or all activities." Thirty individuals had a tremor score of 0, 74 individuals had a score of 1, 22 individuals had a score of 2, 2 individuals had a score of 3, and none had a score of 4. We then grouped the individuals according to the tremor level and compared brainstem volumes between these groups using a linear model, covarying for gender, intracranial volume, scanner, age, and age^2. There were no significant effects of tremor group on brainstem volumes (all $P > 0.13$).

Methods

Methods are available at http://.....

References

1. Guyenet, P. G. The sympathetic control of blood pressure. *Nature reviews Neuroscience* **7,** 335-346 (2006).

2. Del Negro, C. A., Funk, G. D. Breathing matters. *Nature reviews Neuroscience* **19,** 351-367 (2018).

3. Damasio, A., Carvalho, G. B. The nature of feelings: evolutionary and neurobiological origins. *Nature reviews Neuroscience* **14,** 143-152 (2013).

4. Fisman, M. The brain stem in psychosis. *The British journal of psychiatry : the journal of mental science* **126,** 414-422 (1975).

5. Williams, D. R., Lees, A. J. Progressive supranuclear palsy: clinicopathological concepts and diagnostic challenges. *The Lancet Neurology* **8,** 270-279 (2009).

6. Lang, A. E., Lozano, A. M. Parkinson's disease. First of two parts. *The New England journal of medicine* **339,** 1044-1053 (1998).

7. Krishnan, V., Nestler, E. J. The molecular neurobiology of depression. *Nature* **455,** 894-902 (2008).

8. Sara, S. J. The locus coeruleus and noradrenergic modulation of cognition. *Nature reviews Neuroscience* **10,** 211-223 (2009).

9. Nakamura, K. et al. Brain serotonin and dopamine transporter bindings in adults with high-functioning autism. *Archives of general psychiatry* **67,** 59-68 (2010).

10. Grace, A. A. Dysregulation of the dopamine system in the pathophysiology of schizophrenia and depression. *Nature reviews Neuroscience* **17,** 524-532 (2016).

11. Przedborski, S. The two-century journey of Parkinson disease research. *Nature reviews Neuroscience* **18,** 251-259 (2017).

12. van Erp, T. G. et al. Subcortical brain volume abnormalities in 2028 individuals with schizophrenia and 2540 healthy controls via the ENIGMA consortium. *Molecular psychiatry* **21,** 547-553 (2016).

13. Hibar, D. P. et al. Cortical abnormalities in bipolar disorder: an MRI analysis of 6503 individuals from the ENIGMA Bipolar Disorder Working Group. *Molecular psychiatry* **23,** 932-942 (2018).

14. Whelan, C. D. et al. Structural brain abnormalities in the common epilepsies assessed in a worldwide ENIGMA study. *Brain : a journal of neurology* **141,** 391-408 (2018).

15. Schmaal, L. et al. Cortical abnormalities in adults and adolescents with major depression based on brain scans from 20 cohorts worldwide in the ENIGMA Major Depressive Disorder Working Group. *Molecular psychiatry* **6,** 900-909 (2016).

16. Hibar, D. P. et al. Novel genetic loci associated with hippocampal volume. *Nature communications* **8,** 13624 (2017).

17. Franke, B. et al. Genetic influences on schizophrenia and subcortical brain volumes: large-scale proof of concept. *Nature neuroscience* **19,** 420-431 (2016).

18. Hibar, D. P. et al. Common genetic variants influence human subcortical brain structures. *Nature* **520,** 224-229 (2015).

19. Thinking big in mental health. *Nature medicine* **24,** 1 (2018).

20. Iglesias, J. E. et al. Bayesian segmentation of brainstem structures in MRI. *NeuroImage* **113,** 184-195 (2015).

21. Fischl, B. et al. Whole brain segmentation: automated labeling of neuroanatomical structures in the human brain. *Neuron* **33,** 341-355 (2002).

22. Sudlow, C. et al. UK biobank: an open access resource for identifying the causes of a wide range of complex diseases of middle and old age. *PLoS Medicine* **12,** e1001779 (2015).

23. Purcell, S. et al. PLINK: a tool set for whole-genome association and population-based linkage analyses. *American journal of human genetics* **81,** 559-575 (2007).

24. van der Meer, D. et al. Brain scans from 21,297 individuals reveal the genetic architecture of hippocampal subfield volumes. *Molecular psychiatry* 10.1038/s41380-41018-40262-41387 (2018).

25. Bulik-Sullivan, B. et al. An atlas of genetic correlations across human diseases and traits. *Nature genetics* **47,** 1236-1241 (2015).

26. Watanabe, K., Taskesen, E., van Bochoven, A., Posthuma, D. Functional mapping and annotation of genetic associations with FUMA. *Nature communications* **8,** 1826 (2017).

27. Ernst, J., Kellis, M. ChromHMM: automating chromatin-state discovery and characterization. *Nature methods* **9,** 215-216 (2012).

28. Kircher, M. et al. A general framework for estimating the relative pathogenicity of human genetic variants. *Nature genetics* **46,** 310-315 (2014).

29. Pickrell, J. K. et al. Detection and interpretation of shared genetic influences on 42 human traits. *Nature genetics* **48,** 709-717 (2016).

30. de Leeuw, C. A., Mooij, J. M., Heskes, T., Posthuma, D. MAGMA: generalized gene-set analysis of GWAS data. *PLoS computational biology* **11,** e1004219 (2015).

31. Garcia-Fernandez, J. The genesis and evolution of homeobox gene clusters. *Nature reviews Genetics* **6,** 881-892 (2005).

32. Trainor, P. A., Krumlauf, R. Patterning the cranial neural crest: hindbrain segmentation and Hox gene plasticity. *Nature reviews Neuroscience* **1,** 116-124 (2000).

33. Kamburov, A., Stelzl, U., Lehrach, H., Herwig, R. The ConsensusPathDB interaction database: 2013 update. *Nucleic acids research* **41,** D793-800 (2013).

34. Andreassen, O. A. et al. Improved detection of common variants associated with schizophrenia by leveraging pleiotropy with cardiovascular-disease risk factors. *Am J Hum Genet* **92,** 197-209 (2013).

35. Liu, J. Z. et al. Dense genotyping of immune-related disease regions identifies nine new risk loci for primary sclerosing cholangitis. *Nature genetics* **45,** 670-675 (2013).

36. Schork, A. J. et al. New statistical approaches exploit the polygenic architecture of schizophrenia--implications for the underlying neurobiology. *Current opinion in neurobiology* **36,** 89-98 (2016).

37. Smeland, O. B. et al. Genome-wide analysis reveals extensive genetic overlap between schizophrenia, bipolar disorder, and intelligence. *Molecular psychiatry* 10.1038/s41380-41018-40332-x (2019).

38. Smeland, O. B. et al. Identification of Genetic Loci Jointly Influencing Schizophrenia Risk and the Cognitive Traits of Verbal-Numerical Reasoning, Reaction Time, and General Cognitive Function. *JAMA psychiatry* **74,** 1065-1075 (2017).

39. R Core Team. R: A language and environment for statistical computing. *R Foundation for Statistical Computing, Vienna, Austria* (2013).

40. Folstein, M. F., Folstein, S. E., McHugh, P. R. "Mini-mental state". A practical method for grading the cognitive state of patients for the clinician. *Journal of psychiatric research* **12,** 189-198 (1975).

41. Kurtzke, J. F. Rating neurologic impairment in multiple sclerosis: an expanded disability status scale (EDSS). *Neurology* **33,** 1444-1452 (1983).

42. Pedersen, G., Karterud, S. The symptom and function dimensions of the Global Assessment of Functioning (GAF) scale. *Comprehensive psychiatry* **53,** 292-298 (2012).

43. Kay, S. R., Fiszbein, A., Opler, L. A. The positive and negative syndrome scale (PANSS) for schizophrenia. *Schizophrenia bulletin* **13,** 261-276 (1987).

44. Elliott, L. T. et al. Genome-wide association studies of brain imaging phenotypes in UK Biobank. *Nature* **562,** 210-216 (2018).

45. Wang, Y., Mandelkow, E. Tau in physiology and pathology. *Nature Reviews Neuroscience* **17,** 22 (2015).

46. Chang, D. et al. A meta-analysis of genome-wide association studies identifies 17 new Parkinson's disease risk loci. *Nature genetics* **49,** 1511-1516 (2017).

47. Hoglinger, G. U. et al. Identification of common variants influencing risk of the tauopathy progressive supranuclear palsy. *Nature genetics* **43,** 699-705 (2011).

48. Lyons, D. A., Naylor, S. G., Scholze, A., Talbot, W. S. Kif1b is essential for mRNA localization in oligodendrocytes and development of myelinated axons. *Nature genetics* **41,** 854-858 (2009).

49. Zhao, C. et al. Charcot-Marie-Tooth disease type 2A caused by mutation in a microtubule motor KIF1Bbeta. *Cell* **105,** 587-597 (2001).

50. Ahmad, F. J., Yu, W., McNally, F. J., Baas, P. W. An essential role for katanin in severing microtubules in the neuron. *The Journal of cell biology* **145,** 305-315 (1999).

51. Toyo-Oka, K. et al. Recruitment of katanin p60 by phosphorylated NDEL1, an LIS1 interacting protein, is essential for mitotic cell division and neuronal migration. *Human molecular genetics* **14,** 3113-3128 (2005).

52. Checler, F., Vincent, J. P., Kitabgi, P. Purification and characterization of a novel neurotensin-degrading peptidase from rat brain synaptic membranes. *The Journal of biological chemistry* **261,** 11274-11281 (1986).

53. Boules, M. et al. Diverse roles of neurotensin agonists in the central nervous system. *Frontiers in endocrinology* **4,** 36 (2013).

54. Sharma, R. P., Janicak, P. G., Bissette, G., Nemeroff, C. B. CSF neurotensin concentrations and antipsychotic treatment in schizophrenia and schizoaffective disorder. *The American journal of psychiatry* **154,** 1019-1021 (1997).

55. Vuong, T. A. et al. SGTb regulates a surface localization of a guidance receptor BOC to promote neurite outgrowth. *Cellular signalling* **55,** 100-108 (2019).

56. Webb, B. D. et al. HOXB1 founder mutation in humans recapitulates the phenotype of Hoxb1-/- mice. *American journal of human genetics* **91,** 171-179 (2012).

57. Kohler, M. et al. Small-conductance, calcium-activated potassium channels from mammalian brain. *Science (New York, NY)* **273,** 1709-1714 (1996).

58. Zollino, M. et al. Mutations in KANSL1 cause the 17q21.31 microdeletion syndrome phenotype. *Nature genetics* **44,** 636-638 (2012).

59. Frei, O. et al. Bivariate causal mixture model quantifies polygenic overlap between complex traits beyond genetic correlation. *Nature communications* **10,** 2417 (2019).

60. Mirsky, A. F., Duncan, C. C. Pathophysiology of mental illness: a view from the fourth ventricle. *International journal of psychophysiology : official journal of the International Organization of Psychophysiology* **58,** 162-178 (2005).

61. Schildkraut, J. J. The catecholamine hypothesis of affective disorders: a review of supporting evidence. *The American journal of psychiatry* **122,** 509-522 (1965).

62. Ashok, A. H. et al. The dopamine hypothesis of bipolar affective disorder: the state of the art and implications for treatment. *Molecular psychiatry* **22,** 666-679 (2017).

63. Murray, G. K. et al. Substantia nigra/ventral tegmental reward prediction error disruption in psychosis. *Molecular psychiatry* **13,** 239, 267-276 (2008).

64. Rimol, L. M. et al. Cortical thickness and subcortical volumes in schizophrenia and bipolar disorder. *Biological psychiatry* **68,** 41-50 (2010).

65. Alnaes, D. et al. Brain Heterogeneity in Schizophrenia and Its Association With Polygenic Risk. *JAMA psychiatry* **76,** 739-748 (2019).

66. Ledig, C. et al. Structural brain imaging in Alzheimer's disease and mild cognitive impairment: biomarker analysis and shared morphometry database. *Scientific reports* **8,** 11258 (2018).

67. Lee, J. H. et al. Brainstem morphological changes in Alzheimer's disease. *Neuroreport* **26,** 411-415 (2015).

68. Nigro, S. et al. Fully automated segmentation of the pons and midbrain using human T1 MR brain images. *PloS one* **9,** e85618 (2014).

69. Daams, M. et al. Unraveling the neuroimaging predictors for motor dysfunction in long-standing multiple sclerosis. *Neurology* **85,** 248-255 (2015).

70. Lee, C. Y. et al. Differential brainstem atrophy patterns in multiple sclerosis and neuromyelitis optica spectrum disorders. *Journal of magnetic resonance imaging : JMRI* **47,** 1601-1609 (2018).

71. Liu, C. et al. Three dimensional MRI estimates of brain and spinal cord atrophy in multiple sclerosis. *Journal of neurology, neurosurgery, and psychiatry* **66,** 323-330 (1999).

72. Pagonabarraga, J. et al. Neural correlates of minor hallucinations in non-demented patients with Parkinson's disease. *Parkinsonism & related disorders* **20,** 290-296 (2014).

73. Rektorova, I. et al. Grey matter changes in cognitively impaired Parkinson's disease patients. *PloS one* **9,** e85595 (2014).

74. Sawczak, C. M., Barnett, A. J., Cohn, M. Increased Cortical Thickness in Attentional Networks in Parkinson's Disease with Minor Hallucinations. *Parkinsons Dis* **2019,** 5351749 (2019).

75. Goetz, C. G. et al. Movement Disorder Society-sponsored revision of the Unified Parkinson's Disease Rating Scale (MDS-UPDRS): scale presentation and clinimetric testing results. *Movement disorders : official journal of the Movement Disorder Society* **23,** 2129-2170 (2008).

76. Hoehn, M. M., Yahr, M. D. Parkinsonism: onset, progression and mortality. *Neurology* **17,** 427-442 (1967).

77. Boyle, A. P. et al. Annotation of functional variation in personal genomes using RegulomeDB. *Genome research* **22,** 1790-1797 (2012).

78. Kundaje, A. et al. Integrative analysis of 111 reference human epigenomes. *Nature* **518,** 317-330 (2015).

79. Zhu, Z. et al. Integration of summary data from GWAS and eQTL studies predicts complex trait gene targets. *Nature genetics* **48,** 481-487 (2016).

80. Subramanian, A. et al. Gene set enrichment analysis: a knowledge-based approach for interpreting genome-wide expression profiles. *Proceedings of the National Academy of Sciences of the United States of America* **102,** 15545-15550 (2005).

81. Demontis, D. et al. Discovery of the first genome-wide significant risk loci for attention deficit/hyperactivity disorder. *Nature genetics* **51,** 63-75 (2019).

82. Ripke, S. et al. Biological insights from 108 schizophrenia-associated genetic loci. *Nature* **511,** 421-427 (2014).

83. Meta-analysis of GWAS of over 16,000 individuals with autism spectrum disorder highlights a novel locus at 10q24.32 and a significant overlap with schizophrenia. *Molecular autism* **8,** 21 (2017).

84. Stahl, E. A. et al. Genome-wide association study identifies 30 loci associated with bipolar disorder. *Nature genetics* **51,** 793-803 (2019).

85. Wray, N. R. et al. Genome-wide association analyses identify 44 risk variants and refine the genetic architecture of major depression. *Nature genetics* **50,** 668-681 (2018).

86. Hyde, C. L. et al. Identification of 15 genetic loci associated with risk of major depression in individuals of European descent. *Nature genetics* **48,** 1031-1036 (2016).

87. Lambert, J. C. et al. Meta-analysis of 74,046 individuals identifies 11 new susceptibility loci for Alzheimer's disease. *Nature genetics* **45,** 1452-1458 (2013).

88. Sawcer, S. et al. Genetic risk and a primary role for cell-mediated immune mechanisms in multiple sclerosis. *Nature* **476,** 214-219 (2011).

89. Nalls, M. A. et al. Large-scale meta-analysis of genome-wide association data identifies six new risk loci for Parkinson's disease. *Nature genetics* **46,** 989-993 (2014).

90. Andreassen, O. A. et al. Improved detection of common variants associated with schizophrenia and bipolar disorder using pleiotropy-informed conditional false discovery rate. *PLoS genetics* **9,** e1003455 (2013).

91. Nichols, T. et al. Valid conjunction inference with the minimum statistic. *NeuroImage* **25,** 653-660 (2005).

Acknowledgments

The author list between I.A. and M.Z. is in alphabetic order. The authors were funded by the South-Eastern Norway Regional Health Authority 2015-078 (T.E.), 2013-123 (O.A.A.), 2014-097 (L.T.W.), 2015-073 (L.T.W.) and 2016-083 (L.T.W.), by the Research Council of Norway (276082 LifespanHealth (T.K.), 213837 (O.A.A), 223273 NORMENT (O.A.A.), 204966 (L.T.W.), 229129 (O.A.A.), 249795 (L.T.W.), 273345 (L.T.W.) and 283798 SYNSCHIZ (O.A.A.)), Stiftelsen Kristian Gerhard Jebsen, the European Research Council (ERCStG 802998 BRAINMINT (L.T.W.)), NVIDIA Corporation GPU Grant (T.K.), the Ebbe Frøland foundation, and a research grant from Mrs. Throne-Holst. The data used in this study was gathered from various sources and a detailed overview of the included cohorts and acknowledgement of their respective funding sources and cohort-specific details is provided in Supplementary Table 1. Data used in preparation of this article were obtained from the Alzheimer's Disease Neuroimaging Initiative (ADNI) database (adni.loni.usc.edu), from the AddNeuroMed consortium, and from the Pediatric Imaging, Neurocognition and Genetics Study (PING) database (www.chd.ucsd.edu/research/ping-study.html, now shared through the NIMH Data Archive (NDA)). The investigators within the ADNI and PING contributed to the design and implementation of ADNI/PING and/or provided data but did not participate in analysis or writing of this report. This publication is solely the responsibility of the authors and does not necessarily represent the views of the National Institutes of Health or PING investigators. Complete listings of participating sites and study investigators can be found at http://adni.loni.usc.edu/wp-content/uploads/how_to_apply/ADNI_Acknowledgement_List.pdf and https://ping-dataportal.ucsd.edu/sharing/Authors10222012.pdf. The AddNeuroMed consortium was led by Simon Lovestone, Bruno Vellas, Patrizia Mecocci, Magda Tsolaki, Iwona Kłoszewska, and Hilkka Soininen.

We would like to thank the research participants and employees of the ADHD, ASD, SCZ, BD, and MD Working Groups of the Psychiatric Genomics Consortium, the International Genomics of Alzheimer's Project, the International Multiple Sclerosis Genetics Consortium, International Parkinson Disease Genomics Consortium, and 23andMe, Inc. for granting us access to their GWAS summary statistics, and the many people who provided DNA samples for their studies. Data used in the preparation of this article were obtained from the Parkinson's Progression Markers Initiative (PPMI) database (www.ppmi-info.org/data). For up-to-date information on the study, visit www.ppmi-info.org. This work was performed on the TSD (Tjeneste for Sensitive Data) facilities, owned by the University of Oslo, operated and developed by the TSD service group at the University of Oslo, IT-Department (USIT) and on resources provided by UNINETT Sigma2 - the National Infrastructure for High Performance Computing and Data Storage in Norway.

Author contributions

T.E., S.B., L.T.W., and T.K. conceived the study, T.K., L.T.W., and S.B. preprocessed all MRI and genetic data, T.E. and T.K. performed quality control of the MRI data, T.E., S.B., and T.K. performed the analyses, and T.E., S.B., D.v.d.M., O.A.A., L.T.W., and T.K. interpreted the results. All remaining authors contributed to data collection at their respective sites as well as sample-specific tasks. T.E., S.B., and T.K. wrote the first draft of the paper and all authors contributed to and approved the final manuscript.

Competing interests

Some authors received speaker's honoraria from Lundbeck (T.E., G.B., and O.A.A.), Janssen Cilag (T.E.), Merck (E.H.), Sanofi Genzyme (E.H.), and Synovion (O.A.A). A.B. received

speaker's honoraria from Lundbeck, Otsuka, and Janssen Cilag and consultation fees from Biogen and Roche. J.K.B. has been a consultant to, member of advisory board of, and/or speaker for Shire, Roche, Medice, and Servier. E.G.C. has received personal fees from Almirall, Biogen, Merck, Roche and Teva, and grants and personal fees from Novartis and Sanofi. S.C. has received grant support from AstraZeneca as a coinvestigator and has served as a speaker for Otsuka. H.F.F. has received travel support, honoraria for advice or lecturing from Biogen Idec, Sanofi Genzyme, Merck, Novartis, Roche, and Teva and an unrestricted research grant from Novartis. N.I.L. has received consultation fees and travel support from Lundbeck. H.S. has received fees for advisory boards from ACImmune and Merck. P.S. has received honoraria for lecturing and travel support from Merck. M.T. has been member of advisory boards for Merck, IASIS Healthcare, ELPEN and FarmaSyn. M.Z. has received speaker fees for lectures, travel support and membership in advisory boards from Janssen Cilag, Lundbeck, Otsuka, Ferrer Pharma, Trommsdorff, Servier, and Roche. None of these external parties had any role in the analysis, writing or decision to publish this work. All other authors declare no competing interests.

Additional information

Supplementary information is available for this paper at …

Karolinska Schizophrenia Project (KaSP)

Members of the Karolinska Schizophrenia Project (KaSP): L Farde[6], L Flyckt[6], G Engberg[58], S Erhardt S[58], H Fatouros-Bergman[6], S Cervenka[6], L Schwieler[58], F Piehl[59], I Agartz[1,5,6], K Collste[6], P Victorsson[6], A Malmqvist[58], M Hedberg[58], F Orhan[58], C M Sellgren[58]

Online methods

Samples

We collected data from cohorts of participants with common brain disorders and healthy individuals through collaborations, data sharing platforms, and from in-house samples (n = 49,815). All included samples have been part of previously published works and data collection for each sample was performed with participants' written informed consent and with approval by the respective local Institutional Review Boards. Supplementary Table 1 provides details for each sample and refers to previously published works from the included samples.

Preprocessing of MRI data, brainstem segmentations, and quality control procedures

Raw T1-weighted MRI data for all individuals was stored and analyzed locally at the University of Oslo. The whole brainstem, midbrain, pons, SCP, and medulla oblongata were then delineated using Freesurfer 6.0[21] and Bayesian brainstem segmentation[20]. The brainstem segmentation method is based on a probabilistic atlas and Bayesian inference and is robust to changes in MRI scanners and pulse sequence details[20]. We then manually assessed the delineations in all MRI data sets (n = 49,815) by visually inspecting twelve sagittal view figures of the segmentations for each participant, as shown in Supplementary Fig. 1. This visual quality control (QC) procedure for each data set was conducted blind to case-control status. Data sets were excluded from the study if one of the following requirements was not met: 1. the field of view included the whole brainstem, 2. the superior boundary of the midbrain approximated an axial plane through the mammillary body and the superior edge of the quadrigeminal plate, 3. the boundary between mibrain and pons approximated an axial plane through the superior pontine notch and the inferior edge of the quadrigeminal plate, 4. the boundary between between pons and medulla oblongata approximated an axial plane at the level of the inferior potine notch, 5. the inferior boundary of

the medulla oblongata approximated an axial plane at the level of the posterior rim of the foramen magnum, 6. there were no substantial segmentation errors for the anterior and posterior boundaries of midbrain, pons, and medulla oblongata, and 7. the superior boundary of the SCP approximated the inferior boundary of the midbrain tectum, the inferior boundary of the SCP was defined by the merging with the cerebellum, and the anterior boundary of the SCP was defined by the posterior boundary of the pons. This QC procedure excluded 13% (n = 6,462) of the data sets, mainly due to insufficient field of view (e.g., not fully covering the inferior part of the medulla oblongata), insufficient data quality, and segmentation errors in the clinical samples, resulting in a final sample size of n = 43,353 (Supplementary Table 3).

Genome-wide association studies for brainstem volumes and identification of genomic loci

The genetic analyses for the brainstem volumes were based on MRI and genetic data from healthy individuals of the UK Biobank Resource (sample size n = 27,034 after the QC procedures). We restricted all genetic analyses to individuals with White European ancestry, as determined by the UK Biobank study team. We applied standard quality control procedures to the UK Biobank v3 imputed genetic data, removing SNPs with an imputation quality score < 0.5, a minor allele frequency < 0.05, missing in more than 5% of individuals, and failing the Hardy Weinberg equilibrium tests at a P < 1e-6.

We performed GWAS on the brainstem volumes in the 27,034 healthy adults using PLINK 2.0[23]. All GWAS accounted for age, age², sex, scanning site, ICV, genetic batch, and the first ten genetic principal components to account for population stratification. In addition, the GWAS for the midbrain, pons, SCP, and medulla oblongata accounted for whole brainstem volume. The MHC region was excluded from the analysis.

We identified genetic loci related to brainstem volumes using the FUMA platform v1.3.3c[26]. Independent significant SNPs were identified by the genome-wide significant threshold (P < 5e-8) and by their independency ($r^2 \leq 0.6$ within a 1 mb window). Independent significant SNPs with $r^2 < 0.1$ within a 1 mb window were defined as lead SNPs. Genomic risk loci were found by merging lead SNPs if they were closer than 250 kb. Candidate SNPs were defined as all SNPs in LD ($r^2 \geq 0.6$) with one of the independent significant SNPs in the genetic loci.

Functional annotation, gene-based association, and gene-set analysis

We functionally annotated all candidate SNPs of brainstem volumes that were in linkage disequilibrium ($r^2 \geq 0.6$) with one of the independent significant SNPs using the FUMA platform v1.3.3c[26]. FUMA is based on information from 18 biological repositories and tools and functionally annotates GWAS results. The platform prioritizes the most likely causal SNPs and genes by combining positional, eQTL, and chromatin interaction mapping[26]. FUMA annotates significantly associated SNPs with functional categories, combined CADD scores[28], RegulomeDB scores[77], and chromatin states[26]. A CADD score above 12.37 is suggestive of a deleterious protein effect[28]. The RegulomeDB score indicates the regulatory functionality of SNPs based on eQTLs and chromatin marks, whereas the chromatin state indicates the accessibility of genomic regions accessibility using 15 categorical states, as predicted by ChromHMM based on 5 chromatin marks for 127 epigenomes[78,79].

We conducted genome-wide gene-based association and gene-set analyses using MAGMA[30] in FUMA on the complete GWAS input data. MAGMA performs multiple linear regression to obtain gene-based P-values and the Bonferroni-corrected significant threshold was P = 0.05/18158 genes = 2.75e-6. We performed a MAGMA[30] gene-set analysis for curated gene sets and GO terms obtained from MsigDB[80]. To identify over-represented pathways for the

mapped genes, we used the ConsensusPathDB[33]. ConsensusPathDB is a database system that integrates functional interactions, including binary and complex protein-protein, genetic, metabolic, signaling, gene regulatory and drug-target interactions, as well as biochemical pathways[33].

Analyses of genetic overlap between brainstem volumes and eight brain disorders

To further examine the genetic architecture of brainstem volumes and the genetic relationships between brainstem regions and common brain disorders, we obtained GWAS summary statistics for ADHD[81], ASD, SZ, and BD from the Psychiatric Genomics Consortium[82-84], for MD from the Psychiatric Genomics Consortium and 23andMe[85,86], for AD from the International Genomics of Alzheimer's Project[87], for MS from the International Multiple Sclerosis Genetics Consortium[88], and for PD from the International Parkinson Disease Genomics Consortium[46,89]. We then employed conditional Q-Q plots[90] and conditional FDR and conjunctional FDR statistics[34,91] to assess polygenic overlap between brainstem volumes and the eight brain disorders.

The conditional Q-Q plots compare the association with a primary trait across all SNPs and within SNPs strata determined by their association with the secondary trait. Genetic overlap exists if the proportion of SNPs associated with a phenotype increases as a function of the strength of the association with a secondary phenotype[90]. In conditional Q-Q plots, this enrichment is visualized as successive leftward deflections from the null distribution, and can be directly interpreted in terms of the true discovery rate (1−FDR)[34-36]. In this work, we plotted the empirical cumulative distribution of nominal *P*-values in one phenotype (e.g., whole brainstem volume) for all SNPs and for subsets of SNPs with significance levels in another phenotype (e.g., SCZ) below the indicated cut-offs ($P \leq 1$, $P \leq 0.1$, $P \leq 0.01$, and $P \leq 0.001$).

The conditional FDR statistical framework applies genetic association summary statistics from a trait of interest together with those of a conditional trait to estimate the posterior probability that a SNP has no association with the primary trait, given that the *P*-values for that SNP in both the primary and conditional traits are lower than the observed *P*-value[34-36]. This method can enhance the detection of genetic variants associated inserted the primary trait via re-ranking SNPs compared to nominal *P*-value based ranking. Here, we used an FDR level of 0.05 per pairwise comparison for conditional FDR.

To detect genetic jointly associated with the brainstem volumes and the eight clinical conditions, we used the conjunctional FDR method at a threshold of 0.05[34-36]. The conjunctional FDR is an extension of conditional FDR and is defined by the maximum of the two conditional FDR values for a specific SNP. This method estimates a posterior probability that a SNP is null for either trait or both at the same time, given that the *P* values for both phenotypes are as small, or smaller, than the *P*-values for each trait individually. Manhattan plots were constructed based on the ranking of the conjunctional FDR to show the genomic location of the shared genetic risk loci. The empirical null distribution in GWASs is affected by global variance inflation and all p-values were therefore corrected for inflation using a genomic inflation control procedure. All analysis was performed after excluding SNPs in the major extended histocompatibility complex (hg19 location Chr 6: 25119106–33854733) and 8p23.1 regions (hg19 location Chr 8: 7242715–12483982) for all cases and *MAPT* and *APOE* regions for PD and AD, respectively, since complex correlations in regions with intricate LD can bias the FDR estimation. We also ran pairwise genetic correlations between brainstem volumes and the eight psychiatric and neurological disorders using LD score regression[25]. Here, the SNPs were pruned using a pairwise correlation coefficient approximation to LD (r^2), where SNPs were disregarded at $r^2 < 0.2$ and pruning performed with 20 iterations[90].

Statistical analysis of brainstem volumes, brain disorders, and clinical variables

Statistical analyses for group comparisons were conducted using linear models in R statistics[39]. We included all healthy individuals that were imaged on the same scanners as the patients they were compared with, in the respective control groups. For clinical conditions where patients were imaged on multiple scanners, we included scanner site as a covariate in the analyses. For each of the clinical conditions, we ran linear models covarying for sex, age, age-orthogonalized age^2, ICV, and adjusted for multiple testing using FDR (Benjamini-Hochberg). The group analyses for volumes of midbrain, pons, SCP, and medulla oblongata were run both with and without covarying for whole brainstem volume.

Information concerning illness severity was available from individuals with MCI, dementia, MS, SCZ, and PD. 1610 individuals with MCI or dementia had MMSE score[40], whereas 190 individuals with MS had EDSS scores[41]. Linear models were run to examine the relationships between the clinical variables and brainstem volumes covarying for sex, age, age-orthogonalized age^2, ICV, and scanner site. Two neuroradiologists assessed the imaging data from the individuals with MS and found that n = 153 participants had infratentorial MS lesions detectable with MRI, whereas n = 91 did not. 384 individuals with SCZ had function scores of the Global Assessment of Functioning scale[42], whereas 264 individuals had symptom scores from the scale. 616 and 614 individuals with SCZ had positive and negative scores, respectively, from the Positive and Negative Syndrome Scale[43]. 128 individuals with PD had Unified Parkinson's Disease Rating Scale III scores[75] and the Hoehn and Yahr Stage score[76]. To examine whether tremor level might influence the measurements of brainstem volumes in PD, we used the self-report tremor item 2.10 of the Unified Parkinson's Disease Rating Scale III[75] and examined brainstem volumes across these tremor scores using linear models.

Code availability

The code needed to reproduce the results is available from the authors upon request.

The genetic architecture of human brainstem structures and their involvement in common brain disorders

This supplementary file contains Supplementary Tables 1-3.

Supplementary Table 1: Summary of included samples.

Supplementary Table 2: Summary of magnetic resonance imaging characteristics of included samples.

Supplementary Table 3: Size and demographic information of final study samples after quality control procedures.

Supplementary Table 1. Summary of included samples.

Sample	Source	Comment	Reference
ABIDE1	http://fcon_1000.projects.nitrc.org/	Primary support for the work by Adriana Di Martino was provided by the NIMH (K23MH087770) and the Leon Levy Foundation. Primary support for the work by Michael P. Milham and the INDI team was provided by gifts from Joseph P. Healy and the Stavros Niarchos Foundation to the Child Mind Institute, as well as by an NIMH award to MPM (R03MH096321).	[1]
ABIDE2	http://fcon_1000.projects.nitrc.org/	Primary support for the work by Adriana Di Martino and her team was provided by the National Institute of Mental Health (NIMH 5R21MH107045). Primary support for the work by Michael P. Milham and his team provided by the National Institute of Mental Health (NIMH 5R21MH107045); Nathan S. Kline Institute of Psychiatric Research). Additional Support was provided by gifts from Joseph P. Healey, Phyllis Green and Randolph Cowen to the Child Mind Institute.	[2]
ABM	Authors	ABM was supported by the Research Council of Norway (grant number 247372) and Health South East Research Funding Agency (grant number 2105052).	[3]
ADDNEUROMED	Authors	AddNeuroMed consortium was led by Simon Lovestone, Bruno Vellas, Patrizia Mecocci, Magda Tsolaki, Iwona Kłoszewska, Hilkka Soininen. Their work was supported by InnoMed (Innovative Medicines in Europe), an integrated project funded by the European Union of the Sixth Framework program priority (FP6-2004- LIFESCIHEALTH-5).	[4,5]
ADHD200	http://fcon_1000.projects.nitrc.org/	F. Xavier Castellanos, David Kennedy, Michael Milham, and Stewart Mostofsky are responsible for the initial conception of the ADHD-200 Consortium. Consortium steering committee includes Jan Buitelaar, F. Xavier Castellanos, Dan Dickstein, Damien Fair, David Kennedy, Beatriz Luna, Michael Milham (Project Coordinator), Stewart Mostofsky, and Julie Schweitzer. Data aggregation and organization was coordinated by the INDI team, which included Saroja Bangaru, David Gutman, Maarten Mennes, and Michael Milham. Web infrastructure and data storage were coordinated by Robert Buccigrossi, Albert Crowley, Christian Hasselgrove, David Kennedy, Kimberly Pohland, and Nina Preuss. The ADHD-200 Global Competition Coordinators were Damien Fair (Chair of Selection Committee, Editor in Chief for Global Competition Special issue) and Michael Milham	[6,7]
ADHDWUE	Authors	Primary support for the study was provided by the German Research Foundation, grant number DFG KFO 125/2.	[8,9]
ADNI1 ADNI2	http://adni.loni.usc.edu/ http://adni.loni.usc.edu/	Data collection and sharing for this project was funded by the Alzheimer's Disease Neuroimaging Initiative (ADNI) (National Institutes of Health Grant U01 AG024904) and DOD ADNI (Department of Defense award number W81XWH-12-2-0012). ADNI is funded by the National Institute on Aging, the National Institute of Biomedical Imaging and Bioengineering, and through generous contributions from the following: AbbVie, Alzheimer's Association; Alzheimer's Drug Discovery Foundation; Araclon Biotech; BioClinica, Inc.; Biogen; Bristol-Myers Squibb Company; CereSpir, Inc.; Cogstate; Eisai Inc.; Elan Pharmaceuticals, Inc.; Eli Lilly and Company; EuroImmun; F. Hoffmann-La Roche Ltd and its affiliated company Genentech, Inc.; Fujirebio; GE Healthcare; IXICO Ltd.; Janssen Alzheimer Immunotherapy Research & Development, LLC.; Johnson & Johnson Pharmaceutical Research & Development LLC.; Lumosity; Lundbeck; Merck & Co., Inc.; Meso Scale Diagnostics, LLC.; NeuroRx	[10,11]

		Research; Neurotrack Technologies; Novartis Pharmaceuticals Corporation; Pfizer Inc.; Piramal Imaging; Servier; Takeda Pharmaceutical Company; and Transition Therapeutics. The Canadian Institutes of Health Research is providing funds to support ADNI clinical sites in Canada. Private sector contributions are facilitated by the Foundation for the National Institutes of Health (www.fnih.org). The grantee organization is the Northern California Institute for Research and Education, and the study is coordinated by the Alzheimer's Therapeutic Research Institute at the University of Southern California. ADNI data are disseminated by the Laboratory for Neuro Imaging at the University of Southern California.	
BETULA	Authors	Betula was supported by a Wallenberg Scholar Grant (KAW).	[12]
CAMCAN	https://camcan-archive.mrc-cbu.cam.ac.uk/dataaccess/	Data collection and sharing for this project was provided by the Cambridge Centre for Ageing and Neuroscience (CamCAN). CamCAN funding was provided by the UK Biotechnology and Biological Sciences Research Council (grant number BB/H008217/1), together with support from the UK Medical Research Council and University of Cambridge, UK.	[13,14]
CIMH	Authors	CIMH was supported by the Deutsche Forschungsgesellschaft (DFG, projects ZI1253/3-1, ZI1253/3-2, KI 576/14-2, ME 1591/6-2) and the European Community's Seventh Framework Programme (FP7/2007–2013) grant agreement #602450 (IMAGEMEND).	[15,16]
CORR	http://fcon_1000.projects.nitrc.org/		[17]
DLBS	http://fcon_1000.projects.nitrc.org/		[18]
DS000030 (CNP)	https://openfmri.org/	DS* data sets were obtained from the OpenfMRI database. *DS000030* work was supported by the Consortium for Neuropsychiatric Phenomics (NIH Roadmap for Medical Research grants UL1-DE019580, RL1MH083268, RL1MH083269, RL1DA024853, RL1MH083270, RL1LM009833, PL1MH083271, and PL1NS062410). *DS000115* was supported through NIH Grants P50 MH071616 and R01 MH56584. *DS000119* was supported by the National Institutes of Mental Health (NIMH RO1 MH067924). Enami Yasui provided assistance with data collection. *DS000171*: Trisha Patrician and Natalie Stroupe assisted with screening of participants. Allan Schmitt and Franklin Hunsinger collected the MR data.	[19,20]
DS000115 (CCNMD)	https://openfmri.org/		[21,22]
DS000119	https://openfmri.org/		[23]
DS000171	https://openfmri.org/		[24]
DS000202	https://openfmri.org/		[25,26]
DS000222	https://openfmri.org/		[27]
HCP	https://www.humanconnectome.org	Data were provided [in part] by the Human Connectome Project, MGH-USC Consortium (Principal Investigators: Bruce R. Rosen, Arthur W. Toga and Van Wedeen; U01MH093765) funded by the NIH Blueprint Initiative for Neuroscience Research grant; the National Institutes of Health grant P41EB015896; and the Instrumentation Grants S10RR023043, 1S10RR023401, 1S10RR019307.	[28]
HUBIN	Authors	This study was supported by the Swedish Research Council (2006-2992, 2006-986, K2007-62X-15077-04-1, 2008-2167, K2008-62P-20597-01-3. K2010-62X-15078-07-2, K2012-61X-15078-09-3, 2017-00949), the regional agreement on medical training and clinical research between Stockholm County Council and the Karolinska Institutet, the Knut and Alice Wallenberg Foundation, and the HUBIN project.	[29]
HUNT	Authors	The HUNT Study is a collaboration between HUNT Research Centre, Faculty of Medicine and Health Sciences, Norwegian University of Science and Technology (NTNU), Nord-Trøndelag County Council, Central Norway Regional Health Authority, and the Norwegian Institute of Public Health. HUNT-MRI and the genetic analysis were funded by grants	[30,31]

		from the Liaison Committee between the Central Norway Regional Health Authority and NTNU to principal investigator Asta Håberg, and the Norwegian National Advisory Unit for functional MRI. We thank the HUNT MRI participants, MRI technicians and the Department of Diagnostic Imaging at Levanger Hospital, Professor Lars Jacob Stovner (NTNU) and the administrative staff at HUNT.	
IXI	http://brain-development.org/ixi-dataset/		[32]
KASP	Authors	KaSP was supported by grants from the Swedish Medical Research Council (SE: 2009-7053; 2013-2838; SC: 523-2014-3467), the Swedish Brain Foundation, Åhlén-siftelsen, Svenska Läkaresällskapet, Petrus och Augusta Hedlunds Stiftelse, Torsten Söderbergs Stiftelse, the AstraZeneca-Karolinska Institutet Joint Research Program in Translational Science, Söderbergs Königska Stiftelse, Professor Bror Gadelius Minne, Knut och Alice Wallenbergs stiftelse, Stockholm County Council (ALF and PPG), Centre for Psychiatry Research, KID-funding from the Karolinska Institutet.	[33,34]
MALTOSLO	Authors	The study was funded by the South-Eastern Norway Regional Health Authority (2015-2015078), Oslo University Hospital, a research grant from Mrs. Throne-Holst, and the Ebbe Frøland foundation.	[35,36]
NCNG	Authors	The sample collection was supported by grants from the Bergen Research Foundation and the University of Bergen, the Dr Einar Martens Fund, the K.G. Jebsen Foundation, the Research Council of Norway, to SLH, VMS, AJL, and TE. The authors thank Dr. Eike Wehling for recruiting participants in Bergen, and Professor Jonn-Terje Geitung and Haraldplass Deaconess Hospital for access to the MRI facility. Additional support by RCN grants 177458/V50 and 231286/F20.	[37]
NIMAGE	Authors	This project was supported by grants from National Institutes of Health (grant R01MH62873 to SV Faraone) for initial sample recruitment, and from NWO Large Investment (grant 1750102007010 to JK Buitelaar), NWO Brain & Cognition (grant 433-09-242 to JK Buitelaar), ZonMW Grant 60-60600-97-193, and grants from Radboud University Medical Center, University Medical Center Groningen, Accare, and VU University Amsterdam for subsequent assessment waves. NeuroIMAGE also receives funding from the European Community's Seventh Framework Programme (FP7/2007 – 2013) under grant agreements n° 602805 (Aggressotype), n° 278948 (TACTICS), and n° 602450 (IMAGEMEND), and from the European Community's Horizon 2020 Programme (H2020/2014 – 2020) under grant agreements n° 643051 (MiND) and n° 667302 (CoCA).	[38]
NORCOG	Authors	The Norwegian register of persons assessed for cognitive symptoms (NorCog) includes clinical and biological data from memory clinics in Norway (https://www.aldringoghelse.no-/norkog/). The register is owned by Oslo University Hospital and administered by Norwegian National Advisory Unit on Ageing and Health. The NORCOG sample includes individuals with mild cognitive impairment and dementia.	[39]
OASIS	http://www.oasis-brains.org/	The study was supported by grants P50 AG05681, P01 AG03991, R01 AG021910, P50 MH071616, U24 RR021382, R01 MH56584.	[40,41]
PING	http://pingstudy.ucsd.edu/	Data used in the preparation of this article were obtained from the Pediatric Imaging, Neurocognition and Genetics (PING) Study database (http://ping.chd.ucsd.edu/). PING was launched in	[42]

		2009 by the National Institute on Drug Abuse (NIDA) and the Eunice Kennedy Shriver National Institute Of Child Health & Human Development (NICHD) as a 2-year project of the American Recovery and Reinvestment Act. The primary goal of PING has been to create a data resource of highly standardized and carefully curated magnetic resonance imaging (MRI) data, comprehensive genotyping data, and developmental and neuropsychological assessments for a large cohort of developing children aged 3 to 20 years. The scientific aim of the project is, by openly sharing these data, to amplify the power and productivity of investigations of healthy and disordered development in children, and to increase understanding of the origins of variation in neurobehavioral phenotypes. For up-to-date information, see http://ping.chd.ucsd.edu/. Data collection and sharing for this project was funded by the Pediatric Imaging, Neurocognition and Genetics Study (PING) (National Institutes of Health Grant RC2DA029475). PING is funded by the National Institute on Drug Abuse and the Eunice Kennedy Shriver National Institute of Child Health & Human Development. PING data are disseminated by the PING Coordinating Center at the Center for Human Development, University of California, San Diego.	
PNC	https://www.med.upenn.edu	Support for the collection of the data sets was provided by grant RC2MH089983 awarded to R. Gur and RC2MH089924 awarded to H. Hakonarson.	[43,44]
PPMI	http://www.ppmi-info.org/	Parkinson's disease progression markers initiative (PPMI) is an observational clinical study to verify progression markers in PD. The study includes a comprehensive set of clinical, imaging (including structural MRI) and biosample data. The study is sponsored by the Michael J. Fox foundation for Parkinson's Research and is made possible by restricted donations to the Foundation from a consortium of Parkinson's drug development stakeholders. PPMI is led by Principal Investigator Ken Marek, MD, President and Senior Scientist of the Institute for Neurodegenerative Disease in New Haven, Connecticut. Funding partners include abbvie, Allergan, Avid, Biogen, BioLegend, Bristol-Myers Squibb, Celgene, Denali, GE Healthcare, Genentech, GlaxoSmithKline, Lilly, Lundbeck, Merck, Meso Scale Discovery, Pfizer, Piramal, Prevail Therapeutics, Roche, Sanofi Genzyme, Servier, Takeda, Teva, ucb, verily, Voyager Therapeutics, and Golub Capital.	[45]
RSI-MS	Authors	Data collection in this MS cohort was supported by the South-Eastern Norway Regional Health Authority project 39569, Research Council of Norway grant 240102 and 240102, Oslo MS Society, Odd Fellow's Society for MS research. Healthy controls were sampled from the TOP study (same scanner).	[46]
SALD	http://fcon_1000.projects.nitrc.org/		[47]
SCHIZCONNECT1 SCHIZCONNECT2	http://schizconnect.org/ http://schizconnect.org/	Data used in preparation of this article were obtained from the SchizConnect (http://schizconnect.org) database. As such, the investigators within SchizConnect contributed to the design and implementation of SchizConnect and/or provided data but did not participate in analysis or writing of this report. Data collection and sharing for this project was funded by NIMH cooperative agreement 1U01 MH097435 *SCHIZCONNECT1* comprised BrainGluSchi, COBRE and MCIC samples (COINS). *SCHIZCONNECT2* comprised NUSDAST and NUNDA samples. The respective samples were supported by the following grants: *BrainGluSchi*: NIMH R01MH084898-01A1. *COBRE*: 5P20RR021938 /P20GM103472 from the NIH to Dr. Vince Calhoun. *MCIC*: Department of Energy under Award Number DE-FG02-08ER64581. *NUSDAST*: NIMH Grant	[48-53]

		1R01 MH084803. *NUNDA*: MH056584.	
SCORE	Authors	This work was supported by the Swiss National Science Foundation (grant No. 119382).	[54,55]
SLIM	http://fcon_1000.projects.nitrc.org/	Support was provided by grant numbers 31271087; 31470981; 31571137, 31500885, SWU1509383, SWU1509451, cstc2015jcyjA10106, 151023, 2015M572423, 2015M580767, Xm2015037, 14JJD880009.	[56,57]
STROKEMRI/ MOT	Authors	Supported by the Research Council of Norway (249795, 248238), the South-Eastern Norway Regional Health Authority (2014097, 2015044, 2015073, 2016083), and the Norwegian ExtraFoundation for Health and Rehabilitation (2015/FO5146).	[58]
TOP	Authors	The work was funded by the Research Council of Norway (213837, 223273, 204966/F20, 213694, 229129, 249795/F20, 248778), the South-Eastern Norway Regional Health Authority (2013-123, 2014-097, 2015-073, #2017-112) and Stiftelsen Kristian Gerhard Jebsen.	[59-62]
UBA	Authors	European Community‘s Seventh Framework Programme (FP7/2007–2013) grant agreement #602450 (IMAGEMEND).	[63]
UKBB	https://www.ukbiobank.ac.uk/	All subjects with a primary or secondary ICD-10 diagnosis with a mental or neurological disorder were excluded prior to analysis and the remaining subjects included as healthy controls.	[64]
UNIBA	Authors	This work was supported by a “Capitale Umano ad Alta Qualificazione” grant by Fondazione Con Il Sud awarded to Alessandro Bertolino and by a Hoffmann-La Roche Collaboration Grant awarded to Giulio Pergola. This project has received funding from the European Union Seventh Framework Programme for research, technological development and demonstration under grant agreement no. 602450 (IMAGEMEND). This paper reflects only the author's views and the European Union is not liable for any use that may be made of the information contained therein.	[65]
UNIBAS	Authors		[54]

Supplementary Table 2. Summary of magnetic resonance imaging characteristics of included samples.

Sample	Number of scanners/ protocols included	Parameters	References
ABIDE1	20	http://fcon_1000.projects.nitrc.org/indi/abide/scan_params/	[1]
ABIDE2	16		[2]
ABM	2	Philips 3T Ingenia: TR=3000ms, TE=3.61ms, FA=8° (2x same scanner and protocol, except for sagittal phase-encoding vs. axial phase encoding)	[66]
ADDNEUROMED	6	GE 1.5T: TR=8.59, TE=3.8, FA=8° GE 1.5T: TR=10.4, TE=4.09, FA=9° GE 1.5T: TR=10.2, TE=4.1, FA=8° GE 1.5T: TR=10.2, TE=4.1, FA=8° Siemens 1.5T: TR=2400, TE=3.5, FA=8° Picker 1.5T: TR=13, TE=3, FA=20°	[4,5]
ADHD200	6	Philips 1.5 T Gyroscan: TR=8ms, TE=3.76ms, FA=8°; Siemens 3T Allegra: TR=2530ms, TE=3.25ms, FA=8°; Siemens 3T Trio: TR=2300ms, TE=3.58ms, 10°; Siemens 3T Trio: TR=1700ms, TE=3.92ms, FA=12° Siemens 3T Trio: TR=2100ms, TE=3.43ms, FA=8° Siemens 3T Trio: TR=2400ms, TE=3.08ms, FA=8°	[6,7]
ADHDWUE	1	Siemens 1.5T Avanto: TR=2250ms, TE=3.93ms, FA=8°	[8,9]
ADNI1	54	http://adni.loni.usc.edu/methods/mri-tool/mri-analysis/	[10,11]
ADNI2	53		
BETULA	1	GE 3T: TR=8.2ms, TE=3.2ms, FA=12°	[12]
CAMCAN	1	Siemens 3T Trio: TR=2250ms, TE=2.99ms, FA=9°	[13,14]
CIMH	1	Siemens 3T Trio: TR=1570ms, TE=2.75ms, FA=15°	[15,16]
CORR	34	http://fcon_1000.projects.nitrc.org/indi/CoRR/html/_static/scan_parameters/	[17]
DLBS	1	Philips 3T: TR=8.135ms, TE=3.7ms, FA=18°	[18]
DS000030 (CNP)	2	Siemens 3T Trio: TR=1900ms, TE=2.26ms, FA=12°	[19,20]
DS000119	1	Siemens 3T Allegra: TR=1570ms, TE=3.04ms, FA=8°	[23]
DS000171	1	Siemens 3T Skyra: TR=2300ms, TE=2.01ms, FA=9°	[24]
DS000202	1	Philips 3T Achieva: TR=7.6ms, TE=3.7ms, FA=8°	[25,26]
DS000222	1	Siemens 3T Trio: TR=1550ms, TE=2.34ms, FA=9°	[27]
HCP	1	Customized 3T scanner: TR=2400ms, TE=2.14, FA=8°	[28]
HUBIN	1	GE 1.5 T signa Echo-speed: TR=24ms, TE=6.0ms, FA=35°	[29]
HUNT	1	GE 1.5T Signa HDx: TR=10.2ms, TE=4.1ms, FA=10°	[30,31]
IXI	3	Philips 3T: TR=9.6ms, TE=4.6ms, FA=8° Philips 1.5T: TR=9.8ms, TE=4.6ms, FA=8° GE 1.5T: TR=6.0ms, TE=2.5ms	[32]
KASP	1	GE 3T Discovery MR750: TR=7.91ms, TE=3.06ms, FA=12°	[67,68]
MALTOSLO	1	Philips 3T Achieva: TR=8.4ms, TE=2.3ms, FA=7°	[36,69]
NCNG	3	Siemens 1.5T Sonata: TR=2730ms, TE=3.43ms, FA=7°	[37]

		Siements 1.5T Avanto: TR=2400ms, TE=3.61ms, FA=8° GE 1.5T Signa: TR=9.5ms, TE=3.1ms, FA=7°	
NIMAGE	2	Siemens 1.5T Sonata: TR= 2730ms, TE=2.95ms, FA=7° Siemens 1.5T Avanto: TR= 2730ms, TE=2.95ms, FA=7°	[38]
NORCOG	3	GE 3T Signa HDxT: TR=7.8ms, TE=2.956ms, FA=12° (one subset with HNS coil, one subset with 8HRBRAIN coil) GE 3T Discovery GE750: TR=8.16ms, TE=3.18ms, FA=12°	[39]
OASIS	1	Siemens 1.5T Vision: TR=9.7ms, TE=4ms, FA=10°	[40,41]
PING	11	http://pingstudy.ucsd.edu/resources/neuroimaging-cores.html	[42]
PNC	1	Siemens 3T Trio: TR=1810ms, TE=3.51ms, FA=9°	[43,44]
SALD	1	Siemens 3T Trio: TR=1900ms, TE=2.52ms, FA=9°	[47]
SCHIZCONNECT1 (BrainGluSchi, COBRE, MCIC)	5	Siemens 3T Trio: 2530ms, TE=TE = 1.64, 3.5, 5.36, 7.22, 9.08ms, FA=7° Siemens 1.5T Sonata: TR=12ms, TE=4.76, FA=20° Siemens 3T SMS Trio: TR=2530ms, TE=3.81ms, FA=7° Siemens 1.5T Avanto: TR=12ms, TE=4.76ms, FA=20°	[48-53]
SCHIZCONNECT2 (NUNDA, NUSDAST)	2	Siemens 3T Trio: TR=2400ms, TE=3.16ms, FA=8° Siemens 1.5T Vision: TR=9.7ms, TE=4ms, FA=10°	
SCORE	1	Siemens 1.5T Vision: TR=9.7ms, TE=4ms, FA=12°	[54,55]
SLIM	1	Siemens 3T Trio: TR=1900ms, TE=2.52ms, FA=9°	[56,57]
STROKEMRI/ MOT	2	GE 3T Signa HDxT: TR=7.8ms, TE=2.956ms, FA=12° GE 3T Discovery GE750: TR=8.16ms, TE=3.18ms, FA=12°	[58]
TOP/ RSI-MS	4	Siemens 1.5T Sonata: TR=2730ms, TE=3.93ms, FA=7° GE 3T Signa HDxT: TR=7.8ms, TE=2.956ms, FA=12° (one subset with HNS coil, one subset with 8HRBRAIN coil) GE 3T Discovery GE750: TR=8.16ms, TE=3.18ms, FA=12°	[59-62,70]
UBA	1	Siemens 3T Verio: TR=2000ms, TE=3.37ms, FA=8°	[63]
UKBB	3	Siemens 3T Skyra: TR=2000ms, TE=2.01ms, FA=8° (3 identical scanning sites)	[64]
UNIBA	1	GE 3T Signa: TR=25ms, TE=3ms, FA=6°	[65]

Supplementary Table 3. Size and demographic information of final study samples after quality control procedures.

Sample	Number of subjects per group	Age: mean ± sd in years (group)	Sex: f/m
ADHD	681 patients; 992 HC	17.5±9.9 (ADHD); 17.4±9.7 (HC)	702/971
ASD	125 patients; 140 HC	18.7±9.7 (ASD); 17.1±9.8 (HC)	34/231
BD	464 patients; 1,531 HC	33.7±10.7 (BD); 39.1±15.9 (HC)	1,031/946
MDD	211 patients; 93 HC	38.8±13.5 (MDD); 39.5±13.9 (HC)	201/103
PSYMIX	308 patients; 1,430 HC	28.9±9.3 (PSYMIX); 39.3±16.2 (HC)	852/886
SCZ	1,044 patients; 2,079 HC	33.6±11.0 (SCZ); 37.7±15.2 (HC)	1,323/1,800
SCZRISK	91 patients; 402 HC	23.7±5.0 (SCZRISK); 31.2±11.7 (HC)	223/270
DEM	756 patients; 1,921 HC	75.4±7.7 (DEM); 51.4±22.0 (HC)	1,434/1,243
MCI	987 patients; 1,655 HC	72.2±8.4 (MCI); 53.3±21.3 (HC)	1,264/1,378
MS	257 patients; 1,053 HC	40.9±10.0 (MS); 41.4±17.6 (HC)	745/565
PD	138 patients; 67 HC	61.2±9.1 (PD); 60.2±11.3 (HC)	73/132
UK Biobank sample	27,034 HC	55.6±7.4 (HC)	13,931/13,103
All HC	38,299 HC	50.0±15.7 (HC)	19,963/18,336
All participants	43,353		

ADHD; attention-deficit/hyperactivity disorder. ASD; autism spectrum disorders. BD; bipolar disorder. HC; healthy controls. MDD; major depression. PSYMIX; non-SCZ psychosis spectrum diagnoses. SCZ; schizophrenia. SCZRISK; prodromal SCZ or at risk mental state. DEM; dementia. MCI; mild cognitive impairment. MS; multiple sclerosis. PD; Parkinson's disease.

Supplementary references

1. Di Martino A, Yan CG, Li Q, Denio E, Castellanos FX, Alaerts K *et al.* The autism brain imaging data exchange: towards a large-scale evaluation of the intrinsic brain architecture in autism. *Molecular psychiatry* 2014; **19:** 659-667.

2. Di Martino A, O'Connor D, Chen B, Alaerts K, Anderson JS, Assaf M *et al.* Enhancing studies of the connectome in autism using the autism brain imaging data exchange II. *Sci Data* 2017; **4:** 170010.

3. Maglanoc LA, Landro NI, Jonassen R, Kaufmann T, Cordova-Palomera A, Hilland E *et al.* Data-Driven Clustering Reveals a Link Between Symptoms and Functional Brain Connectivity in Depression. *Biological psychiatry Cognitive neuroscience and neuroimaging* 2018.

4. Liu Y, Paajanen T, Zhang Y, Westman E, Wahlund LO, Simmons A *et al.* Combination analysis of neuropsychological tests and structural MRI measures in differentiating AD, MCI and control groups--the AddNeuroMed study. *Neurobiol Aging* 2011; **32:** 1198-1206.

5. Lovestone S, Francis P, Strandgaard K. Biomarkers for disease modification trials--the innovative medicines initiative and AddNeuroMed. *J Nutr Health Aging* 2007; **11:** 359-361.

6. Brown MR, Sidhu GS, Greiner R, Asgarian N, Bastani M, Silverstone PH *et al.* ADHD-200 Global Competition: diagnosing ADHD using personal characteristic data can outperform resting state fMRI measurements. *Front Syst Neurosci* 2012; **6:** 69.

7. Consortium HD. The ADHD-200 Consortium: A Model to Advance the Translational Potential of Neuroimaging in Clinical Neuroscience. *Front Syst Neurosci* 2012; **6:** 62.

8. Guadalupe T, Mathias SR, vanErp TGM, Whelan CD, Zwiers MP, Abe Y *et al.* Human subcortical brain asymmetries in 15,847 people worldwide reveal effects of age and sex. *Brain Imaging Behav* 2017; **11:** 1497-1514.

9. Conzelmann A, Mucha RF, Jacob CP, Weyers P, Romanos J, Gerdes AB *et al.* Abnormal affective responsiveness in attention-deficit/hyperactivity disorder: subtype differences. *Biological psychiatry* 2009; **65:** 578-585.

10. Weiner MW, Aisen PS, Jack CR, Jr., Jagust WJ, Trojanowski JQ, Shaw L *et al.* The Alzheimer's disease neuroimaging initiative: progress report and future plans. *Alzheimers Dement* 2010; **6:** 202-211 e207.

11. Wyman BT, Harvey DJ, Crawford K, Bernstein MA, Carmichael O, Cole PE *et al.* Standardization of analysis sets for reporting results from ADNI MRI data. *Alzheimers Dement* 2013; **9:** 332-337.

12. Nilsson L-G, Adolfsson R, Bäckman L, de Frias CM, Molander B, Nyberg L. Betula: A Prospective Cohort Study on Memory, Health and Aging. *Aging, Neuropsychology, and Cognition* 2004; **11:** 134-148.

13. Taylor JR, Williams N, Cusack R, Auer T, Shafto MA, Dixon M *et al.* The Cambridge Centre for Ageing and Neuroscience (Cam-CAN) data repository: Structural and functional MRI, MEG, and cognitive data from a cross-sectional adult lifespan sample. *Neuroimage* 2017; **144:** 262-269.

14. Shafto MA, Tyler LK, Dixon M, Taylor JR, Rowe JB, Cusack R *et al.* The Cambridge Centre for Ageing and Neuroscience (Cam-CAN) study protocol: a cross-sectional, lifespan, multidisciplinary examination of healthy cognitive ageing. *BMC Neurol* 2014; **14:** 204.

15. Eisenacher S, Rausch F, Ainser F, Mier D, Veckenstedt R, Schirmbeck F *et al.* Investigation of metamemory functioning in the at-risk mental state for psychosis. *Psychological medicine* 2015; **45:** 3329-3340.

16. Rausch F, Mier D, Eifler S, Esslinger C, Schilling C, Schirmbeck F *et al.* Reduced activation in ventral striatum and ventral tegmental area during probabilistic decision-making in schizophrenia. *Schizophrenia research* 2014; **156:** 143-149.

17. Zuo XN, Anderson JS, Bellec P, Birn RM, Biswal BB, Blautzik J *et al.* An open science resource for establishing reliability and reproducibility in functional connectomics. *Scientific data* 2014; **1:** 140049.

18. Lu H, Xu F, Rodrigue KM, Kennedy KM, Cheng Y, Flicker B *et al.* Alterations in cerebral metabolic rate and blood supply across the adult lifespan. *Cereb Cortex* 2011; **21:** 1426-1434.

19. Gorgolewski KJ, Durnez J, Poldrack RA. Preprocessed Consortium for Neuropsychiatric Phenomics dataset. *F1000Res* 2017; **6:** 1262.

20. Poldrack RA, Congdon E, Triplett W, Gorgolewski KJ, Karlsgodt KH, Mumford JA *et al.* A phenome-wide examination of neural and cognitive function. *Sci Data* 2016; **3:** 160110.

21. Repovs G, Barch DM. Working memory related brain network connectivity in individuals with schizophrenia and their siblings. *Frontiers in human neuroscience* 2012; **6:** 137.

22. Repovs G, Csernansky JG, Barch DM. Brain network connectivity in individuals with schizophrenia and their siblings. *Biological psychiatry* 2011; **69:** 967-973.

23. Velanova K, Wheeler ME, Luna B. Maturational changes in anterior cingulate and frontoparietal recruitment support the development of error processing and inhibitory control. *Cereb Cortex* 2008; **18:** 2505-2522.

24. Lepping RJ, Ruth AA, Cary R. Development of a validated emotionally provocative musical stimulus set for researc. *Psychology of music* 2016; **44**.

25. Van Schuerbeek P, Baeken C, De Mey J. The Heterogeneity in Retrieved Relations between the Personality Trait 'Harm Avoidance' and Gray Matter Volumes Due to Variations in the VBM and ROI Labeling Processing Settings. *PloS one* 2016; **11:** e0153865.

26. Van Schuerbeek P, Baeken C, De Raedt R, De Mey J, Luypaert R. Individual differences in local gray and white matter volumes reflect differences in temperament and character: a voxel-based morphometry study in healthy young females. *Brain Res* 2011; **1371:** 32-42.

27. FitzGerald THB, Hammerer D, Friston KJ, Li SC, Dolan RJ. Sequential inference as a mode of cognition and its correlates in fronto-parietal and hippocampal brain regions. *PLoS Comput Biol* 2017; **13:** e1005418.

28. Van Essen DC, Smith SM, Barch DM, Behrens TE, Yacoub E, Ugurbil K *et al.* The WU-Minn Human Connectome Project: an overview. *Neuroimage* 2013; **80:** 62-79.

29. Haukvik UK, Schaer M, Nesvag R, McNeil T, Hartberg CB, Jonsson EG *et al.* Cortical folding in Broca's area relates to obstetric complications in schizophrenia patients and healthy controls. *Psychol Med* 2012; **42:** 1329-1337.

30. Haberg AK, Hammer TA, Kvistad KA, Rydland J, Muller TB, Eikenes L *et al.* Incidental Intracranial Findings and Their Clinical Impact; The HUNT MRI Study in a General Population of 1006 Participants between 50-66 Years. *PloS one* 2016; **11:** e0151080.

31. Krokstad S, Langhammer A, Hveem K, Holmen TL, Midthjell K, Stene TR *et al.* Cohort Profile: the HUNT Study, Norway. *Int J Epidemiol* 2013; **42:** 968-977.

32. Liu K, Yao S, Chen K, Zhang J, Yao L, Li K *et al.* Structural Brain Network Changes across the Adult Lifespan. *Front Aging Neurosci* 2017; **9:** 275.

33. Collste K, Plaven-Sigray P, Fatouros-Bergman H, Victorsson P, Schain M, Forsberg A *et al.* Lower levels of the glial cell marker TSPO in drug-naive first-episode psychosis patients as measured using PET and [(11)C]PBR28. *Molecular psychiatry* 2017; **22:** 850-856.

34. Orhan F, Fatouros-Bergman H, Goiny M, Malmqvist A, Piehl F, Cervenka S *et al.* CSF GABA is reduced in first-episode psychosis and associates to symptom severity. *Molecular psychiatry* 2018; **23:** 1244-1250.

35. Elvsashagen T, Westlye LT, Boen E, Hol PK, Andreassen OA, Boye B *et al.* Bipolar II disorder is associated with thinning of prefrontal and temporal cortices involved in affect regulation. *Bipolar Disord*, vol. doi: 10.1111/bdi.121172013.

36. Elvsashagen T, Westlye LT, Boen E, Hol PK, Andersson S, Andreassen OA *et al.* Evidence for reduced dentate gyrus and fimbria volume in bipolar II disorder. *Bipolar disorders* 2013; **15:** 167-176.

37. Espeseth T, Christoforou A, Lundervold AJ, Steen VM, Le Hellard S, Reinvang I. Imaging and cognitive genetics: the Norwegian Cognitive NeuroGenetics sample. *Twin Res Hum Genet* 2012; **15:** 442-452.

38. von Rhein D, Mennes M, van Ewijk H, Groenman AP, Zwiers MP, Oosterlaan J *et al.* The NeuroIMAGE study: a prospective phenotypic, cognitive, genetic and MRI study in children with attention-deficit/hyperactivity disorder. Design and descriptives. *Eur Child Adolesc Psychiatry* 2015; **24:** 265-281.

39. Doan NT, Engvig A, Zaske K, Persson K, Lund MJ, Kaufmann T *et al.* Distinguishing early and late brain aging from the Alzheimer's disease spectrum: consistent morphological patterns across independent samples. *Neuroimage* 2017; **158:** 282-295.

40. Buckner RL, Head D, Parker J, Fotenos AF, Marcus D, Morris JC *et al.* A unified approach for morphometric and functional data analysis in young, old, and demented adults using automated atlas-based head size normalization: reliability and validation against manual measurement of total intracranial volume. *Neuroimage* 2004; **23:** 724-738.

41. Fotenos AF, Snyder AZ, Girton LE, Morris JC, Buckner RL. Normative estimates of cross-sectional and longitudinal brain volume decline in aging and AD. *Neurology* 2005; **64:** 1032-1039.

42. Jernigan TL, Brown TT, Hagler DJ, Jr., Akshoomoff N, Bartsch H, Newman E *et al.* The Pediatric Imaging, Neurocognition, and Genetics (PING) Data Repository. *Neuroimage* 2016; **124:** 1149-1154.

43. Satterthwaite TD, Connolly JJ, Ruparel K, Calkins ME, Jackson C, Elliott MA *et al.* The Philadelphia Neurodevelopmental Cohort: A publicly available resource for the study of normal and abnormal brain development in youth. *Neuroimage* 2016; **124:** 1115-1119.

44. Satterthwaite TD, Elliott MA, Ruparel K, Loughead J, Prabhakaran K, Calkins ME *et al.* Neuroimaging of the Philadelphia neurodevelopmental cohort. *Neuroimage* 2014; **86:** 544-553.

45. The Parkinson Progression Marker Initiative (PPMI). *Progress in neurobiology* 2011; **95:** 629-635.

46. Sowa P, Harbo HF, White NS, Celius EG, Bartsch H, Berg-Hansen P *et al.* Restriction spectrum imaging of white matter and its relation to neurological disability in multiple sclerosis. 2018; 1352458518765671.

47. Wei D, Zhuang K, Chen Q, Yang W, Luiu W, Wang K *et al.* Structural and functional MRI from a cross-sectional Southwest University Adult lifespan Dataset (SALD). *bioRxiv* 2018.

48. Bustillo JR, Jones T, Chen H, Lemke N, Abbott C, Qualls C *et al.* Glutamatergic and Neuronal Dysfunction in Gray and White Matter: A Spectroscopic Imaging Study in a Large Schizophrenia Sample. *Schizophr Bull* 2017; **43:** 611-619.

49. Cetin MS, Christensen F, Abbott CC, Stephen JM, Mayer AR, Canive JM *et al.* Thalamus and posterior temporal lobe show greater inter-network connectivity at rest and across sensory paradigms in schizophrenia. *Neuroimage* 2014; **97:** 117-126.

50. Gollub RL, Shoemaker JM, King MD, White T, Ehrlich S, Sponheim SR *et al.* The MCIC collection: a shared repository of multi-modal, multi-site brain image data from a clinical investigation of schizophrenia. *Neuroinformatics* 2013; **11:** 367-388.

51. Kogan A, Alpert K, Ambite JL, Marcus DS, Wang L. Northwestern University schizophrenia data sharing for SchizConnect: A longitudinal dataset for large-scale integration. *Neuroimage* 2016; **124:** 1196-1201.

52. Wang L, Alpert KI, Calhoun VD, Cobia DJ, Keator DB, King MD *et al.* SchizConnect: Mediating neuroimaging databases on schizophrenia and related disorders for large-scale integration. *Neuroimage* 2016; **124:** 1155-1167.

53. Ambite JL, Tallis M, Alpert K, Keator DB, King M, Landis D *et al.* SchizConnect: Virtual Data Integration in Neuroimaging. *Data Integr Life Sci* 2015; **9162:** 37-51.

54. Borgwardt S, Koutsouleris N, Aston J, Studerus E, Smieskova R, Riecher-Rossler A *et al.* Distinguishing prodromal from first-episode psychosis using neuroanatomical single-subject pattern recognition. *Schizophr Bull* 2013; **39:** 1105-1114.

55. Dukart J, Smieskova R, Harrisberger F, Lenz C, Schmidt A, Walter A *et al.* Age-related brain structural alterations as an intermediate phenotype of psychosis. *Journal of psychiatry & neuroscience : JPN* 2017; **42:** 307-319.

56. Wang Y, Wei D, Li W, Qiu J. Individual differences in brain structure and resting-state functional connectivity associated with type A behavior pattern. *Neuroscience* 2014; **272:** 217-228.

57. Zhu W, Chen Q, Tang C, Cao G, Hou Y, Qiu J. Brain structure links everyday creativity to creative achievement. *Brain Cogn* 2016; **103:** 70-76.

58. Dorum ES, Alnaes D, Kaufmann T, Richard G, Lund MJ, Tonnesen S *et al.* Age-related differences in brain network activation and co-activation during multiple object tracking. *Brain Behav* 2016; **6:** e00533.

59. Kaufmann T, Alnaes D, Brandt CL, Doan NT, Kauppi K, Bettella F *et al.* Task modulations and clinical manifestations in the brain functional connectome in 1615 fMRI datasets. *Neuroimage* 2016; **147:** 243-252.

60. Kaufmann T, Skatun KC, Alnaes D, Doan NT, Duff EP, Tonnesen S *et al.* Disintegration of Sensorimotor Brain Networks in Schizophrenia. *Schizophr Bull* 2015.

61. Skåtun KC, Kaufmann T, Tonnesen S, Biele G, Melle I, Agartz I *et al.* Global brain connectivity alterations in patients with schizophrenia and bipolar spectrum disorders. *Journal of psychiatry & neuroscience : JPN* 2016; **41:** 150159.

62. Brandt CL, Kaufmann T, Agartz I, Hugdahl K, Jensen J, Ueland T *et al.* Cognitive Effort and Schizophrenia Modulate Large-Scale Functional Brain Connectivity. *Schizophr Bull* 2015.

63. Heck A, Fastenrath M, Ackermann S, Auschra B, Bickel H, Coynel D *et al.* Converging genetic and functional brain imaging evidence links neuronal excitability to working memory, psychiatric disease, and brain activity. *Neuron* 2014; **81:** 1203-1213.

64. Alfaro-Almagro F, Jenkinson M, Bangerter NK, Andersson JLR, Griffanti L, Douaud G *et al.* Image processing and Quality Control for the first 10,000 brain imaging datasets from UK Biobank. *Neuroimage* 2018; **166:** 400-424.

65. Pergola G, Trizio S, Di Carlo P, Taurisano P, Mancini M, Amoroso N *et al.* Grey matter volume patterns in thalamic nuclei are associated with familial risk for schizophrenia. *Schizophrenia research* 2017; **180:** 13-20.

66. Maglanoc LA, Landro NI, Jonassen R, Kaufmann T, Cordova-Palomera A, Hilland E *et al.* Data-Driven Clustering Reveals a Link Between Symptoms and Functional Brain Connectivity in Depression. *Biol Psychiatry Cogn Neurosci Neuroimaging* 2019; **4:** 16-26.

67. Collste K, Plaven-Sigray P, Fatouros-Bergman H, Victorsson P, Schain M, Forsberg A *et al.* Lower levels of the glial cell marker TSPO in drug-naive first-episode psychosis patients as measured using PET and [(11)C]PBR28. *Molecular psychiatry* 2017; **22:** 850-856.

68. Orhan F, Fatouros-Bergman H, Goiny M, Malmqvist A, Piehl F, Karolinska Schizophrenia Project C *et al.* CSF GABA is reduced in first-episode psychosis and associates to symptom severity. *Molecular psychiatry* 2017.

69. Elvsashagen T, Westlye LT, Boen E, Hol PK, Andreassen OA, Boye B *et al.* Bipolar II disorder is associated with thinning of prefrontal and temporal cortices involved in affect regulation. *Bipolar disorders* 2013; **15:** 855-864.

70. Sowa P, Harbo HF, White NS, Celius EG, Bartsch H, Berg-Hansen P *et al.* Restriction spectrum imaging of white matter and its relation to neurological disability in multiple sclerosis. *Mult Scler* 2018; 1352458518765671.